A MICROSATELLITE EVALUATION OF THE GENETIC STATUS OF THE $P27^{KIP1}$ AND $P21^{CIP1/WAF1}$ GENES IN OESOPHAGEAL CANCER.

BY

ZAKIR GAFFOOR

Submitted in partial fulfillment to the requirements for the degree of a Masters in Medical Science in the Pfizer Molecular Biology Research Facility, Doris Duke Medical Research Institute, Faculty of Medicine, Nelson R Mandela School of Medicine, University of KwaZulu-Natal.

Acknowledgements

There are a number of people to whom I owe the deepest gratitude. I have not mentioned everyone by name, but I am thankful for their assistance nonetheless.

I would to thank Dr. Richard Naidoo for supervising this project with patience. To all the people from the Pfizer Molecular Biology Research Facility, thanks for always being there for me.

I dedicate this master's dissertation to my family, especially my wonderful parents. I am here today because of their love, hard work and sacrifice. I wish I had the words to fully describe my gratitude to them.

Finally, I must thank Almighty God, who is the ultimate source of infinite wisdom and knowledge, both hidden and revealed.

DECLARATION

The experimental work presented in this thesis represents the original work of the author and has not been submitted to any other university. Where use was made of the work of others, it has been duly acknowledged in the text.

The research described in this study was carried out under the supervision of Dr. R. Naidoo in the Pfizer Molecular Biology Research Facility, Nelson R Mandela School of Medicine, University of KwaZulu-Natal, Durban

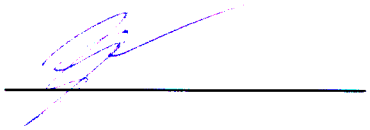

Zakir Gaffoor

July 2008

Publications

The results are expected to be published in the future.

Presentations

The results are expected to be presented at a future conference.

TABLE OF CONTENTS

LIST OF FIGURES

LIST OF FIGURES

CONTINUED...

LIST OF TABLES

LIST OF APPENDICES

LIST OF ABBREVIATIONS

°C	Degrees Celcius
A	Adenine
APS	Ammonium persulphate
bp	Base pair
C	Cytosine
Cdk	Cyclin-dependant kinase
COOH	Carboxyl
CpG	Cytosine-phosphate-guanine
CT	Computed tomographic
Cum Survival	Cumulative survival
CY5	CyTM5 amidite (5'-cyamine-d[seq]) fluorochrome
DNA	Deoxy-ribonucleic acid
dNTP	Deoxynucleotide triphosphate
EDTA	Ethylene-diamine-tetraacetic acid
EUS	Endoscopic ultrasonography
G	Guanine
G0	Gap-quiescent
G1	Gap 1
G1/S	Gap 1/Synthesis cell cycle junction
G2	Gap 2
Gly	Glycine
H	Homozygous, no change
H&E	Haemotoxylin and eosin
HNPCC	Hereditary nonpolyposis colorectal cancer
HPV	Human papilloma virus
i.e	That is
KCl	Potassium chloride
kD	kilo Dalton
LOH	Loss of heterozygosity
LOH-AI	Loss of heterozygosity-allelic imbalance
M	Mitotic
mA	Milliamp
MD	Moderate differentiated
med	Median
mg	Milligram
Mg^{2+}	Magnesium ion
$MgCl_2$	Magnesium chloride
ml	millilitre
mM	Millimolar

mRNA	messenger Ribonucleic acid
MSI	Microsatellite instability
NAI	No allelic imbalance
nm	nanometre
OC	Oesophageal cancer
OSCC	oesophageal squamous cell carcinoma
PCNA	proliferating cell nuclear antigen
PCR	Polymerase chain reaction
PCR-SSCP	Polymerase chain reaction-single strand conformational polymorphism
PD	Poor differentiated
PET	Positron emission tomography
pmol	Picomol
pRb	Phosphorylated retinoblastoma protein
Rb1	Retinoblastoma tumour suppressor gene
RNA	Ribonucleic acid
SNP	single nucleotide polymorphism
SV40	Simian virus 40
T	Thymine
TBE	Tris-boric acid-EDTA
TEMED	N, N, N', N'-tetramethyl-ethylendiamine
Thr	Threonine
TNM	Tumour, node, metastases
TSG	Tumour suppressor gene
U	Enzymatic unit of activity
v	Version
V	Volt
Val	Valine
viz	Namely
vs	Versus
W	Watt
WD	Well differentiated
µl	microlitre

ABSTRACT

p21$^{Cip1/WAF1}$ and *p27*^{Kip1} are cyclin-dependant kinase inhibitors that form an integral part of the cell cycle process. These proteins function as cell-cycle inhibitors, and are able to induce cell cycle arrest by binding to cyclin complexes at key stages. *p21* and *p27* have been found to be down-regulated in various cancers.

This study investigated aberrations at microsatellite markers linked to the *p21* and *p27* cell cycle genes, in a large cohort of oesophageal squamous cell carcinomas in South Africa. Fluorescent-based PCR were performed on markers linked to both the *p21* and *p27*. The products were run with a 50-500bp marker on 6% denaturing polyacrylamide gels, on the ALFexpress™ DNA sequencer. The detection and analysis of PCR products was achieved using the ALFexpress™ and Fragment Manager™ software programmes.

Our findings indicate that markers linked to *p27* display infrequent aberrations, with loss of heterozygosity ranging from 19% to 37%, and microsatellite instability at 3% to 7%. However, significant relationships between decreased survival time, and aberrations in markers D12S391 and D12S364, were found to exist. Marker D6S1575 linked to *p21* displayed frequent allelic loss at 47%, and was comparable to similar studies on the 6p region Further, LOH-A1 in this marker was found to be significantly associated with poorly differentiated tumours.

The findings from our study indicate that microsatellite aberrations occur infrequently at the *p21* and *p27* loci in oesophageal cancer, with the exception of marker D6S1575. In addition,

this study clearly demonstrates the accuracy and sensitivity of the technology employed. This is the first microsatellite-based investigation of the *p21/p27* gene loci in oesophageal cancer in South Africa, using a fluorescent-based PCR assay.

CHAPTER ONE

LITERATURE REVIEW

1. Oesophageal Cancer

There are a variety of cancers that may occur in the oesophagus. Of these, adenocarcinoma and squamous cell carcinoma, account for the overwhelming majority of cases. According to the latest available statistics from the South African National Cancer Registry, oesophageal cancer (OC) is the third and fourth most commonly occurring cancer in South African men and women respectively (South African National Cancer Registry, Cancer Statistics 1997). [Internet]. Available from: http://www.cansa.org.za [Accessed 02/04/2006]. The latter report also provided Age Standardised Rates/100 000 people for OC as 12.6 and 5.58 in males and females respectively. Amongst OC diagnosed patients in South Africa, squamous cell carcinomas form the major proportion of cases, with adenocarcinomas still a relatively rare occurrence (Isaacson, 2005). This is in contrast with what has been reported in the Western world, where incidences of adenocarcinomas have been increasing (Zhang *et al.*, 2004).

OC normally begins with progressive dysphagia over a relatively short time period of several weeks (Blot, 1994). Dysphagia manifests with the progressive difficulty in swallowing solids, as a result of the constriction of the lumen of the oesophagus to 14mm or less (Urba *et al.*, 2001). Over time, patients experience difficulty with swallowing liquid

foods and saliva. This progressive worsening over time is indicative of a growing tumour. Dysphagia is almost universally accompanied by dramatic weight loss. A number of other symptoms and signs accompany these events and some are listed below:

- Compression of the recurrent laryngeal nerve.
- Compression of sympathetic nerves.
- Nerve compression elsewhere leading up to spinal pain, hiccups, or paralysis of the diaphragm.
- Pulmonary metastasis leading to dyspnea.
- The presence of solid tumour intraluminally may lead to odynophagia, vomiting, haematemesis, maelena, anaemia, lung abscess and pneumonia.

OC usually metastasises to the lungs and liver, and sometimes to other more distant sites. Diagnosis is achieved through various ways. These include barium X-ray, endoscopy, computed tomographic (CT) and endoscopic ultrasound. Endoscopy with biopsy and cytological analysis is currently the preferred method of diagnosis. Figure 1 below presents a classical anatomical representation of oesophageal structure in relation to surrounding organs.

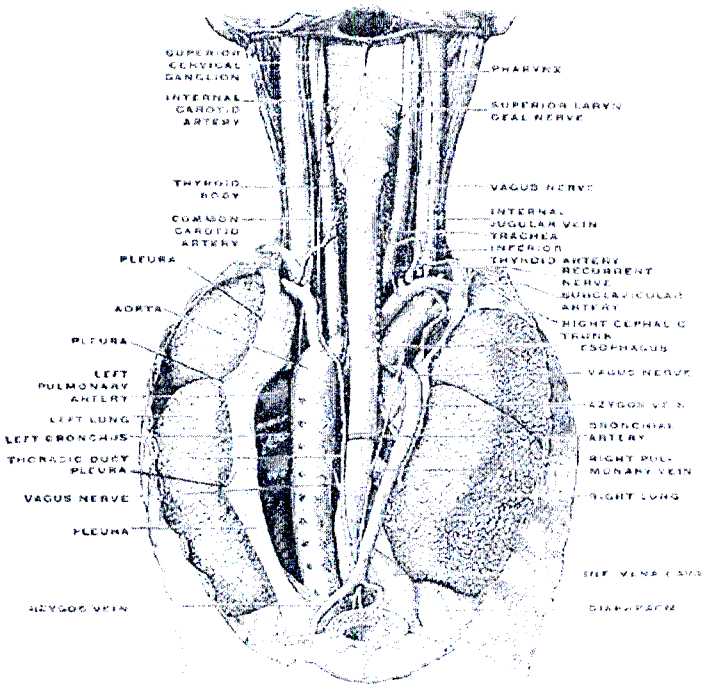

Figure 1: Diagrammatic representation of the oesophagus in the cervical cavity. Taken from Gray, H. (2000) *Anatomy of the Human Body*. New York, Bartleby.com. Available from: www.bartleby.com/107/. [Accessed 02/11/2005].

1.1 Oesophageal squamous cell carcinoma

Squamous cell carcinoma of the oesophagus, or epidermoid carcinoma, is a result of epidermal lesions that transform into intra-luminally expanding tumours. The aetiology of oesophageal squamous cell carcinoma (OSCC) is relatively well documented, although no causative agent or condition has been exclusively identified as the major contributing factor in tumourigenesis. There are a number of factors that have been significantly linked, often in combination, with disease

aggressivity and outcome. Figure 2 below is an endoscopic image of the oesophagus with intra-luminal tumour growth. The series of images that follows in figure 3 are micrographs that illustrate the progressive expansion of tumours into the surrounding tissue.

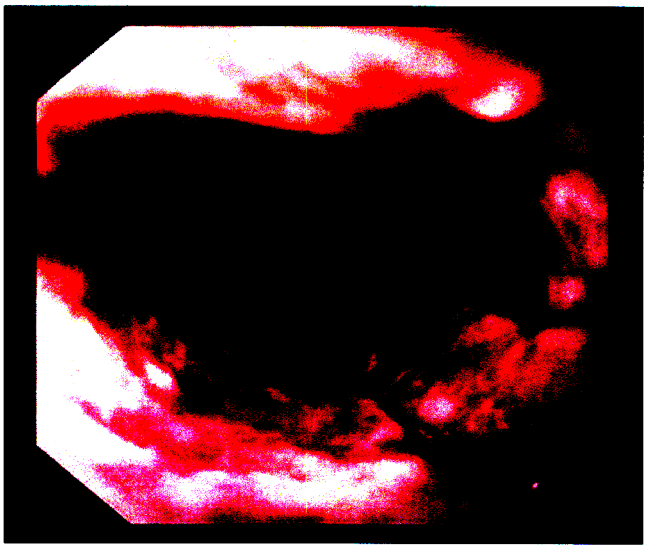

Figure 2: Lumen of an oesophagus as seen through an endoscope, with tumour that is represented as an intra-luminal growth. The tumour caused a narrowing of the oesophagus that is seen in the image shown above. Taken from: Beers, MH. and Berkow, R (2000) *Chapter 34, Tumors of the Gastrointestinal Tract, The Merck Manual of Diagnosis & Therapy* [Internet]. Whitehouse Station, New Jersey, Merck & Co., Inc. Available from: www.merck.com. [Accessed 02/11/2005].

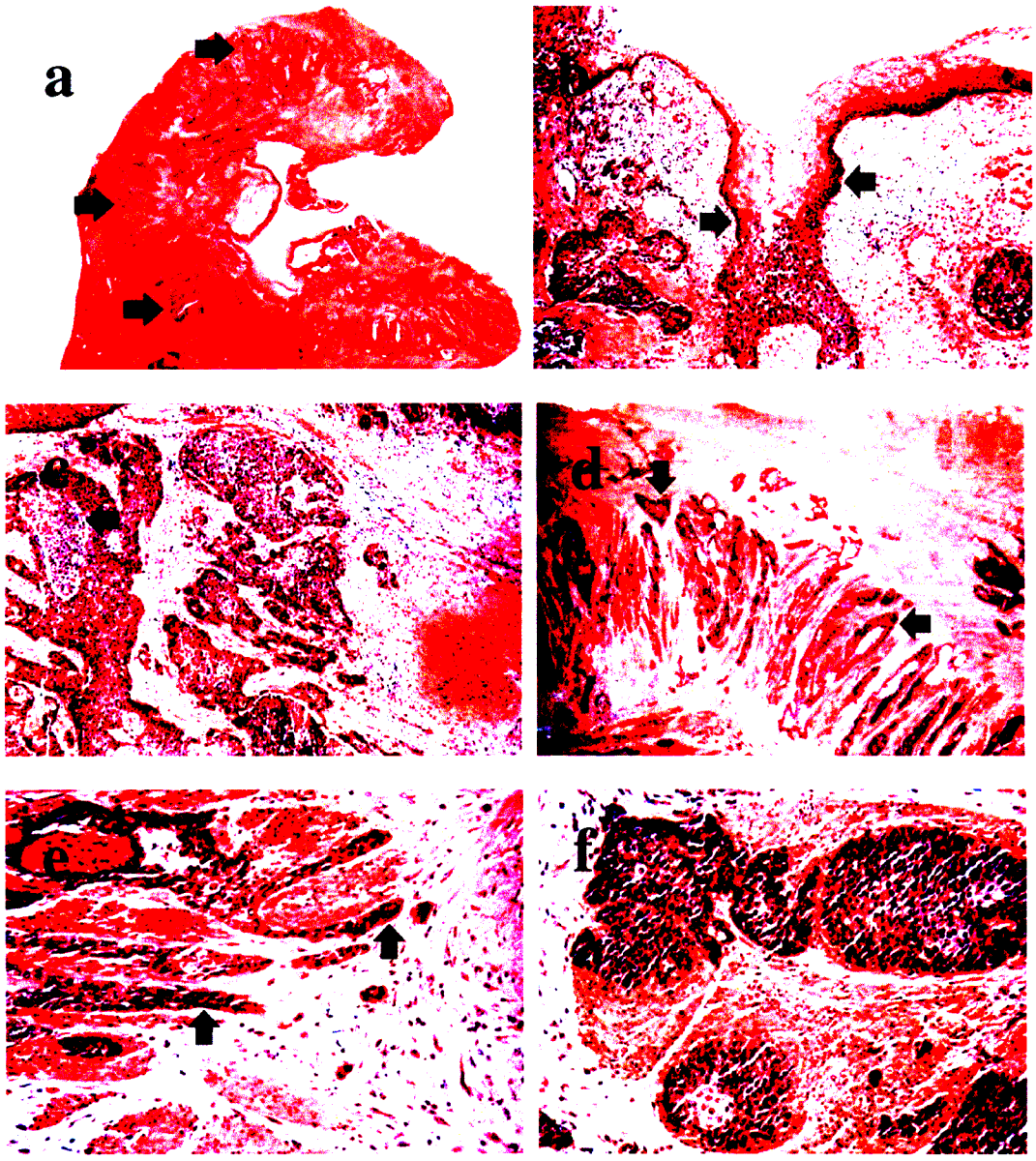

Figure 3: Low power photomicrographs of the oesophagus at various stages of squamous cell tumourigenesis, with features indicated by solid black arrows. (a) The area of constriction shown in this micrograph shows extensive invasion of tumour into the oesophageal wall. (b) Junction between native oesophageal squamous mucosa and the origin of the contiguous invasive carcinoma. (c) Areas of tumour cells that show central necrosis are indicated by the arrow. (d) Groups of tumour cells begin to invade the adjacent lamina propria. (e) Bands of tumour cells

begin to invade the muscularis propria. (f) The tumour moves to adjacent muscularis propria. Taken from: (2005) *Cancer and Tumors, Cancer of the Esophagus* [Internet], Available from: http://www.emedicinehealth.com/articles/ [Accessed 02/11/2005].

1.2 Adenocarcinoma of the oesophagus

Adenocarcinoma of the oesophagus is more common in the Western World, especially among Caucasian population groups. It has been reported extensively that primary adenocarcinomas are almost exclusively a result of Barrett's oesophagus. The latter is a condition, which occurs as a result of chronic gastro-oesophageal reflux disease. The effect of stomach acids on the stratified squamous epithelium that lines the oesophagus is dramatic: The cells become columnar, glandular and similar to that found in the stomach lining, resulting in what is termed an intestinal metaplasia. This process takes place during the healing period of acute oesophagitis. Subsequent dysplasia has been found to be associated with the development of oesophageal adenocarcinoma. This was demonstrated by Sampliner (1998), where increasingly severe dysplasia corresponded to an increase in patients who developed cancer.

Figure 4 below shows an adenocarcinoma of the oesophagus:

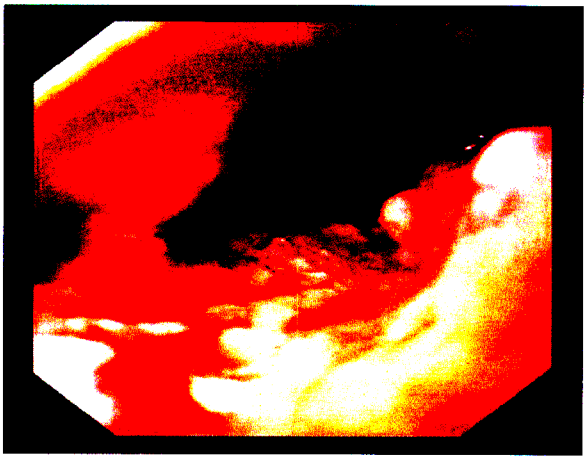

Figure 4: Adenocarcinoma of the oesophagus. Taken from: Beers, MH. and Berkow, R (2000) *Chapter 34, Tumors of the Gastrointestinal Tract, The Merck Manual of Diagnosis & Therapy* [Internet]. Whitehouse Station, New Jersey, Merck & Co., Inc. Available from: www.merck.com. [Accessed 02/11/2005].

1.3 Prognosis, therapeutic and diagnostic strategies: an overview

The prognosis for patients with oesophageal cancers is particularly poor, with a long-term survival rate of less than 5%. Therapeutic strategies are based on numerous factors, such as accurate tumour staging and grading, location and the precise determination of tumour size. These basic assessments are often lacking in resource-poor health settings, and may therefore affect any treatment decisions taken.

The treatment options for OSCC include surgical resection and/or radiotherapy and chemotherapy. The surgical treatment of OC is discussed in greater detail later in the chapter. The size and stage of the tumour and the surgical experience available will often

determine the type of surgery that is to be performed. A complete or *En Bloc* resection, with the intended outcome being a cure, would require the complete removal of all tumour tissue, as well as the proximal and distal margins of normal associated tissue. In addition, all potentially cancerous lymph nodes must be removed, as well as a portion of the distal stomach. *En Bloc* resection requires gastric pull up, oesophagogastric anastomosis, small-bowel interposition or colonic interposition. Because an oesophagectomy results in bilateral vagotomy, pyloroplasty is required to ensure efficient gastric drainage (Reed, 1999).

Surgery is associated with a high mortality rate. In addition, a complete surgical resection is found to be less effective in patients over the age of 75. The same can be said for those patients that present with tumours that extend through the oesophageal wall, lymph node metastases, less than 40% cardiac ejection fraction, and a forced expiratory volume of less than 1.5 litres. However, palliative surgery is successful in that more than 90% of patients are thereafter able to consume a soft to solid diet (Crofts, 2000).

The accurate staging of tumours is critical to the type of therapeutic strategy that needs to be employed. The following methods are in current use, and a critical assessment of their efficacy in diagnosis of the disease is presented below:

1.3.1 Computed tomographic scanning

Computed tomographic (CT) scanning, whilst being the most frequent type of staging tool used in use, has been found to be inefficient in assessing T status in patients. It is also not very accurate in determining regional lymph node metastases. Studies have reported that in more than 40% of cases, CT scanning underestimates tumour stage (Reed, 1999). With regard to T status assessment, the accuracy was reported to range between 55% and 63% (Sondenaa *et al.*, 1992 and Consigliere *et al.*, 1992).

1.3.2 Endoscopic ultrasonography

Endoscopic ultrasonography (EUS) allows for a 360° view of the oesophageal wall and its component layers, and is considered to be the most accurate, non-invasive method for T and N staging of tumours (Reed, 1999). Numerous studies have reported on the accuracy of EUS as a staging tool, where the technique was found to be more effective than CT scanning (Ziegler K *et al.*, 1991; Botet *et al.*, 1991; Tio *et al.*, 1989; Grimm *et al.*, 1993 and Vilgrain *et al.*, 1990).

1.3.3 Thoracoscopic and laparoscopic staging

Studies using the method of thoracoscopic and laparoscopic staging are accurate in the identification of lymph node metastases (Krasna *et al.*, 1996 and Luketich *et al.*, 1997). The major drawback of this technique is its invasive nature, which involves general anaesthesia and hospital stay. The technique is still in development, and studies are being conducted so as to verify its feasibility.

1.3.4 Positron emission tomography

Positron emission tomography (PET) as a diagnostic tool is being investigated as an addition to what is currently used. Studies thus far have been able to detect previously unsuspected metastatic cancer in almost 20% of patients that had previously been regarded as candidates for surgical resection (Block *et al.*, 1997 and Luketich *et al.*, 1997).

1.4 The oesophageal cancer tumour staging system

Oesophageal cancer is classified in accordance with the guidelines that have been laid out in the 2002 American Joint Committee on Cancer tumour-node-metastasis (TNM) classification system (Table 1). The current guideline was upgraded from an earlier version to include the number of regional and distal positive nodes in the staging of tumours. It was thought that whilst the current system was adequately expanded in the description of tumour invasion in the oesophageal wall (T status), better descriptors of regional lymph node (N status) and distal (M) metastases were required (Urba *et al.*, 2001 and Swanson *et al.*, 2001).

This involved the quantification of positive nodes detected, their locations, and defining their overall prognostic value. Furthermore, the number of metastatic lymph nodes, which is normally considered by most surgeons to be an important indicator of survival, has been included in the current staging system (Enzinger and Mayer, 2003; Fein R *et al.*, 1985; Marriette *et al.*, 2001 and Hori *et al.*, 1997).

Table 1: The TNM staging system for oesophageal cancer*

T status Tis Carcinoma *in situ* T1 Tumour invading lamina propria or submucosa T2 Tumour invading muscularis propria T3 Tumour invading adventitia T4 Tumour invading adjacent structures
N status N0 No regional lymph node metastases N1 Regional lymph node metastases
M status M0 No distant metastases M1 Distant metastases
Tumours of the lower oesophagus M1a Not applicable M1b Non-regional lymph nodes and/or other distant metastasis
Tumours of the mid-thoracic oesophagus M1a Metastasis in cervical nodes M1b Other distant metastasis

*Table 1 has been adapted from Reed, 1999.

Following diagnosis of OC in a patient, the information is combined to give a certain stage of tumour and disease development. Table 2 that follows is a representation of this:

Table 2: Stage Grouping*

Stage 0	Tis	N0	M0
Stage I	T1	N0	M0
Stage IIA	T2	N0	M0
	T3	N0	M0
Stage IIB	T1	N	M0
	T2	N1	M0
Stage III	T3	N1	M0
	T4	Any N	M0
Stage IV	Any T	Any N	M1
Stage IVA	Any T	Any N	M1a
Stage IVB	Any T	Any N	M1b

* information sourced from Greene *et al.* (Eds.) , 2002.

1.5 Oesophageal cancer by stage

Stage 0, the earliest stage in OC, refers to the condition where the carcinoma is *in situ*, i.e., the tumour is limited to the epithelial layer of the oesophageal wall, or the innermost lining of the oesophagus.

In Stage I the cancer has invaded other layers of the oesophageal wall, such as the lamina propria or the submucosa. At this stage the cancer has not spread to the muscularis propria, or to regional and distant lymph nodes.

In stage IIA, the cancer has spread into the muscularis propria, and has also invaded the adventitia. However, lymph node metastasis has not yet occurred. Stage IIB is similar, except that the cancer has not spread to the adventitia, and can also be found in regional lymph nodes. Metastasis to other organs has not occurred.

Stage III is characterised by tumour invasion of the entire oesophageal wall into surrounding organs, such as the trachea and lungs. The cancer may have also spread to regional lymph nodes, but not to distant nodes or organ sites.

At Stage IV, the cancer has spread to distant organs and lymph nodes. Depending on the location of the primary tumour in the oesophagus, metastasis to non-regional lymph nodes can be considered to be distant metastases.

1.6 The surgical treatment of oesophageal cancer

Surgical removal is the most common option for patients with early stage OC. There are different strategies employed, and surgical techniques vary in terms of the benefits and drawbacks they may offer to patients. Oesophagectomy refers to the removal of part of the oesophagus that contains the tumour, as well as surrounding normal tissue and lower distal

part of the gastro-oesophageal junction. A gastric pull-up is then performed, where the stomach is re-attached to the remainder of the oesophagus. This is commonly achieved via the transthoracic or the transhiatal approach. An example of a transthoracic surgical procedure would be the Ivor-Lewis oesophagogastrectomy. The surgeon using this method would make incisions in the right thorax and abdomen (right-transthoracic), with the anastomosis situated in the upper chest (Crofts, 2000). Another right-transthoracic approach may be used for primary tumours located higher up the oesophagus, and this involves placing the anastomosis in the neck. The technique is also known as the three-field or Mckeown method (Reed, 19990 and Allum *et al.*, 2002). The transhiatal technique involves abdominal and left cervical incisions and avoids a thoracotomy (Bains, 1995). The anastomosis is always placed in the neck during the latter procedure. The other methods include a left thoracic and left thoracoabdominal oesophagogastrectomy (Reed, 1999).

1.7 The aetiology and epidemiology of oesophageal squamous cell carcinoma

The aetiology and epidemiology of OSCC is not well understood. However, recent advances have observed important changes to the profile of the disease. Most notably, epidemiological studies in the western world show the disease to be associated with lifestyle (Enzinger and Mayer, 2003).

OSCC is associated with a number of risk factors. These include environmental and physiological conditions, and thus far, no single agent has been explicitly indicated as the

cause of cancer development. OSCC, like most other cancers, have a number of factors that impact on the development of the disease. In the western world, OSCC has been described as a disease that affects the elderly, with the majority of cases being diagnosed after the age of 65 (Blot, 1994). In the last decade or so, the molecular aspects of this disease have been more intensively studied in OSCC 'hotspots' around the world. The very high frequencies of OSCC among these populations are not always clearly associated with any known combination of risk factors. This has lead to the conclusion among many investigators that there may be a molecular basis for tumourigenesis within these geographical locations. This will be discussed later in the chapter.

1.7.1 Dietary factors

Certain dietary factors have been shown to be a risk factor in the development of OSCC. In particular, nitrosamine compounds in food sources are known to predispose consumers to the disease (Wu *et al.*, 1993). These carcinogens arise out of food sources being contaminated with the fungus *Fusarium moniliforme*, and several investigators have reported a link between such contamination and OSCC (Schoental and Joffe, 1974; Marasas *et al.*, 1979 and Isaacson, 2005). Experimentally, OSCC has been induced in rats by the application of test nitrosamine compounds, and is regarded as evidence for the carcinogenic role of such chemicals (Gurski *et al.*, 1999). There is, however, no such specific evidence in humans to date. Among black males in South Africa, a link has been drawn between the consumption of maize products and the development of OSCC (Isaacson, 2005). This is related to a change from sorghum to maize as a staple diet. It is

known that maize supports the growth of fungal contaminants to a greater extent than sorghum. In addition, the traditional beer that is fermented from maize has been described as a risk factor (Isaacson, 2005).

1.7.2. Alcohol consumption

Reports indicate that alcohol consumption, especially when combined with smoking, is a major risk factor associated with the development of OSCC and to a limited extent, adenocarcinoma as well (Allum *et al.*, 2002). Many studies have detailed the correlation between increasing risk of OSCC development and increasing alcohol consumption (Hu *et al.*, 1994; Rolon *et al.*, 1995; Castelletto *et al.*, 1994; Stoner and Gupta, 2001; Yokoyama *et al.*, 2002 and Wu *et al.*, 2005).

1.7.3. Tobacco consumption

Chemical carcinogens that are found in tobacco smoke include nitrosamines, polycyclic aromatic hydrocarbons, phenols and various other chemical compounds, and are highly damaging to exposed human mucosa. All of these compounds are associated with an increase in OSCC (Tuyns *et al.*, 1980 and Ribiero *et al.*, 1996). Consuming alcohol whilst smoking or chewing tobacco also allows for ethanol to act as a solvent for tobacco-related carcinogens. This may facilitate the penetration of the oesophageal mucosa by these compounds (Yokoyama *et al.*, 2002 and Wu *et al.*, 2005). Smoking may also contribute to the increased mutagenesis of key genes that regulate the cell cycle process, thereby

playing a role in the development of cancer (Biramijamal *et al.*, 2001 and Ahrendt *et al.*, 2000).

1.7.4. Human papilloma virus infection

The role of human papilloma virus (HPV) infection as a risk factor has been demonstrated in OSCC 'hotspot' areas (Syrjanen, 2002 and Farhadi *et al.*, 2005). HPV types 16 and 18 are already known to be the primary risk factor associated with cervical cancer (Munoz *et al.*, 2003). Lately, roles for HPV sub-types in the development of other cancers have also been established. With regard to OC, these reports portray a mixed picture in terms of the risk associated with HPV. DNA-based detection of HPV variants in oesophageal tissue, including, normal and cancerous, has been used to provide evidence of HPV involvement in tumourigenesis (Chen *et al.*, 1994; Syrjanen, 2002 and Farhadi *et al.*, 2005). This has yielded different results from varying geographical locations (Syrjanen, 2002). The trend that has emerged, however, is that high levels of HPV variants are often associated with OC 'hotspots' around the world. These high-risk areas include eastern South Africa, China and Iran (Saidi *et al.*, 2000; Syrjanen, 2002 and Farhadi *et al.*, 2005).

1.7.5. Irritation of the oesophagus through chemical and other agents

Any substance that causes mucosal inflammation or chronic irritation of the oesophagus, may lead to an increased risk for the development of OSCC (Enzinger and Mayer, 2003). Lye, a strongly corrosive chemical that is found in household cleaners, may increase the risk of OSCC development in children who accidently swallow lye-containing substances

(American Cancer Society, Cancer Facts & Figures, 2004). Other substances, such as caustic soda, may be extremely damaging to the oesophageal wall. Indeed, OSCC may develop more than 40 years after a single episode. (American Cancer Society, Cancer Facts & Figures, 2004). [Internet]. Available from: http://www.americancancersociety.com. [Accessed 02/112005].

1.7.6. Conditions that predispose patients to OSCC development.

1.7.6.1 Plummer-Vinson syndrome

The condition describes a combination of abnormalities that include oesophageal webs, dysphagia and anaemia. The syndrome may also be associated with abnormalities in a number of other organ sites (Larsson *et al.*, 1975 and Enzinger and Mayer, 2003). According to the American Cancer Society, 1 in 10 patients with the syndrome go on to develop OSCC (American Cancer Society, Cancer Facts & Figures, 2004). [Internet]. Available from: http://www.americancancersociety.com. [Accessed 02/112005].

1.7.6.2 Achalasia

Achalasia refers to the condition whereby the lower oesophageal sphincter does not relax sufficiently enough to allow food to pass through into the stomach. This results in food being retained in the lower oesophagus, leading to dilation in that region. The patient suffering from achalasia will also typically experience difficulty in swallowing food (American Cancer Society, Cancer Facts & Figures, 2004). [Internet]. Available from: http://www.americancancersociety.com. [Accessed 02/112005]. It is not well established

as to how achalasia increases the risk for OSCC, but more than 6% of achalasia patients go on to develop the disease (Sandler *et al.*, 1995).

1.7.6.3 Epidermoid carcinoma of the head and neck

People with a history of head and neck cancers are more likely to have OSCC, because both conditions are strongly associated with tobacco and alcohol consumption (Enzinger and Mayer, 2003). In a report in which OSCC had been previously unsuspected, 2% of head and neck cancer patients were found to have the disease (Erkal *et al.*, 2001).

1.8 The molecular basis for the development of cancer: an overview

Cancer is a disease that arises out of certain molecular processes that have more recently been well documented. The disease is also slow to progress, with the time from the precancer stage to the detection of a solid tumour, approximately 20 years (Loeb *et al.*, 2003). The normal-precancer-cancer sequence of development was observed early on, and epidemiological studies postulated that there were a number of rate-limiting steps in the progression through the cancer development sequence (Peto, 1982). It is thought that these rate-limiting steps represent mutations of certain key genes that are important in the overall regulation of cell growth. Furthermore, these mutations would result in the aberrant functioning of genes responsible for apoptosis, cell cycle progression and genetic stability (Sherr, 2000; Loeb *et al.*, 2003 and Martinez *et al.*, 2003). The genetic basis for cancer is thought to occur via two possible pathways *viz.*, clonal evolution and the mutator phenotype hypothesis. These mechanisms may, or may not, be mutually exclusive.

1.8.1 Clonal evolution

Investigators into the biology of cancer have, over the years, come to understand that the disease is the result of a series of molecular events that may occur in concert, or as initially isolated events. An isolated or random mutation in a gene may provide a developing pre-cancerous cell with a selective advantage over normally replicating cells, and thus lead to its eventual clonal propagation (Nowell, 1976). Such mutations are commonly reported in all cancers.

1.8.2 The mutator phenotype hypothesis

The mutator phenotype hypothesis is another accepted model for the molecular development of cancer. The prevailing view is that normal mutation rates would be insufficient in creating the large number of mutations that are reported in all cancer types. Mutations that would act to increase the overall rate of mutations can account for the type of mutation rate seen in tumour cells (Loeb *et al.*, 2003).

This hypothesis was originally proposed in the DNA mismatch repair gene model. These genes are responsible for maintaining a very high level of fidelity during DNA replication. Mutations in such genes lead to 'DNA slippage', whereby an incorrectly incorporated nucleotide would create a frameshift mutation or single nucleotide polymorphism (SNP). These SNP's are a result of DNA mismatch repair enzymes themselves incurring loss of function (Naidoo *et al.*, 2005). Such aberrations have been well documented in hereditary

nonpolyposis colorectal cancer (HNPCC) where it is estimated that more than 100, 000 microsatellite markers in any given HNPCC genome is highly polymorphic for length. These genetic aberrations, which are reported as microsatellite instability and loss of heterozygosity, are a result of mutations in mismatch repair genes (Ionov *et al.*, 1993; Fishel *et al.*, 1993 and Brentnall *et al.*, 1996).

In addition to the above mechanisms, other genes that control important cellular processes, have also been found to impact cancer development through a mutator phenotype process (Kallioniemi *et al.*, 1992).

1.9 The process of carcinogenesis

Carcinogenesis is a complex series of genetic and molecular changes that occur as a result of stimulation *via* chemical or physical means. (Hennings *et al.*, 1993) have discussed the process as consisting of three distinct stages *viz.*, initiation, promotion and progression. Initiation is characterised by an irreversible change in a gene or group of genes. These include point mutations, insertions and deletions. Promotion is the propagation of cells that have been 'initiated' into a mutational event, and progression is the accumulation of cells with genetic mutations that eventually leads to tumour growth. When carcinogenic chemicals have been applied to mouse models, it was found that there were three main steps in the initiation stage of chemical carcinogenesis: carcinogen metabolism; DNA damage and repair; and cell proliferation (Hennings *et al.*, 1993).

The process of initiation has been well studied in mouse models using chemical mutagens. These carcinogens, once metabolically activated, are strong electrophiles which disrupt the DNA through covalent binding. The resultant carcinogen-DNA adducts are then subjected to DNA repair processes. The subsequent failure of efficient DNA repair results in the accumulation of genetic errors in dividing cells. This in turn may result in genes downstream being inactivated (Nelson *et al.*, 1992 and Minamoto *et al.*, 1999).

The promotion stage can be observed with the addition of a chemical that stimulates the proliferation of previously initiated cells(Martinez *et al.*, 2003). This stage of chemical carcinogenesis favours the clonal selection of mutated cells that are pre-tumour (Martinez *et al.*, 2003). In addition, promotion is also reversible, since removal of chemical agents may lead to the prevention or reduced frequency of tumour formation (Iwamoto *et al.*, 2000).

1.10 Epigenetics and cancer

Epigenetics may be defined as a process by which cellular behaviour is affected by something apart from mutational events (Lam, 2000). Usually, a mutation in the coding region of an important gene is detectable *via* resultant phenotypic and genotypic characteristics. However, genes may be 'silenced' in other ways that do not involve a direct mutation. The loss of expression of a gene in this manner is termed 'epigenetic silencing'. Epigenetic events regulate gene expression and are also important in early embryonic development (Martinez *et al.*, 2003).

The most widely reported epigenetic event is DNA hypermethylation (Holliday, 2005). This occurs when a methyl group is added to position 5 of the ring of cytosine in a CG base pair sequence (Holliday, 2005 and Myers and Ries, 1989). Regions of DNA in the 5' promoter regions of almost 50% of known human genes are thought to contain so-called 'CpG islands', or regions of CG sequences that are hypermethylated (Martinez *et al.*, 2003). *De novo* methylation, or methylation of normally unmethylated DNA is usually associated with a tumourigenic event, since patterns of hypermethylation in CpG islands are thought to be inherited (Holliday, 2005).

Hypermethylation suppresses gene expression. This may be important in early embryonic development as certain genes are switched on and off through silencing (Holliday, 2005). In cancerous or pre-cancerous cells, DNA hypermethylation is often evident, with certain genes showing CpG hypermethylation and increased histone deacetylase activity (Baylin, 2001). Histone deactylases are sequestered by CpG-methyl binding proteins, resulting in condensation of chromatin structure around the hypermethylation site (Baylin, 2001). Ultimately, the genes associated with these methylated sites are left unavailable to transcription factors, etc., resulting in the 'epigenetic silencing' of the gene.

There are numerous hypermethylated genes that are reported to be silenced or linked in some way to the progression of cancer. A number of studies have investigated these genes, because their silencing often leads to a loss of cell cycle control, genetic instability and

altered cell-cell interactions in a variety of cancers (Hiltunen *et al.*, 1997; Kane *et al.*, 1997 and Nass *et al.*, 2000).

1.11 The molecular basis of oesophageal squamous cell carcinoma development

The process of tumourigenesis in OSCC would likely follow a similar developmental mode to that seen in other cancers, since the basis of all cancer initiation seems to be an accumulation of genetic and epigenetic events. The molecular biology of OSCC is important, since diagnosis and prognosis *via* the TNM staging system is limited to the expertise of the clinician, and the health resource setting that they may find themselves in. Furthermore, since most patients with OSCC are diagnosed at a relatively late stage of disease progression, the prognosis is invariably poor.

Molecular research into the aetiology and pathogenesis of the disease might therefore be useful in providing better diagnostic tools, as well as possible gene therapy targets. The precise mechanisms that govern the metaplasia-dysplasia sequence of events in OSCC need to be well studied at the molecular level before such tools can be identified.

Like other cancers, OSCC development is influenced by tumour suppressor genes (TSG), oncogenes, apoptosis-related genes, and genetic events such as microsatellite instability (MSI) and loss of heterozygosity (LOH) (Lehrbach *et al.*, 2003 and McCabe and Dlamini, 2005). There are also some reports that describe a clustering of the disease amongst communities in regions of the world that are known high-risk areas (Mandard *et al.*, 2000).

These indicate a genetic pre-disposition for the disease among high-risk population groups.

With regard to the specific genetic events that are associated with OSCC, the most commonly observed appear to be mutations of the *p53* TSG, as well as other cell cycle and apoptosis related genes (Mandard *et al.*, 2000; Sepehr *et al.*, 2001 and Lehrbach *et al.*, 2003). More recently, numerous reports have documented these and other such mutational and epigenetic events associated with OSCC. Lam (2000) is of the opinion that few of these studies have sound scientific basis, due to a lack of clinico-pathological data for OSCC specimens that were used in such studies. Histological information is deemed equally important, since OSCC cases consist of a heterogenous mix of tumour types and grades, with each displaying different pathogenic modes, as well as different clinical outcomes (Lam, 2000).

1.11.1 The role of tumour suppressor genes in oesophageal squamous cell carcinoma development

TSGs are defined as recessive genes that result in cancer development when both alleles are lost (Hollywood and Barton, 1994). These genes may function as indirect points of cell-cycle control, in the sense that they often control the expression of proteins that function as cell cycle regulators (Toyoshima and Hunter, 1994 and Sherr, 2000). There are a number of TSGs that have been implicated in tumour development. Such genes, like the cyclin-dependant kinase inhibitors, control the processes of cell proliferation and

dormancy. The importance of cell cycle-related genes in cancer, with a particular emphasis on OSCC and the *p21/p27* genes, will be discussed in more detail later in the chapter.

1.11.1.1 *p53*

The *p53* TSG and its aberrations are the most commonly studied in all human cancers (Lam, 2000). Furthermore, there is a wealth of information with regard to *p53* mutations and OSCC (Lam, 2000). The p53 gene, which is located on chromosome 17, has an open reading frame of 1179 base pairs, and is one of the genes that are responsible for maintaining cell division integrity (Lam, 2000; Lehrbach *et al.*, 2003; Martinez *et al.*, 2003; and McCabe and Dlamini, 2005). The gene does this by one of two pathways:

p53 over-expression may stop the progression of the G1 stage of the cell cycle into G2 if there is DNA damage present. This allows for DNA repair to take place. If the damage is irreparable, *p53* may act to activate the cell apoptotic pathway, leading to the extermination of aberrant cells (el-Deiry *et al.*, 1993; el-Deiry *et al.*, 1994; Kato *et al.*, 2000 and Sherr, 2000). *p53* is not required for normal development, as demonstrated by mutagenic studies, but seems to be activated in times of cell stress (el-Deiry *et al.*, 1994). The gene is known to respond to a variety of cellular stresses, including genotoxic stress, redox fluctuation, cell adhesion changes and oncogenic pressure (Martinez *et al.*, 2003). The maintainance of low *p53* levels under normal cell conditions is achieved through ubiquination and proteosome-mediated degradation, and an important gene in this process is *MDM2*. By binding to the N-terminus of *p53*, the gene becomes targeted for degradation. When ionising radiation, for example, is applied, a series of phosphorylation

events take place in the N-terminal region of *p53*. This in turn would prevent *MDM2* binding, resulting in a spike in cellular *p53* levels (Sherr, 2000 and Lehrbach *et al.*, 2003). Activation of the *p53* gene involves pathways that are complex in nature and diversity, as might be expected from the various stimuli and downstream effector genes that *p53* interacts with. Various agents, both chemical and physical, may seek to interfere with *p53* levels under stress conditions, and *p53* mutational events are often a result of these stresses.

Numerous types of *p53* gene inactivation have been described. The most widely reported involve actual mutations of the gene. The first is a mutation in the coding region of the gene that generates events such as single nucleotide polymorphisms (SNPs) or point mutations (Lehrbach *et al.*, 2003). Such mutations lead to a non-functional protein product that accounts for more than 50% of sporadic human tumours (Lam, 2000). *p53* mutations may also be inherited in the normal mendelian fashion, leading to conditions such as Li-Fraumeni syndrome (Hollywood and Barton, 1994). Inactivation of *p53* might also occur via non-mutational pathways. Such epigenetic silencing may be a result of hypermethylation, but more commonly involves viral proteins when cancer is involved. The HPV-E6 gene product has been observed to eliminate *p53* via 26S proteosome-mediated degradation. The *p53* protein has also been shown to occur in a bound state with SV40 viral particles, resulting in its effective removal from cell stress-related duties (Stoner and Gupta, 2001).

Another way in which *p53* is functionally inactivated is by physical removal of the gene product from the site of action. This involves sequestration of the protein into distinct cytoplasmic locations, which prevents *p53* entry into the nucleus. Access to genes that are responsible for mounting a cellular response to genotoxic stress is thus prevented (Sherr, 2000).

A significant proportion of *p53* mutations occur within four conservative domain regions spanning exons 5 and 8 of the gene (Lam, 2000). Very few, or none, are reported to occur in other exons. Notable exceptions include one each found in exons 10 and 11 respectively (Casson, 1998 and Wagata *et al.*, 1993). It has been found that the SNPs associated with *p53* are distributed geographically. In the developed world, such point mutations are found to occur evenly across exons 5 through 8, with the highest frequency observed at codons 175 and 278 (Wagata *et al.*, 1993). In areas of China that are known to be high-risk for OSCC, codon 175 in exon 5 displays the highest frequency, whilst in Taiwan and nearby Hong Kong, mutations were detected with the highest frequency in exons 6, 7 and 8 respectively (Wang *et al.*, 1998). These mutations are thought to offer selective growth advantages and are associated with the progression of the disease to an invasive state (Wang *et al.*, 2003a).

In adenocarcinoma of the oesophagus, it is reported that up to 85% of *p53* mutations occur at GC→AT transition points, with approximately 69% occurring at CpG rich islands (Wang *et al.*, 2003b).

Studies done in North America and Europe have shown that G→T substitutions in *p53* are significantly linked to smokers (Montesano *et al.*, 1996). It is important to note that the same mutations occur at similar frequencies between smokers and non-smokers in China, and possibly other high-risk OSCC regions of the world (Lam and Ma, 1997 and Bennett *et al.*, 1997). This trend firstly reflects the ethnic diversity with which OSCC occurs. Secondly, geographic variability of *p53* mutations may also highlight the effect that differing environmental factors may have on disease initiation and outcome. In their investigation, Lam *et al.* (1997) found a shorter survival rate that positively correlated with increased *p53* mutations. In addition, they reported that the relationship between OSCC and *p53* aberrations varied according to ethnicity.

The presence of *p53* mutations may be a particularly important prognostic indicator in OSCC. In *p53* mutated-OSCC, the disease is found to be chemotherapy (Wang *et al.*, 2003a).

1.11.1.2 Other tumour suppressor genes

Other genes apart from *p53* that are related to the cell cycle, *viz.*, *p21*, *p27*, *p15*, *p16* and *Rb*, have been reported to play a similarly important role in OSCC. The *p21/p27* family of cyclin-dependant kinase (cdk) inhibitors is discussed in detail later in the chapter.

TSG's that are not directly involved in the cell cycle have also been investigated in OSCC. These include the *MCC*, *APC* and *DCC* genes, which have been shown to be mutated or functionally lost in other human cancers. The *MCC* and *APC* genes are both located at

chromosomal position 5q21, and display a number of sequence similarities (Ashton-Rickardt *et al.*, 1991). The *APC* gene, which is associated with familial adenomatous polyposis coli, is most frequently associated with colorectal tumours in its deleted or mutated form.

APC is suspected to be lost to a certain extent in OSCC, as demonstrated by LOH studies (Boynton *et al.*, 1992). The data is conflicting however, as other investigators have observed no significant mutational events in the *APC* gene amongst the OSCC cases analysed (Ogasawara *et al.*, 1994).

The *DCC* gene, which is significantly diminished or functionally absent through mutation in colorectal cancers, may also play a role in OSCC. Some reports have observed tenuous correlations between *DCC* mutated genotypes and disease progression and outcome (Miyake *et al.*, 1994; Chetty *et al.*, 1998 and Ramburan *et al.*, 2004). In particular, Ramburan *et al.* (2004) found that multiple aberrations of the *DCC* locus played a role in the progression of nephroblastomas. These researchers found a significant correlation between frequent LOH and unfavourable histology in tumours. Furthermore, aberrations in more than one *DCC*-related marker were found in all patients who had died.

In hereditary breast cancer, the *BRCA1* gene is famously mutated in almost all known cases, and has provided new gene therapy and drug-based targets in the treatment of the disease. With regard to OSCC, aberrant *BRCA1* is much less commonly found, with a

limited number of reports describing links between the gene and disease (Mori *et al.*, 1994).

1.11.2 Apoptosis-related genes

Apoptosis is defined as a distinctive form of cell death, in which single cells are deleted amongst normal cells, and is of particular importance in human cancer (Cooke and Stanton, 1994). It has been observed that cancer cells respond to chemotherapy and/or radiotherapy in different ways. One of the features of OSCC is that spontaneous apoptosis can be induced by such therapy (Ohbu *et al.*, 1995; Moreira *et al.*, 1995; Hamada *et al.*, 1996; Ohashi *et al.*, 1997 and Shears *et al.*, 1998).

The *bcl-2* apoptotic regulatory gene, which has been widely investigated, is an inhibitor of apoptosis. Proteins from the *bcl-2* family may act in either a pro-apoptotic or anti-apoptotic manner. *bcl-2* over-expression was found to occur in OSCC, ranging from 33% to 74% of patients studied, (Ohbu *et al.*, 1995; Puglisi *et al.*, 1996; Parenti *et al.*, 1997; Ohbu *et al.*, 1997 and Sarbia *et al.*, 1998a). Further, other proteins of the *bcl-2* family have been studied, and include the *bax* and *bcl-*X_L proteins. These were observed to be over-expressed in 100% and 53% of OSCC cases respectively (Sarbia *et al.*, 1998a).

1.11.3 Oncogenes and oesophageal squamous cell carcinoma

Oncogenes are defined as those genes that, when expressed, have the potential to transform normal cells into cancer cells (Hollywood and Barton, 1994). These genes are

derived from their normal counterparts, but become oncogenic in nature through the process of mutation. Activated oncogenes are thought to reduce a cells apoptotic potential (Martinez *et al.*, 2003).

There are a number of identifiable classes of oncogenes that are categorised according to their physiological function and location. These include growth factors and their receptors: membrane associated guanine nucleotide-binding proteins; various kinase proteins as well as a number of other cellular proteins (Martinez *et al.*, 2003). The growth factors and their receptors are an important and widely studied class of oncogenes, as a result of being intimately linked to the process of cell proliferation (Sherr, 2000).

EGF, *TGF*, *α* and *c-sis* are oncogenic growth factors that are thought to play a role in OSCC development (Wong *et al.*, 1994; Jones *et al.*, 1993 and Yoshida *et al.*, 1990). Other oncogenes, such as *hst-1* and *hst-2*, as well as *cyclin D1*, have been shown to be over-amplified *in vitro*. It appears that *cyclin D1* is most important with regards to OSCC, since that gene alone is over-expressed (Lam, 2000).

Growth factor receptors, which are trans-membrane proteins that receive extracellular signals, are another class of oncogenes that has been studied (Hollywood and Barton, 1994). The genes *erbB-1* and *erbB-2* are growth factor receptors, and their over-expression in OSCC is found in a significant proportion of cases. Such studies have reported frequencies of between 30% and 90% (Ozawa *et al.*, 1989 and Hirai *et al.*, 1998). In particular *erbB-1* over-expression has been correlated with a decrease in the 5-year

survival rate. Since high expression of *erbB-1* is associated with poor prognosis, its detection may allow surgeons to make better choices with regard to the best surgical procedure, preferably one that is the least invasive (Hirai *et al.*, 1998).

Another class of oncogenes are the nuclear-associated factors. Cell cycle-related oncogenes, such as *cyclin D1*, fall into this category. *Cyclin D1* is an important part of the cell cycle machinery, and forms complexes with cyclin-dependant kinases. These complexes act to regulate passage of cycling cells through various checkpoints, more notably the G1/S phase junction. *Cyclin D1*, if over-expressed, would act to enhance the cell proliferative process, since more cyclin would be sequestered into kinase complexes. The end result would be an increased tumourigenic effect. Over-expression of *cyclin D1* has been demonstrated in OSCC cell lines (Zhu *et al.*, 1996 and Nakagawa *et al.*, 1995). In addition, *Cyclin D1* over-expression has been found to occur in OSCC patients, and more importantly, to be a marker of poor prognosis (Doki *et al.*, 1997; Gramlich *et al.*, 1994 and Ishikawa *et al.*, 1998).

Cyclin D1 is one of the more important oncogenes with regard to OSCC, since gene over-expression has been correlated with lymph node metastases and distant metastases, advanced tumour stage and grade, and a higher proliferative capacity. Other studies have described *E-cadherin*, a cell adhesion molecule, to be associated with OSCC development. An expression profile that displays *E-cadherin* stability and lower *cyclin D1* levels has been observed to be the best prognosis, and *vice versa* (Lehrbach *et al.*, 2003). Data from

many similar reports have led to the conclusion that *cyclin D1* plays a significant role in OSCC.

1.11.4 Chromosomal aberrations and oesophageal squamous cell carcinoma

Aberrations that compromise the integrity of DNA are a common feature of cancer and apoptosis. The latter event is characterized by massive DNA fragmentation and general chromosomal degradation, and usually precedes catastrophic cell death (McCabe and Dlamini, 2005). With regard to cancer, the processes are often more subtle. Mutations that have been discovered in cancer cells include translocations, chromosomal re-arrangements, random insertions, and other such events that are easily identified using standard cytogenetic techniques (Mathew *et al.*, 2001). A number of reports have described various genes that are affected in these ways across various cancer types. Such genetic instability is indeed one of the hallmarks of cancer. At the sequence level, the instability is yet more complex, and may involve epigenetic processes as well. Microsatellite instability (MSI) and loss of heterozygosity (LOH) are some of the mutational processes that have been linked to a number of cancers. MSI and LOH in OSCC is broadly the focus of this dissertation, and an overview is provided in the following subsection.

1.12 Microsatellite aberrations and disease: an historical perspective

Microsatellites are short stretches of DNA that consist of tandemly repeated sequences of one to five base pairs in length. Microsatellites are ubiquitous across genera, and are evenly scattered throughout the genome of an organism, including humans. The role of microsatellites in humans is largely unknown, despite the association of numerous disease states with microsatellite polymorphisms (Bennett, 2000). These tandem repeats are known to be stably inherited and highly conserved. In addition, microsatellite length is unique to each individual, but different between individuals, thereby making them excellent genetic markers (Muc and Naidoo, 2002).

Microsatellites may vary in length, from a few oligonucleotides to several hundred base pairs, with a hundred or so base pairs being the average length (Bennett, 2000). Each tandem repeat sequence may range in length, from the mononucleotides to the pentanucleotides (Muc and Naidoo, 2002). Microsatellite variability between individuals arises out of the DNA mismatch repair system in replicating cells. When the newly replicated strand mispairs with the template strand, the region of mispairing is said to 'loop out' by the number of nucleotides that were missed, usually one to five. If the loop is on the template strand, DNA mismatch repair enzymes act to excise the unpaired loop, resulting in the loss of that repeat unit. If the loop is on the newly synthesised strand, the result is the addition of a repeat unit (Bennett, 2000). The total number of each type of microsatellite decreases with increase in repeat length. This may be due to the theory that

mispairing is less likely to occur over a larger number of nucleotides (Thibodeau *et al.*, 1993 and Bennett, 2000).

The biological function of microsatellites is not well understood in humans. The resulting pathology of their aberrant replication, however, is fairly well documented. In particular, the tri-nucleotide associated diseases are well characterised, and include such conditions such as Huntingtons disease, myotonic dystrophy, as well some types of spino-cerebellar ataxia (Brook *et al.*, 1992; Gusella *et al.*, 1993; Orr *et al.*, 1993 and Schols *et al.*, 1995). The tri-nucleotide repeat diseases are mainly of a neurological nature, and seem to result from the microsatellite expanding outside of the 'allowed' or normal polymorphic range. Such tri-nucleotides usually occur within a gene linked to the disease in question, and results in the inactivation of that gene as a result of moving into the coding region (Debrauwere *et al.*, 1997). If located outside the gene, the instability in the repeat would be sufficient to affect the functioning of the gene. Importantly, the length of the tri-nucleotide repeat seems to correlate positively with disease severity, and therefore outcome. In addition, it is known that the longer a repeat expands, the more sensitive it becomes to further instability (Bennett, 2000). The result for affected individuals in successive generations is earlier disease onset or even an increased severity of disease symptoms (Bennett, 2000).

An interesting point of discussion is the fact that to date, tri-nucleotide repeat associated diseases have only been found in humans. Not even in our closely related primate species, some of which share a 99% sequence homology with the human genome, are these repeats

associated with any disease (Bennett, 2000). The observation that the diseases identified are almost all neurological in nature is equally interesting. This has led to the hypothesis that trinucleotides found in genes that are associated with neurological function, are there as a result of natural selection. Their presence may have conferred a selective advantage to humans in terms of brain function (Bennett, 2000).

1.12.1 Microsatellite alterations in human cancer

To date, microsatellite instability has been used as a tool in identifying sequences where tumour suppressor genes may be located in cancer (Muc and Naidoo, 2002). This involved evaluating LOH, or loss of allelic DNA, in a tumour sample, in comparison with a normal sample. If the tumour sample has lost genetic material in relation to the normal sample, the patient is said to display LOH for that microsatellite marker. LOH that is consistently observed in a large sample size would be indicative of a deletion event. The location of the microsatellite marker would likely be a region of tumour suppressor activity (Oda *et al.*, 1997).

The techniques used to determine such changes have evolved to allow for the simple, accurate and rapid screening of large numbers of markers in a variety of human cancers. Initially, autoradiography and silver staining were used to view the DNA fragments that had been separated in polyacrylamide gels. Later on, a fluorescent-based detection system became the gold standard in studies that were focused on the detection of microsatellite aberrations (Cawkwell *et al.*, 1995; Oda *et al.*, 1997 and Muc and Naidoo, 2002). Briefly,

the technique utilizes fluorescently labelled primers in microsatellite PCR. The PCR products containing bound fluorophore are then detected *via* the excitation of light of a particular wavelength. The resulting flurorescence is recorded as a peak that is directly proportional to the amount of fluorescence emitted by the sample. The comparison with a reference standard allows for the precise size of the microsatellite marker to be determined.

1.13 The cell cycle theory

An important feature of eukaryotic cell survival is its ordered progression through the cell cycle. The cell cycle can be described as the progression of a replicating cell through numerous, rigidly enforced checkpoints, the latter of which are usually located at the transition points between one phase of the cell cycle and the next (Sherr, 2000). With regard to the latter, the system consists of alternating S (DNA synthesis) and M (mitotic) phases, with gap (G) phases in between (Figure 5).

Movement through these checkpoints is a complex process, and is effected, in part, through the assembly, activation and inactivation of specific key protein complexes, known collectively as cyclin dependant kinases, or Cdk's. (Polyak *et al.*, 1994) and (Moller, 2000). These Cdk's consist of two major subunits *viz.*, a kinase subunit with catalytic activity and a cyclin subunit (Ferrando *et al.*, 1996); (Moller, 2000) and (Sherr, 2000).

Towards late G1 phase of the cell cycle, a key area of regulation in the cell cycle occurs, and is known as the restriction point (Polyak *et al.*, 1994). Once the cell cycle has progressed beyond this point, it is said to proceed autonomously (Polyak *et al.*, 1994); (Moller, 2000) and (Sherr, 2000). Movement through the restriction point, which occurs at the G1-S phase transition, is regulated by a number of different pathways, in particular the Retinoblastoma tumour suppressor gene (*Rb1*) pathway (Sherr, 2000).

The product of this pathway is phosphorylated to form pRb, the process of which is triggered by the accumulation of cyclin E and D-Cdk complexes (Shackelford *et al.*, 1999). Phosphorylation of *Rb* prevents this gene from functioning in its growth-repressive capacity, thereby allowing the cell cycle to proceed past the restriction point (Moller, 2000). This is illustrated in Figure 5.

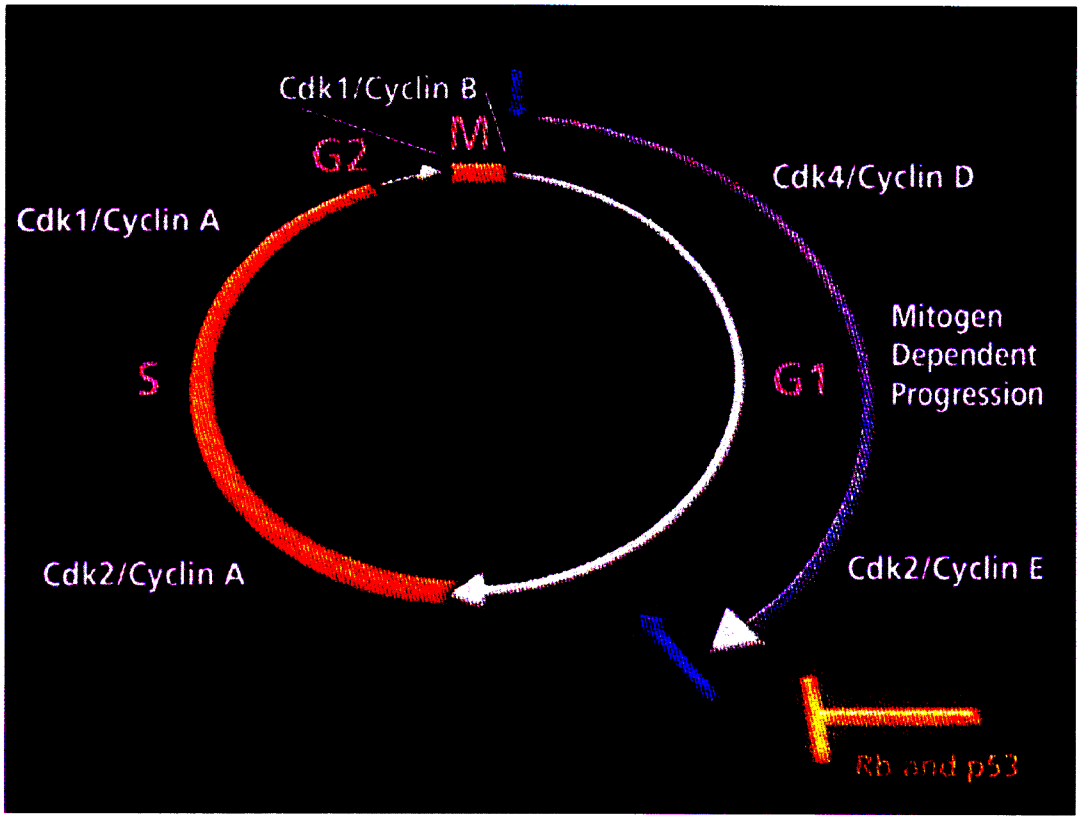

Figure 5: The cell cycle. Taken from the American Association for Cancer Research's newsletter on the conference: Cell Cycle and Cancer: Pathways and Therapies. December 1-5, 2004, Florida.

1.13.1 The Cyclin-Cdk complexes

1.13.1.1 The D-Type cyclins

The D-type cyclins consist of *D1, D2* and *D3* and are found to be active in the G1 and G1-S phase transitions of the cell cycle (Shackelford *et al.*, 1999). These three isoforms are expressed differently amongst various cell types (Matsushime *et al.*, 1991); (Motokura *et al.*, 1991) and (Ajchenbaum *et al.*, 1993).

The cyclin D subunits combine and interact with their distinctive catalytic partners *viz.*, the Cdk's, to produce functional holoenzymes that drive the cell cycle machinery during the G1 and G1-S phase transition. Cyclin D has been shown to be most active in early to mid G1 phase, and requires a continuous stream of mitogenic stimuli in order to maintain its levels and drive cycling cells beyond the restriction point and the G1-S phase transition. This was demonstrated by Matsushime and co-workers (1991), where cycling cells were subjected to a starvation of externally applied growth factors (mitogenic stimuli), resulting in cyclin D levels diminishing rapidly and cells exiting the proliferative stage into the quiescent G0 stage of the cell cycle.

Thus, the assembly of active cyclin-cdk complexes during G1 phase depends on, to a greater extent, the reception and integration of mitogenic stimuli. It has been suggested, on the basis of these and other data, that cyclin D complexes regulate the movement of cells, from the G0 phase into G1 phase and beyond through the G1-S transition point (Ajchenbaum *et al.*, 1993).

Studies on cyclin D1 and D2 'knockout' mice have suggested that the D cyclins exhibit what Shackelford and co-workers (1999) have described as 'functional redundancy'. This refers to the phenomenon of mice remaining viable despite being nullizygous for either cyclin D1 or D2. Studies later conducted on human ovarian and testicular tumours have also shown high cyclin D2 mRNA expression in some of these (Sicinski *et al.*, 1996).

These and other differences, including their tissue-specific expression, occur amongst the D-type cyclins.

The D-type cyclins combine with two distinctive catalytic partners referred to as Cdk4 and Cdk6. Interactions with the latter can lead to the creation of at least six different cyclin-cdk complexes that are identifiable and expressed in a tissue specific manner (Sherr, 2000).

The catalytically active cyclin D-Cdk4/6 complexes require the sequestration of proteins from the Cip/Kip family of Cdk inhibitors in order to form complexes that are capable of phosphorylating the Retinoblastoma (pRb) protein, which thereafter results in the cell cycle being moved through the G1 phase.

1.13.1.2 *Cyclin E* complexes

Another cyclin-cdk complex that plays an important role during the G1-S phase transition of the cell cycle is cyclin E/Cdk2. E2F transcription factors are released when pRb is phosphorylated by cyclin D complexes, allowing for E2F factors to induce the expression of cyclin E and A genes. Once expressed, cyclin E combines with its catalytic partner, Cdk2, to form the activated cyclin E-Cdk2 state. This complex is thought to follow a similar pattern to that observed for cyclin D complexes in terms of broad function, displaying a marked increase in cyclin E expression at the G1-S phase junction (Shackelford *et al.*, 1999).

Unlike the D-type cyclin-Cdk complexes, cyclin E-Cdk2 displays *in vitro* kinase activity towards a wider range of protein substrates, including pRb and Histone H1 (Koff *et al.*, 1992). Studies thus far have shown that cyclin E-Cdk2 complexes drive the cell cycle through S phase, and in addition, it also appears that Cdk2 expression is required for the entry of the cell cycle into S phase (Ohtsubo *et al.*, 1995).

Cyclin E-Cdk2 appears to complete the phosphorylation of pRb, a process that is initiated early on in G1 phase by cyclin D complexes (Sherr, 2000). Interaction between the two cyclin-Cdk types was demonstrated by (Lundberg and Weinberg, 1998) where the selective inhibition of Cdk4, Cdk6 or Cdk2 lead to cyclin D-Cdk4/6 complexes being unable to phosphorylate pRb.

1.13.2 The *pRb/E2F* pathway

The accumulation of cyclin D-Cdk complexes during G1 phase triggers the phosphorylation of the Rb protein, which is itself bound to what are collectively known as the E2F transcription factors (Sherr, 2000). pRb, in its hypophosphorylated state and bound to E2F. This complex therefore functions in a growth-repressive capacity that limits or halts cell cycle progression. As such, the functional role and regulation of either pRb or E2F are inextricably linked.

A large number of studies have described the role that the E2F transcription factors play during the G1-S phase transition. E2F factors regulate a number of key genes that are

either directly or indirectly required by the cell cycle process. These genes include those that code for DNA Polymerase α, proliferating cell nuclear antigen (PCNA), nucleotide biosynthetic activities and DNA repair genes, amongst others (Nevins, 2001). The requirements for the assembly of pre-replication complexes at origins of replication are under the control of E2F (Leone *et al.*, 2001). In addition, E2F is a transcription factor which is critical in directing the expression of cyclin E, A and Cdk2.

Cyclin D-Cdk4/6 complexes and cyclin E-Cdk2 collectively interact in the phosphorylation of pRb-E2F. Cyclin D-Cdk4/6 complexes phosphorylate pRb-E2F, thereby releasing E2F transcription factors that are known to actively promote the expression of cyclin E, amongst other proteins. As part of a functioning cyclin D-Cdk4/6 complex, the $p27^{Kip1}$ Cdk inhibitor is required as a co-factor (LaBaer *et al.*, 1997) and (Cheng *et al.*, 1999). Sherr (2000) is of the opinion that virtually all $p27^{Kip1}$ molecules in cycling cells exist as part of p27-cyclin D-Cdk4/6 complexes. Once cyclin E-Cdk2 complexes are activated, they are able to phosphorylate unbound p27Kip1, altering the conformation of the Cdk inhibitor. In this state, it can be recognized by ubiquitin ligases and targeted for degradation by proteasomes (Pagano *et al.*, 1995). Whilst $p27^{Kip1}$ is being degraded, it is almost simultaneously being sequestered as co-factors into cyclin D-Cdk4/6 complexes. Thus, there is virtually no unbound $p27^{Kip1}$ remaining to function in its growth suppressive capacity as a Cdk inhibitor. Furthermore, the absence of $p27^{Kip1}$ resulting from this process drives the cell cycle irreversibly beyond the restriction point.

1.13.3 The *Cip/Kip* family of Cdk inhibitors

Other aspects of cell cycle regulation include the activity of Cdk inhibitors. These proteins function as inhibitors of the cell cycle process, and are therefore capable of inducing cell cycle arrest. Inhibitor proteins function by binding specifically to a diverse range of cyclin-Cdk complexes, rendering them non-functional (Polyak *et al.*, 1994). These include two classes of Cdk inhibitors.

The first, known as the Cip/Kip family, includes $p21^{Cip1/WAF1}$, $p27^{Kip1}$ and $p57^{Kip2}$ (Harper *et al.*, 1993); (Polyak *et al.*, 1994); (el-Deiry *et al.*, 1993) and (Toyoshima and Hunter, 1994). The second class is known as the INK4 inhibitors, and consists of $p16^{INK4a}$, $p15^{INK4b}$, $p18^{INK4c}$ and $p19^{INK4d}$ (el-Deiry *et al.*, 1994); (Shackelford *et al.*, 1999) and (Sherr, 2000).

1.13.3.1 The *p21 Cip1/WAF1* gene

Harper and coworkers (1993) first identified the Cdk inhibitor *p21 Cip1*, which encodes a 164 amino acid protein of 21 kilo Daltons (kD). This amino acid sequence was found to be identical in sequence and location to the WAF1 inhibitor protein (el-Deiry *et al.*, 1993).The gene that encodes the Cip1 (or WAF1) protein is commonly referred to as *p21 Cip1/WAF1*, and has been localised to the chromosomal region 6p21.2 (el-Deiry *et al.*, 1993). The Cip1/WAF1 inhibitor protein, is transcriptionally activated by the *p53* tumour suppressor gene, and functions as a tumour suppressor (Mousses *et al.*, 1995). It has therefore been suggested that Cip1/WAF1, which functionally occurs as part of a

quarternary complex (cyclin-Cdk and a proliferating nuclear antigen), mediates the effect of *p53* on G1 phase arrest (Mousses *et al.*, 1995).

In addition, Cip1/WAF1 associates with several cyclin-Cdk complexes involving cyclins A, B, D, E and Cdk2, Cdk4, Cdk5 and Cdc2 (Xiong *et al.*, 1993). Cip1/WAF1 acts as a broad, negative regulator of the G1-S phase transition, and therefore plays an important regulatory role in the overall cell proliferation process, leading to tumourigenesis (Harper *et al.*, 1993).

1.13.3.2 The $p27^{Kip1}$ gene

$p27^{Kip1}$ is located at chromosomal region 12p13, and shares many sequence and function-specific similarities with $p21^{Cip1/WAF1}$ (Toyoshima and Hunter, 1994) and (Moller, 2000). The amino terminal of $p27^{Kip1}$ shares a 44% homology with $p21^{Cip1/WAF1}$, and this region also displays significant Cdk inhibitory activity (Polyak *et al.*, 1994) and (Moller, 2000). The $p27^{Kip1}$ gene encodes a protein of 27kD, with an amino acid sequence length of 198 (Polyak *et al.*, 1994). The product of the gene binds specifically to cyclin E-Cdk2 complexes and prevents their activation, which in turn inhibits previously activated complexes. According to Polyak and coworkers (1994), $p27^{Kip1}$ overexpression prevents cell entry into the S phase of the cell cycle.

1.13.4 *p21Cip1*$^{/WAF1}$ and *p27*^{Kip1} and their roles in cancer

1.13.4.1 *p27*^{Kip1}

Aberrantly low levels of the *p27* protein have been reported in a wide variety of human carcinomas. These expression levels have been directly correlated to a significant extent with disease aggressiveness and poor prognosis. It has also been widely reported that mutations of the *p27* gene occur rarely in human cancers. In addition, the frequency and prognostic/therapeutic value has been poorly characterised.

1.13.4.1.1 An overview of important *p27*^{Kip1} mutational studies conducted in various cancers

Since the *p27* gene is very rarely homozygously mutated, it does not fulfill the strict requirements that were originally proposed regarding the status of a tumour suppressor gene (Knudson, 1971). Later development in the understanding of how genes function has led to *p27* being classified as a tumour suppressor gene.

p27 is known to be haplo-insuffient. The latter refers to a state whereby one allele of a gene exists in a mutated state, with the other allele being neither mutated nor silenced *i.e.*, the gene is heterozygous for a condition. This was shown to be the case for *p27* in mice knockout studies that were conducted, where both *p27* nullizygous and heterozygous mice showed a predisposition to the development of tumours upon challenge with carcinogenic

agents (Geng *et al.*, 2001). This study established a causal link between the low levels of *p27* expression commonly reported in cancers, and the genes ability to act as a tumour suppressor gene. The researchers did not report any mutation in the wild-type allele itself, but rather pointed to the dosage sensitivity of the *p27* protein in the development of sporadic human tumours.

(Kawamata *et al.*, 1995) conducted one of the first full-scale studies on the genetic status of the $p27^{Kip1}$ gene in cancer. Evaluation of 432 different cancers and 20 cancer cell lines for genetic alterations using PCR-SSCP (PCR-single-strand-conformational polymorphism) and Southern Blotting revealed one silent mutation (GCG→GCA) in a gastric cancer case, and one polymorphism, resulting from a T→G base substitution (GTC→GGC). This resulted in an amino acid change from valine to glycine. The striking aspect of this study was the large number of cancers analysed, as well as the various histological grades of tumours that were taken into account in the study design. This provided a statistically significant indication of the genetic status of $p27^{Kip1}$ amongst a variety of cancers.

One of the first studies describing aberrations of *p27* was conducted on breast cancer (Spirin *et al.*, 1996). Two point mutations were discovered; the first being a polymorphism at codon 142, which was reported for the first time, with the latter being a nonsense mutation at codon 104. The mutation at codon 142 was found to be a G→A base substitution, creating a so-called 'silent' mutation with no change in amino acid sequence (ACG→ACA; Thr→Thr). The second alteration was a hemizygous nonsense mutation

resulting from a CT base substitution, creating a stop codon at 104 (CAG→TAG). This study indicated that mutations of the *p27* gene are rare events in breast cancer, but may contribute to tumourigenesis in an isolated number of cases. Similar results were also obtained in another study on primary breast carcinomas (Ferrando *et al.*, 1996).

Other studies conducted more recently have indicated similar observations to that described above. Polymorphisms were found to be present in isolated cases of corticotrophin-secreting tumours (Dahia *et al.*, 1998). Another study that was conducted on *p27* mutations analysed SNP variants for association with advanced prostate cancer (Kibel *et al.*, 2003). Specific polymorphic genotypes of *p27* have been shown to be associated with advanced prostate carcinoma. In addition, it has been recommended that genetic screening for these variants may aid in determining patients that are most at risk for developing advanced prostate carcinoma (Kibel *et al.*, 2003).

1.13.4.2 $p21^{Cip1/WAF1}$ mutation studies

p21 mutations have also been shown to be uncommon. Mice knockout studies have also failed to significantly demonstrate any tumour susceptibility in *p21*-deficient mice (Deng *et al.*, 1995). Mutations that have been identified were found in isolated cases of Burkitt's lymphoma (Bhatia *et al.*, 1995); melanoma (Vidal *et al.*, 1995) and breast carcinoma (Balbin *et al.*, 1996). (Ralhan *et al.*, 2000) conducted studies on oral malignant and pre-malignant lesions and their association with *p21* aberrations. They discovered a polymorphism (codon 149; A→G) in the PCNA-binding COOH terminal domain of the

p21 gene that was present to a greater extent in cancerous tissue as compared to normal controls.

A limited number of other studies have more recently reported *p21* mutations; however, none have displayed a significant correlation with the development of such cancers and therefore appear to be isolated events.

1.13.5 Expression of $p27^{Kip1}$ and $p21^{Cip1/WAF1}$ in cancer

Aberrant expression patterns of *p27* and *p21* have been more widely reported in a variety of human cancers. With regard to *p27*, low expression has been associated with cancer progression. In addition, this has been shown to be an indicator of poor prognosis and disease aggressiveness. Table 3 below provides a brief list of recent studies that attest to this finding:

Table 3: Low $p27^{Kip1}$ expression in human cancers

cancer type	reference
Colorectal	(Loda *et al.*, 1997)
Breast	(Catzavelos *et al.*, 1997; Porter *et al.*, 1997 and Wu *et al.*, 1999)
Prostate	(Tsihlias *et al.*, 1998; Cote *et al.*, 1998 and Cordon-Cardo *et al.*, 1998)
Oesophageal	(Singh *et al.*, 1998 and Anayama *et al.*, 1998)
Ovarian	(Newcomb *et al.*, 1999)
Lung	(Catzavelos *et al.*, 1999)
Pancreatic	(Lu *et al.*, 1999)
Melanoma	(Florenes *et al.*, 1998)
Non-Hodgkin's lymphoma	(Erlanson *et al.*, 1998; Moller *et al.*, 1999 and Saez *et al.*, 1999)

For *p21*, over-expression has been found to be an independent, unfavourable prognostic factor in a variety of cancers. A few of these studies are listed in table 4 below:

Table 4: $p21^{Cip1/WAF1}$ expression in human cancers

cancer type	reference
Ovarian	(Baekelandt *et al.*, 1999)
Brain	(Jung *et al.*, 1995)
Lung adenocarcinoma	(Hayashi *et al.*, 1997)
Bladder	(Stein *et al.*, 1998)
Oesophageal	(Sarbia *et al.*, 1998b)
Pancreatic	(Harada *et al.*, 1997)
Breast	(Barbareschi *et al.*, 1996)

1.14 Aims and objectives

The aim of the project was to determine the genetic status of the $p21^{CIP1/WAF1}$ and $p27^{Kip1}$ genes in a cohort of OSCC specimens. This was achieved *via* analysis of LOH-AI and MSI in markers linked to these genes. In attaining this objective, a secondary aim of the project was to investigate the efficacy of using a fluorescence-based detection system. Specific objectives of the project were:

a. To select informative markers linked to the genes of interest, for the assessment of microsatellite variability.
b. To design and optimize fluorescence-based Polymerase Chain Reaction (PCR) assays for microsatellite detection.
c. To collect clinico-pathological data with reference to the specimens obtained.

d. To analyse and compare microsatellite data with clinico-pathological features.

e. To determine the potential of such markers as tools of diagnostic and prognostic prediction.

CHAPTER 2

Materials and Methods

2.1 Ethical Approval

Ethical approval for the project, which included the informed consent of study participants, was obtained from the Higher Degrees Committee, Nelson R. Mandela School of Medicine in 2003.

2.2 Case Selection

Ninety six cases of OSCC, each consisting of a normal and corresponding tumour pair, were obtained for the study. The cases consisted of archival specimens, which had been fixed in formalin and embedded in paraffin wax.

2.3 DNA isolation

2.3.1 Preparation of paraffin wax-embedded tissue sections for DNA isolation:

Glass slides containing 8μm sections of paraffin wax-embedded, normal and tumour oesophageal tissue and their corresponding Haemotoxylin and Eosin (H & E) stained slides were obtained for DNA isolation. Each H & E stained slide had the normal and tumour regions

of tissue identified by a pathologist, and then demarcated using a maker pen for comparison with its corresponding tissue slides. The normal and tumour regions were thus identified for DNA isolation. The tissue samples were subsequently scraped and transferred into sterile, 1.5ml Eppendorf tubes. 200 µl of DNA Tissue Lysis Buffer (Appendix A1) was added to each of the tubes, followed by 20 µl of Proteinase K (20mg/ml). The sample tubes were then sealed with Parafilm™, and incubated overnight at approximately 60°C.

2.3.2 Phenol-Chloroform extraction.

Following tissue homogenization and protein digestion (as described in section 2.3.1 above), a standard phenol-chloroform extraction procedure was adopted for DNA isolation (Maniatis *et al.*, 1989).

After the overnight incubation step, the Parafilm™ seals were removed and each tube was vortexed. The tubes were then placed on a heating block that had been set at 90°C, for a time period of 20 minutes. 400 µl of phenol-chloroform-isoamyl alcohol (1:1:1) (Appendix A2) was then pipetted into each tube. The samples were then vortexed briefly and centrifuged at 12000rpm for 5 minutes using a standard bench-top centrifuge (Sorvall® MC 12V, DuPont Inc., USA). The upper aqueous phase was then transferred to a set of appropriately labeled 1.5ml Eppendorf ™ tubes, each of which contained 1 µl glycogen, 40µl of 3M sodium acetate (Appendix A3) and 2 volumes (2 X 400µl =800µl) of cold (-20°C) absolute ethanol. The samples were then mixed briefly by inversion and placed in a freezer at -20°C for 30 minutes or longer.

This was followed by centrifugation at maximum speed (14000rpm) for 20 minutes. The supernatant was removed by careful pipetting, and the remaining pellet was washed with 75 µl of 80% ethanol (Appendix A4). Following a centrifugation step of 3 min at maximum speed, the supernatant was removed carefully and the pellet allowed to air dry completely so as to remove any last traces of ethanol. The pellets were then resuspended in 60 µl of sterile distilled water.

2.4 DNA quantification

DNA samples were quantified spectrophotometrically using a GeneQuant® II DNA/RNA Calculator (Pharmacia Biotech, Sweden). A 1:100 dilution of each sample was read at a wavelength of 280nm, and the results were computed into concentration units of µg/ml.

2.5 Assessment of DNA quality - Insulin PCR

A Polymerase Chain Reaction (PCR) of the ubiquitous human insulin gene was performed on all DNA samples isolated, so as to assess whether the samples were of an amplifiable quality. PCR for a 236 bp fragment targeting the exon 2 region of the gene was performed. The primer set, synthesised at the Department of Biochemistry, University of Cape Town, consisted of the following sequences:

5′-ACC CAG ATC ACT GTC CTT CTG CC-3′ (forward)

5′-AGG GGC AGC AAT GGG CGG TTG-3′ (reverse)

To each 200µl PCR tube (Axygen Scientific, USA) the following reagents were added per reaction:

- Sterile distilled water
- 1 X PCR Reaction Buffer (from 10 X stock containing 100mM Tris-HCl, 15mM $MgCl_2$ and 500mM KCl, pH 8.3), Roche Molecular Biochemical's (Mannheim, Germany)
- 10 pmol/µl forward primer
- 10 pmol/µl reverse primer
- 0.2mM of each dNTP (from 10mM mixed dNTP stock), Roche Molecular Biochemical's (Mannheim, Germany)
- 1U of DNA Taq Polymerase (from 5U/µl stock), Roche Molecular Biochemical's (Mannheim, Germany)
- Approximately 100µg/ml DNA template

Positive (high molecular weight DNA sample) and negative (water) controls were included alongside samples being amplified. The target region was amplified on a GeneAmp™ 9700 PCR System (Applied Biosystems, California, USA) using the following thermal cycling conditions:

An initial denaturation step of 1minute at 94°C, followed by 30 cycles of 94°C for 1 minute; primer annealing at 64°C for 1 minute and then a primer extension step at 72°C for 2 minutes.

This was followed by a final extension step at 72°C for 7 minutes. The samples were then held at 4°C.

2.6 Agarose gel electrophoresis

PCR products of the exon 2 region of the insulin gene were run on 2% agarose gels to assess the viability of the PCR reaction performed, by comparing the size(s) of any product(s) obtained to a DNA molecular weight marker. Molecular Weight Marker VIII (Roche Molecular Biochemical's, Mannheim, Germany) was used in this study. The gel consisted of 1.4g of molecular biology grade agarose (Sigma, USA) that was dissolved in 70ml of 1 X Tris-Boric Acid-EDTA (TBE, Appendix A5) buffer by heating. 2-3µl of ethidium bromide was then mixed into the molten agarose and poured into a casting tray fitted with gel combs, where the gel was allowed to cool and set for approximately 30 minutes. The gel was then placed in an electrophoresis tank (Scie-Plas, U.K.) containing freshly made 1 X TBE running buffer to a sufficient depth. 10 µl of each sample was mixed with 3 µl of bromophenol blue (Appendix A6) dye and then loaded into the wells, with the first well containing Molecular Weight Marker VIII. The gel was then electrophoresed at 100 volts for approximately 1 hour at room temperature, or until sufficient band separation had been achieved.

2.7 Annotation and labeling of DNA samples for identification

Samples were labeled appropriately with an odd or even number so as to distinguish between normal and tumour samples respectively.

2.8 Microsatellite PCR

2.8.1 Selection of microsattelite markers that flank genes of interest

6 microsatellite markers that flank the $p21^{CIP1}$ and $p27^{Kip1}$ genes were selected for the study (Appendix B).

2.8.2 Online Public Genome Resources

The Genome Database (http: //www.gdb.org), an online public genome resource database, as well as Pubmed (http://www.ncbi.nlm.nih.gov/entrez/query.fcgi), were searched for microsatellite markers linked to the genes of interest. Markers were searched for primer sequences, amplification product size, chromosomal location and related literature.

2.8.3 Design and construction of primer sequences

Primer sequences were synthesized by Inqaba Biotechnology®, South Africa, with a fluorescent CY dye attached to the 5' end of each forward primer sequence. The primer sequence sets for each of the six microsatellite markers, as well as their amplified oligonucleotide lengths and linked genes, are tabulated in Appendix B.

2.8.4 Preliminary PCR test run

For each marker, one sample pair (normal and tumour) was amplified under standard PCR conditions as a preliminary test of PCR viability. To each 200µl PCR tube, the following reagents were added per reaction:

- Sterile distilled water
- 1 X PCR Reaction Buffer (from 10 X stock containing 100mM Tris-HCl, 15mM $MgCl_2$ and 500mM KCl, pH 8.3), Roche Molecular Biochemical's (Mannheim, Germany)
- 10 pmol/µl forward primer (from 100pmol/µl stock), Inqaba Biotechnology, South Africa.
- 10 pmol/µl reverse primer (from 100pmol/µl stock), Inqaba Biotechnology, South Africa).
- 0.2mM of each dNTP (from 10mM mixed dNTP stock), Roche Molecular Biochemical's (Mannheim, Germany)
- 1U of DNA Taq Polymerase (from 5U/µl stock), Roche Molecular Biochemical's (Mannheim, Germany)
- Approximately 100µg/ml DNA template

Positive (high molecular weight DNA sample) and negative (water) controls were included alongside samples being amplified.

The PCR thermal cycling conditions were as follows:

An initial denaturation step of 1minute at 95°C, followed by 35 cycles of 95°C for 30 seconds; primer annealing at 55°C for 30 seconds and then a primer extension step at 72°C for 30 seconds. This was followed by a final extension step of 72°C for 10 minutes. The reaction was then held at 4°C.

The PCR products thus obtained were analyzed, or stored at 4°C for later use.

2.8.5 $MgCl_2$ optimization

A $MgCl_2$ titration was performed on all markers (one case per marker), so as to determine the concentration of Mg^{2+} required for optimal PCR performance. Mg^{2+} concentrations of 1.5, 3 and 5mM respectively were evaluated, and the reagents used for the reaction, as well as PCR reaction conditions, were the same as that listed in section 2.7.4 above, with the exception of the PCR reaction buffer used. For the titration, 1 X PCR Reaction Buffer (from 10 X stock), without added $MgCl_2$, was used. The required amounts of Mg^{2+} for the reaction were then added from 25mM $MgCl_2$ stock. The buffer and $MgCl_2$ were obtained from a PCR Core Kit. (Roche Molecular Biochemicals, Mannheim, Germany).

2.8.6 Template concentration optimisation

The optimal template concentration was determined for each marker (one case per marker) by varying the amount of template DNA added. Amounts of 1, 3 and 5µl of DNA (100µg/ml) were evaluated, using the same reagent concentrations and PCR conditions as described in section 2.7.4 above.

2.8.7 Annealing temperature optimisation

The optimal annealing temperature for each marker was determined by running the PCR reaction using annealing temperatures ranging from 50° to 55°C.

2.9 Preparation of polyacrylamide sequencing gel

Urea (12.6g) was weighed out on a Mettler Toledo PB3002-S DeltaRange® (Switzerland) bench-top balance into a 50ml glass beaker. The urea was dissolved in approximately 20ml of distilled water with a magnetic stirrer under medium heat conditions. 3ml of acrylamide, in the form of a 50% stock of Long Ranger™ Gel Solution (BioWhittaker Molecular Applications, USA) was then added, followed by 3.6ml of 10 X TBE. The solution was mixed thoroughly before being topped up to a final volume of 30ml with distilled water, and then stored in polyethylene squeeze bottles at 4 °C for later use.

Prior to the gel being poured, 30µl of N, N, N', N'-tetramethyl-ethylendiamin (TEMED, Merck, Germany) and 300µl of freshly made 10% ammonium persulphate (APS) solution (Appendix A7) were added and mixed in thoroughly.

2.9.1 Gel Cassette cleaning, assembly and loading

The gel cassette (Pharmacia Biotech) consisted of a thermal short plate, accompanying cover glass, glass spacers (0.3mm) and metal clip-on attachments that held the short plate and cover

glass together. The short plate and cover glass were cleaned thoroughly with equal amounts of distilled water and 100% ethanol in combination, so as to remove all traces of residual gel and other residue. The spacers were then positioned along the left and right edges of the thermoplates. The cleaned and dust-free plates were then assembled and fixed into position using the metal clamps, and a lane comb was inserted between the plates. The pre-mixed acrylamide solution (as described above) was then squeezed between the plates through the lower edge of the gel cassette, and the gel was allowed to polymerize and set for approximately 45 minutes.

2.9.2 Attachment of gel cassette to the ALFexpress™ DNA sequencer

The gel cassette containing the polymerized gel was attached to the sequencer by connecting the cassette into place through the push-fit connectors. These connectors held the cassette in place and also allowed for water to be circulated through the thermoplates. With the cassette attached, 1 litre of 1 X TBE buffer was poured into each of the lower and upper buffer chambers. The positive electrode was then attached to the appropriate point and placed in the lower buffer chamber. The sequencer was then switched on, and the temperature allowed to reach at least 37°C before the gel comb was carefully removed.

2.10 Sample preparation

The microsatellite PCR products were mixed with a blue dextran loading dye (AmerSham Biosciences, USA) in equal volumes (3µl each), before being denatured at 96 °C for 3 minutes in a GeneAmp™ 9700 PCR System thermocycler (Applied Biosystems, California, USA). The

samples were then immediately held on ice to so as to prevent re-annealing, prior to being loaded on a gel.

2.11 Gel loading

Using a syringe filled with buffer, the lanes were thoroughly washed to remove any residual urea and non-polymerized gel solution. Elongated gel-loading tips were used to carefully load the samples into the lanes. Lane 1 was loaded with a Cy5-labelled external size marker (ALFexpress Sizer ™ 50-500, AmerSham Biosciences, USA) to allow for the determination and comparison of sample sizes.

2.12 Run conditions used on the ALFexpress™ sequencer

The following parameters were used for running gels on the ALFexpress™ sequencer:

- Voltage 1600V
- Power 25W
- Current 60mA
- Temperature 55-60°C range
- Sampling interval 1 second
- Running time 180 minutes

Before each run was started, the above parameters were programmed into the sequencer.

2.13 Fragment analysis

Two software packages were used to analyse data viz., ALFexpress™ and Fragment Manager™ (Pharmacia Biotech). Data files were saved into the Fragment Manager™ programme for analysis. The amplified product length(s) were determined by comparing the peak location to the external standard marker.

2.14 Statistical analysis

Statistical analysis was performed using the SPSS® v. 11.0 for Windows software programme. Non-parametric tests were used. These included the Kruskal-Wallis test, chi-squared test and cross tabulation, as well as the Kaplan-Meier test for survival.

CHAPTER 3

Results

3.1 Light microscopic evaluation

All the oesophagectomies received were determined to be squamous cell carcinomas, and were graded by a pathologist in one of three ways: well, moderate or poorly differentiated. Tumours that were well differentiated displayed widespread keratinisation of cells. An arrow in Figure 6 below indicates this:

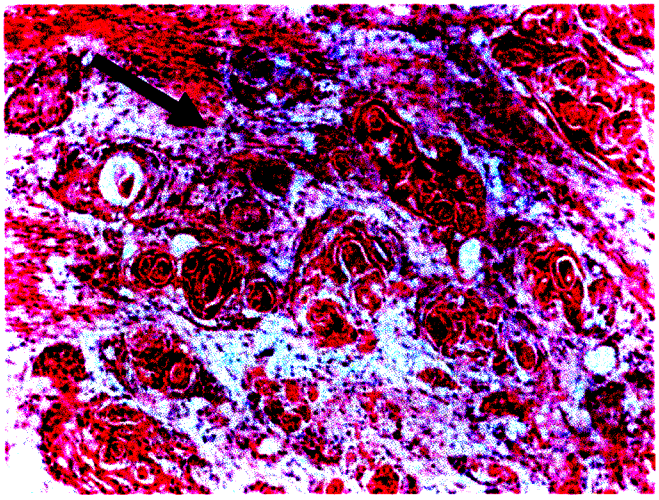

Figure 6: A well differentiated, OSCC case displaying widespread keratinisation of cells. With permission from Naidoo, 1998 (PhD dissertation, University of Natal).

3.2 Insulin PCR and agarose gel electrophoresis

PCR for the exon 2 region of the insulin gene was performed to assess the quality of the DNA isolated. The PCR product of this reaction was a 236bp fragment. A representative image of an agarose gel containing the amplified insulin fragment is shown in figure 7 below:

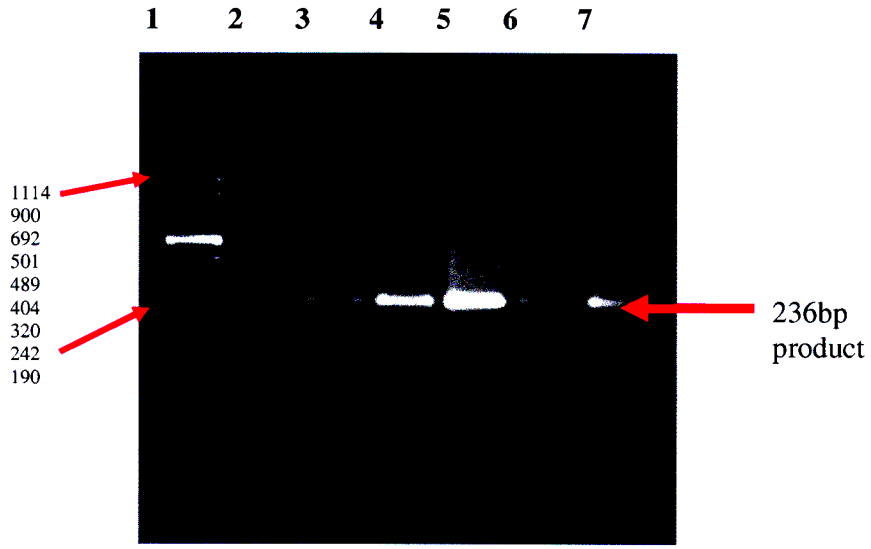

Figure 7: Agarose gel electrophoresis of insulin PCR products. The gel was run at room temperature for 45 minutes, and later viewed on a BioRad ChemiDoc® UV trans-illuminator (Biorad Laboratories, California). Lane 1 contains the DNA molecular weight marker VIII® (Roche Diagnostics, Germany). Lane 2 contains the negative template (water) and lane 3 contains a positive control. The bands in lanes 4-7 are the amplified PCR products (236bp).

3.3 Microsatellite PCR

Microsatellite PCR was carried out as detailed in chapter 2.

3.3.1 Preliminary PCR test run

The test run was conducted as detailed in Chapter 2 (2.8.4). Amplification was achieved for all markers tested.

3.3.2 $MgCl_2$ optimization

A $MgCl_2$ titration was performed as detailed in Chapter 2 (2.8.5). A representative electrophoretogram of this titration is shown for marker D6S1575 (Appendix F, Figure 1). No significant difference between peak size and shape was noted with the three $MgCl_2$ concentrations used, for any of the six markers tested. It was decided that the concentration of 2.5mM would be used, since this was the concentration used in the preliminary PCR test reaction.

3.3.3 Template concentration optimization

The optimal template concentration was determined as detailed in Chapter 2 (2.8.6). A representative electrophoretogram of this titration is shown for marker D12S391 (Appendix F, Figure 2). A concentration of 100 µl/ml did not allow for significant and consistent

amplification in any of the markers tested. Amplification was achieved with 300 µl/ml and 500 µl/ml concentrations. With regard to the latter, no significant difference was observed between these two concentrations, in terms of amplification. It was decided that a concentration of 300 µl/ml would be used, since this allowed for sufficient amplification, using the least amount of template possible.

3.3.4 Annealing temperature optimization

The optimal annealing temperature was determined to be 55°C for all the markers tested. A representative electrophoretogram of this titration is shown for marker D12S358 (Appendix F, Figure 3). For temperatures below 55°C, *viz.* 50°C and 53°C, the primers did not bind to the template strand stringently enough, and non-specific amplification occurred. Using a temperature of 55°C significantly decreased this, whilst allowing for sufficient amplification of the marker product.

3.4 Interpretation of data

Representative electophoretograms for LOH-AI and MSI of each marker is attached as Appendix C. The microsatellite genotypes that were observed were interpreted in one of the following ways:

3.4.1 Homozygous, no change (H)

Figure 8 is an example of a homozygous case showing no change. If a tumour and its corresponding normal sample showed a single peak with the same shape and size, the case was reported to be homozygous, with no change between the two peaks. Such a case would be considered uninformative.

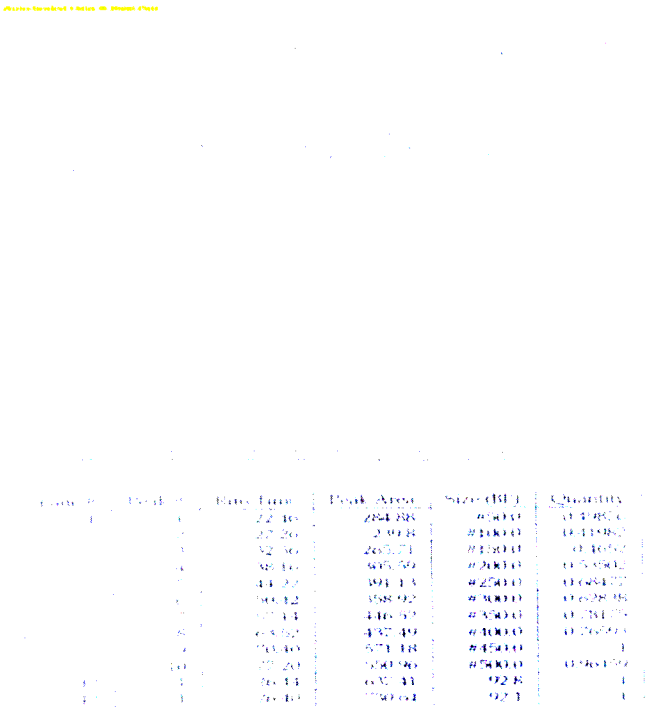

Figure 8: Electrophoretogram displaying the H genotype, as seen in marker D6S1575. Lane 1 contains the 50-500bp CY5-labelled marker. Lane 2 contains PCR product amplified from normal DNA, with the corresponding tumour sample in lane 3. The table lists the peaks that were recorded, as well as their size(s). As can be seen, only one peak was detected in the normal and tumour samples, with no change between them (H).

3.4.2 No allelic imbalance (NAI)

Figure 9 is a representative example of a case displaying NAI. This genotype was characterized by cases that showed two peaks for both normal and tumour samples. These cases were considered to be heterozygous.

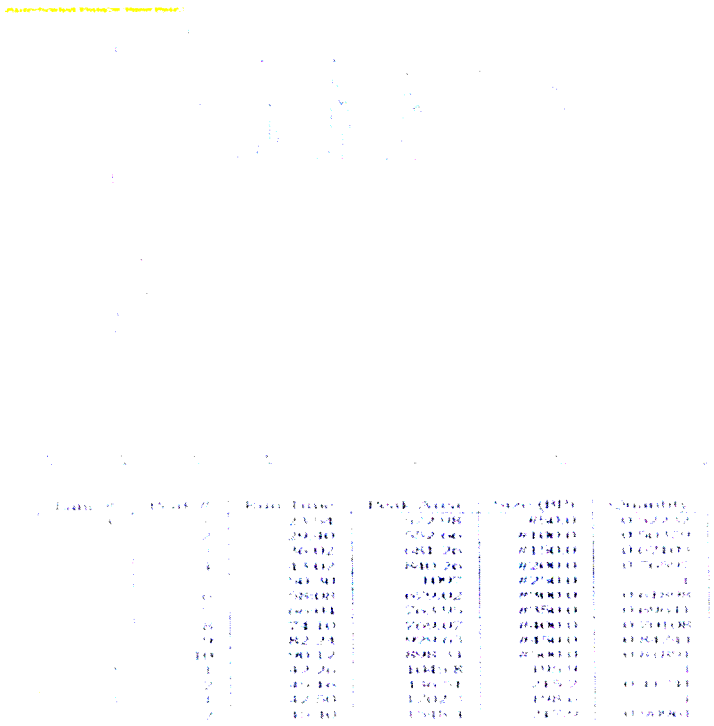

Figure 9: Electrophoretogram displaying the NAI genotype, as seen in marker D12S320. Lane 1 contains the 50-500bp CY5-labelled marker. Lane 2 contains the normal PCR product, with the corresponding tumour sample in lane 3. The table lists the number of peaks recorded, as well as their size(s). Two peaks were detected in both normal and tumour samples, with no change between them (NAI).

3.4.3 Loss of Heterozygosity-Allelic Imbalance (LOH-AI)

Figure 10 shows a case that was recorded as LOH-AI. When a tumour sample displayed a loss of an allele, in comparison with the paired normal genotype, the case was recorded as LOH-AI. Cases that also displayed significant differences in allele sizes (allelic imbalance), but no allelic loss, were also grouped into this category.

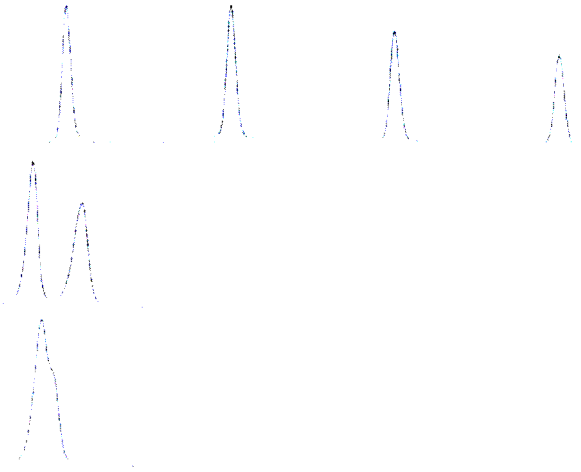

Lane #	Peak #	Run Time	Peak Area	Size (BP)	Quantity
1	1	22.52	169.56	#50.0	1
	2	27.36	134.84	#100.0	0.79522
	3	32.50	145.27	#150.0	0.85971
	4	38.24	131.64	#200.0	0.77635
	5	44.24	133.68	#250.0	0.78836
	6	50.40	109.34	#300.0	0.64482
	7	57.04	98.964	#350.0	0.58365
	8	63.38	86.635	#400.0	0.51094
	9	70.18	66.772	#450.0	0.3938
	10	76.54	41.681	#500.0	0.24582
12	1	26.34	152.64	89.6	1
	2	28.04	149.66	104.6	0.98053
13	1	26.50	430.29	92.3	1

Figure 10: Electrophoretogram displaying the LOH-AI genotype, as seen in marker D6S1575. Lane 1 contained the 50-500bp CY5-labelled marker. Lane 2 contained normal PCR product, with the corresponding tumour sample in lane 3. The table lists the number of peaks that were recorded, as well as their size(s). Two peaks were detected in the normal sample (lane 2), with the second peak being lost in the tumour sample in lane 3 (LOH-AI).

3.4.4 Microsatellite Instability (MSI)

Figure 11 shows a representative case of MSI. The gain of an allele, represented by an additional peak in the tumour sample with reference to the corresponding normal sample, was reported as MSI.

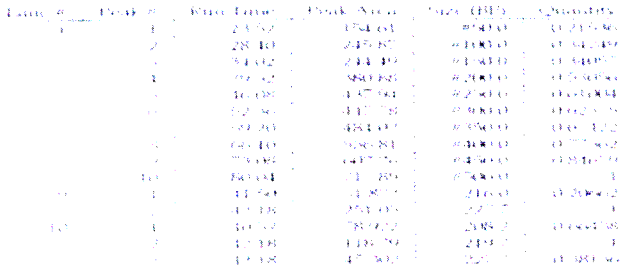

Figure 11: Electrophoretogram displaying the MSI genotype, as seen in marker D12S391. Lane 1 contained the 50-500bp CY5-labelled marker. Lane 2 contained normal PCR product, with the corresponding tumour sample in lane 3. The table lists the number of peaks that were recorded, as well as their size(s). Two peaks were detected in the normal sample (lane 2), with an additional 3rd peak in the tumour sample in lane 3 (MSI).

3.5 Overall results of microsatellite PCR

The results of LOH-AI/MSI analysis for the 96 OC cases are shown in Tables 5 and 6 below. Data for each marker, along with the corresponding clinical information is attached in appendices D1 and D2.

Table 5: Genetic aberrations at markers near *p27*^{Kip1}

Frequency of LOH/AI and MSI		
Marker	**LOH-AI/I* (%)**	**MSI/N (%)**
D12S391	8/43 (19)	3/96 (3)
D12S320	10/38 (26)	3/96 (3)
D12S364	8/30 (27)	7/96 (7)
D12S358	7/19 (37)	4/96 (4)

I* = no. of informative cases (I* = NAI+LOH-AI); N = population size

The frequencies for LOH-AI were calculated as a percentage of the number of informative cases (I*).

For all the markers, the main microsatellite genotype recorded was H, which ranged from 49% to 78% of all cases (Figures 12 & 13). NAI was also a major feature, and ranged from 8% to 35%. Figure 12 shows the distribution of these and other microsatellite alterations for the markers listed in table 5:

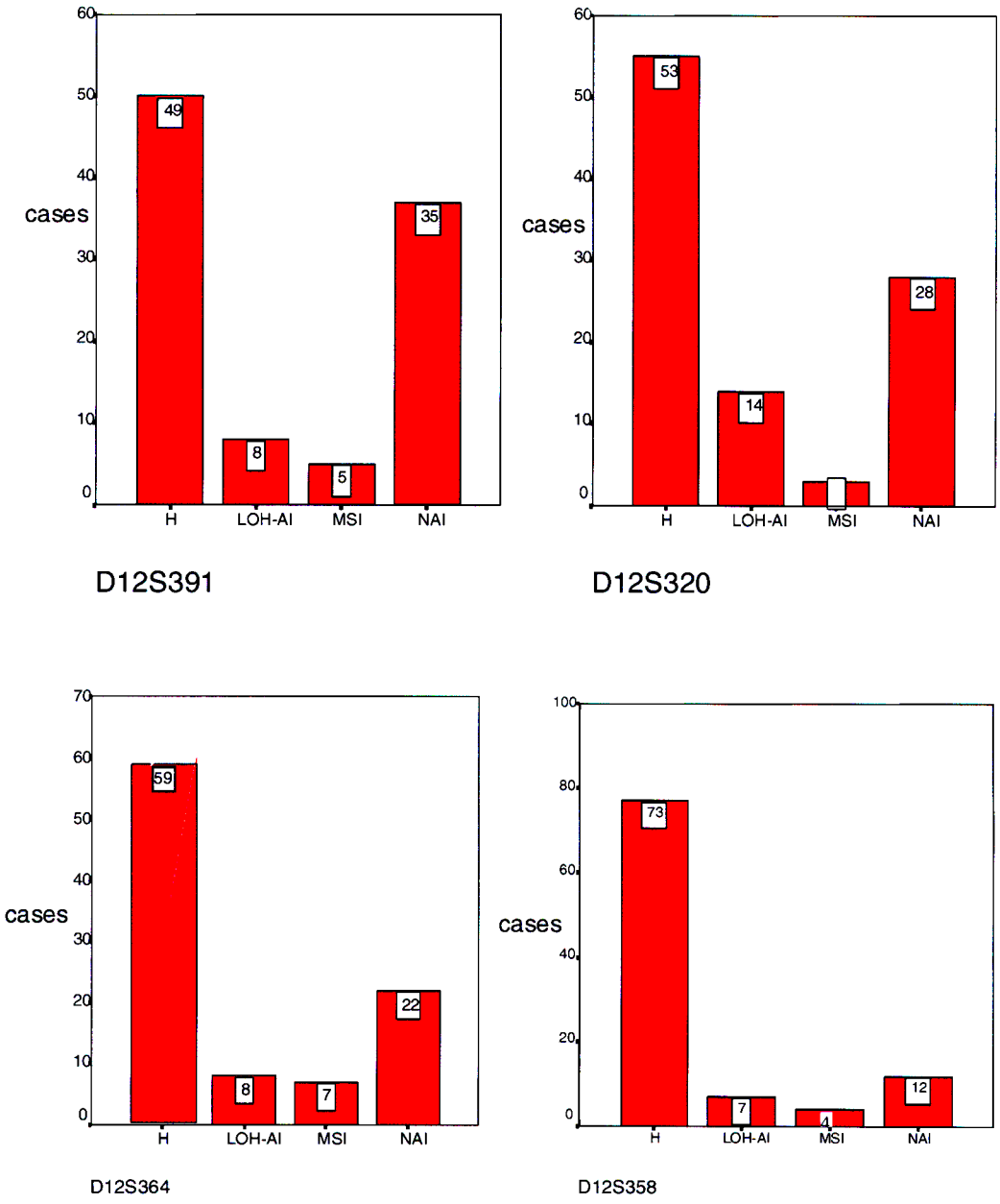

Figure 12: Microsatellite genotype distribution of markers near the *p27*^{Kip1} gene.

The data in table 6 show the results for LOH-AI and MSI that were recorded for markers near the *p21*$^{Cip1/WAF1}$ gene. Figure 13 below shows bar graphs that illustrate the distribution of these and other microsatellite alterations for the markers listed in table 6.

Table 6: Genetic aberrations at markers near *p21*$^{Cip1/WAF1}$

Frequency of LOH/AI and MSI		
Marker	**LOH-AI/I* (%)**	**MSI/N (%)**
D6S1575	7/15 (47)	3/96 (3)
D6S1645	10/30 (33)	3/96(3)

I* = no. of informative cases (I* = NAI+LOH-AI); N = population size

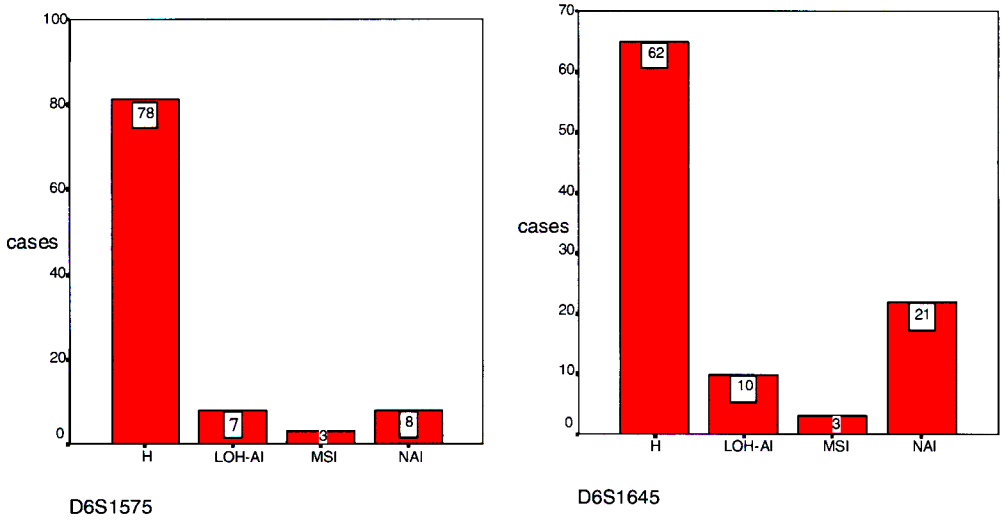

Figure 13: Microsatellite genotype distribution of markers near the p21$^{Cip1/WAF1}$ gene.

3.6 Analysis of microsatellite data with clinico-pathological data

Clinical and pathological data was obtained for as many cases as possible. Table 7 below summarizes the type of data that were collected *via* the Department of Pathology. Statistical analysis was performed using the data that were available at the time of study.

Table 7: Clinico-pathological data collected for statistical analyses

Clinico-pathological feature	**No. of cases with valid entries/96**
Age (yrs)	96
Sex Ratio (Male:Female)	54:42
Stage	
0	1
I	0
IIA	45
IIB	11
III	39
No stage assigned	4
Grade	
Well differentiated (WD)	25
Moderately differentiated (MD)	61
Poorly differentiated (PD)	10
Not graded	4
Lymph node metastases	**No. of cases with valid entries/84**
No	37
Yes	47
TNM staging	**No. of cases with valid entries/96**
$T_2N_0M_0$	16
$T_2N_1M_0$	12
$T_3N_0M_0$	29
$T_3N_1M_0$	29
$T_4N_0M_0$	4
$T_4N_1M_0$	5
$T_{is}N_0M_0$	1
Outcome	
Alive	54
Dead	20
Not recorded	26
Survival	74

3.7 Statistical Analysis

The data (Table 7 above) were analysed with the results obtained from each of the six microsatellite markers. Using the statistical software programme SPSS® v. 11.0 for Windows, various analyses were undertaken. These included descriptive statistics, such as the calculation of the mean and standard deviation for each of the parameters described, for each of the six markers studied. Trend analysis was performed, and this consisted of cross tabulations. The Kruskal-Wallis and Chi-squared tests were used to determine the relationships between microsatellite data and clinical-pathological features.

3.7.1 Descriptive statistics of categorical and clinico-pathological data

3.7.1.1 Age

Figure 14 is a bar graph of the age category. As can be seen from the graph, the mean age is 56 years and the standard deviation is 10.91, for a total sample size of 96.

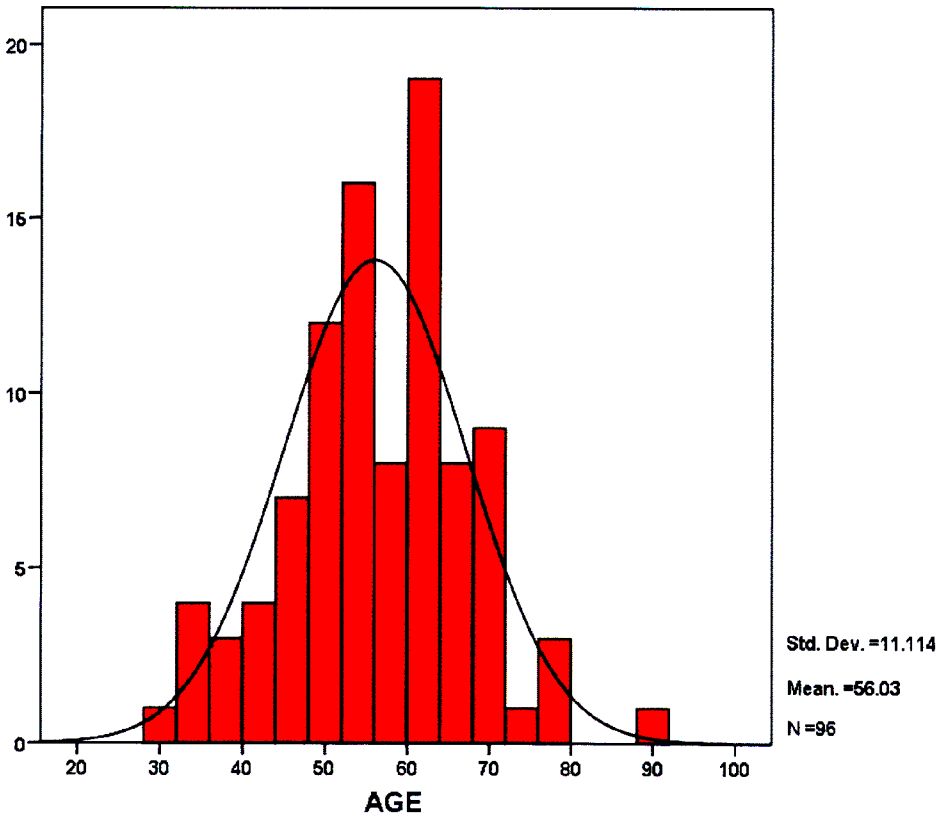

Figure 14: Bar graph showing the distribution of age groups of study participants.

3.7.1.2 Sex

Figure 15 is a bar graph that illustrates the sex distribution of study participants. 56% of samples were collected from males, whilst 44 % of samples came from females.

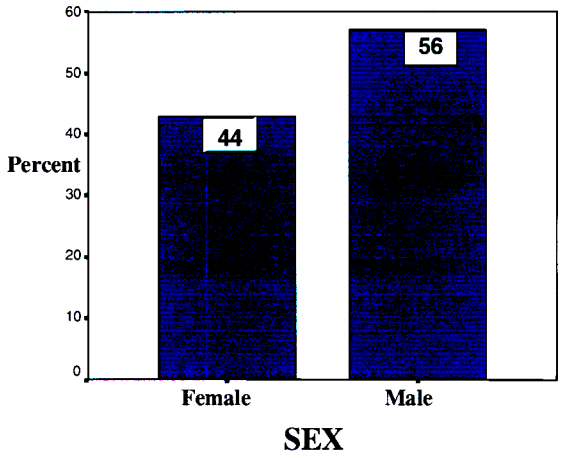

Figure 15: Bar graph showing the distribution of males and females in study participants.

3.7.1.3 Tumour stage

Figure 16 indicates graphically the frequencies of each tumour stage that was used in this study. The percentages for each stage are also given on each representative bar. The majority of tumour stages that were investigated in this study consisted of stage IIA (47%) and stage III (41%). Refer to the section on tumour staging and grading (chapter 1) for more information regarding different tumour stages.

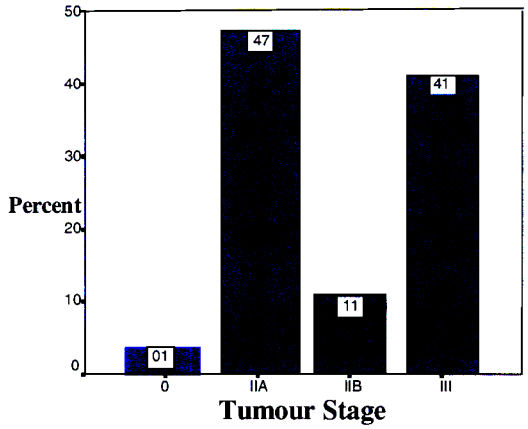

Figure 16: Bar graph showing the distribution of tumour stages in the samples collected from study participants.

3.7.1.4 Tumour grade

A large percentage of tumours (64%) were found to be of a moderately differentiated (MD) grade (figure 17). Refer to the section on tumour staging and grading (chapter 1) for more information regarding this.

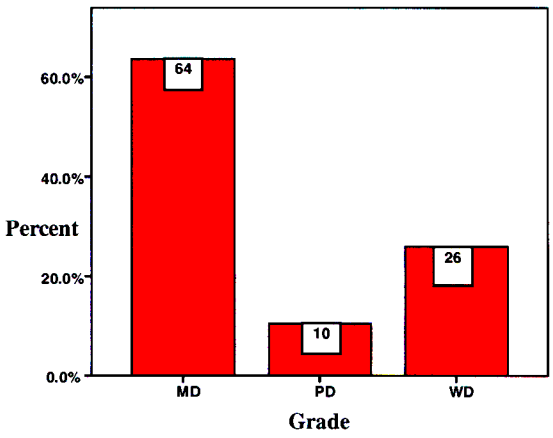

Figure 17: Bar graph for tumour grade distribution.

3.7.1.5 TNM staging

The percentages of each category of staging are shown in figure 18 below. Stages 3, 1, 0 and 3, 0, 0 accounted for 30% of all cases respectively.

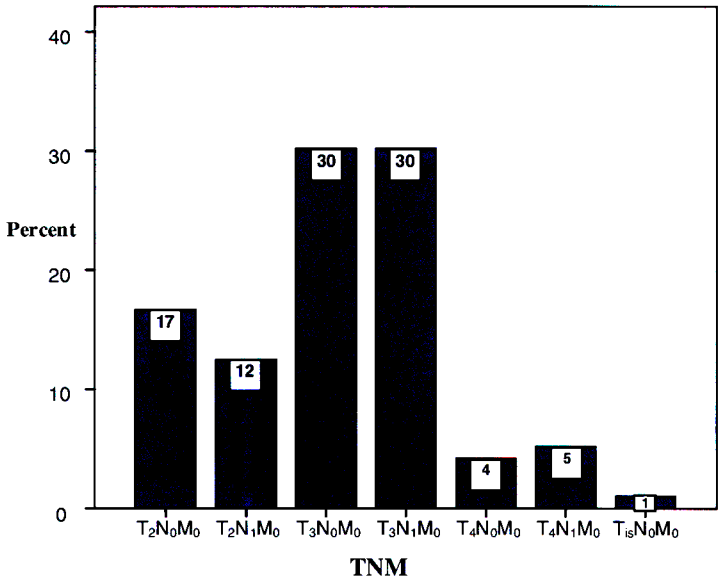

Figure 18: TNM staging distribution among study participants.

3.7.1.6 Lymph node metastases

Of the 84 cases that had valid entries for the presence/absence of lymph node metastases, 56% were positive and 44% were not. Data for the remaining 16 cases could not be obtained. Figure 19 illustrates this:

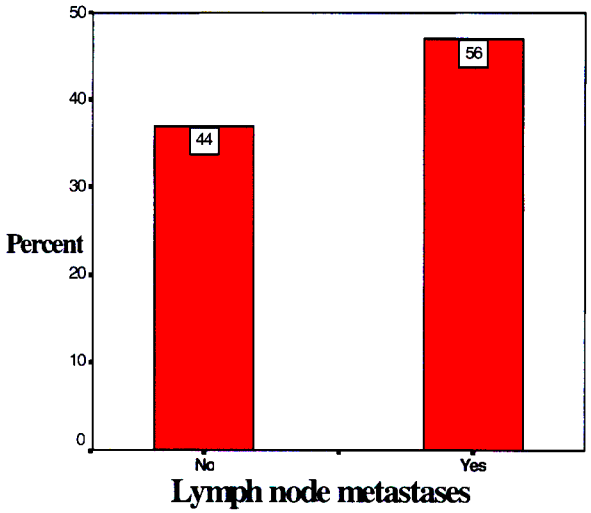

Figure 19: Distribution of the presence/absence of lymph node metastases among study participants.

3.7.1.7 Outcome

With regard to patient outcome, it was recorded that 73% of patients were alive and 27% had died, by the end of the study period. Figure 20 below illustrates this:

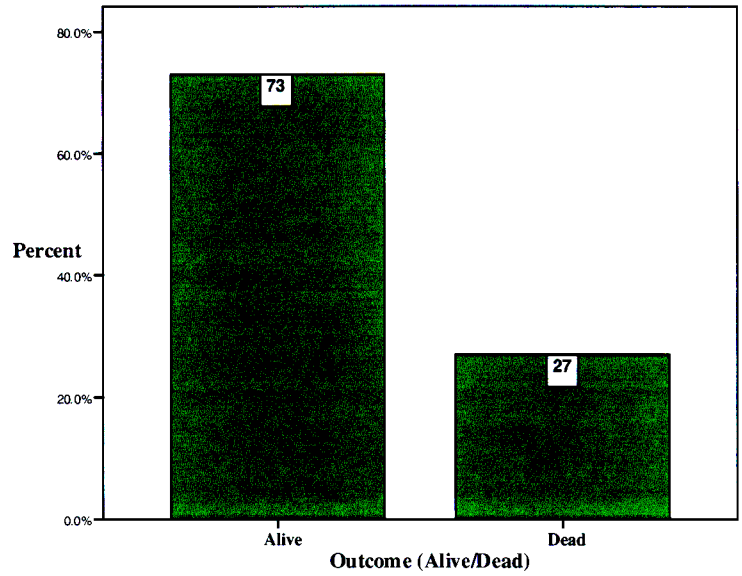

Figure 20: Distribution of patient outcome among study participants.

3.7.1.8 Survival time

Patient survival was recorded as the number of weeks of survival following surgical resection, up to a pre-determined cut-off date (Table 8). From 74 valid entries, the mean number of weeks of survival was found to be approximately 26 weeks.

Table 8: Descriptive statistics for survival time

		Survival/weeks
N	Valid	74
Mean		26.53
Median		8.00
Std. Deviation		45.78
Skewness		3.581
Std. Error of Skewness		.279
Minimum		0
Maximum		284
Percentile	25	5.00
	50	8.00
	75	24.00

3.7.2 Trend analysis

The data were determined to be not normally distributed, and non-parametric tests were carried out.

3.7.2.1 Kruskal-Wallis test for age *vs.* marker genotypes

A Kruskal-Wallis test was performed for age of patient versus the microsatellite aberrations recorded for each marker. The results show no significant association between patient age and microsatellite aberrations for any of the markers ($p>0.05$). The results of the test are shown in appendix E3. The following bar graphs (Figures 21 and 22) describe the trends that were seen in this study for patient age vs. microsatellite genotypes. MSI is associated with advanced age in markers D6S1575, D12S364 and D12S358 respectively [Figures 22(b), 21(a) and 21(b)]. Advanced age is also associated with LOH-AI in markers D12S320, D12S391 and D6S1645 respectively [Figures 21(c), 21(d) and 22(a)].

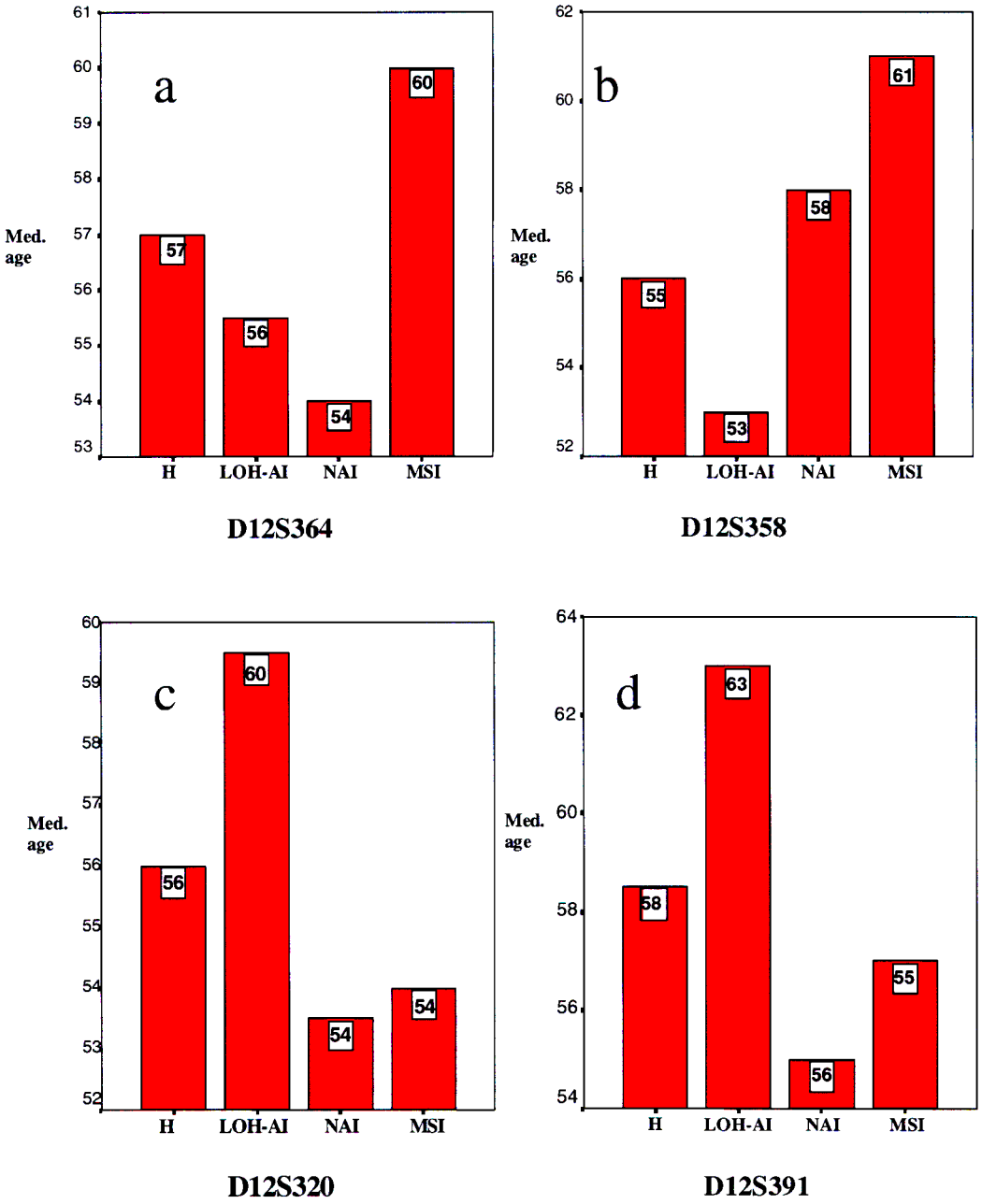

Figure 21: Bar graph plots of median age *vs.* microsatellite genotype for the $p27^{Kip1}$-linked markers.

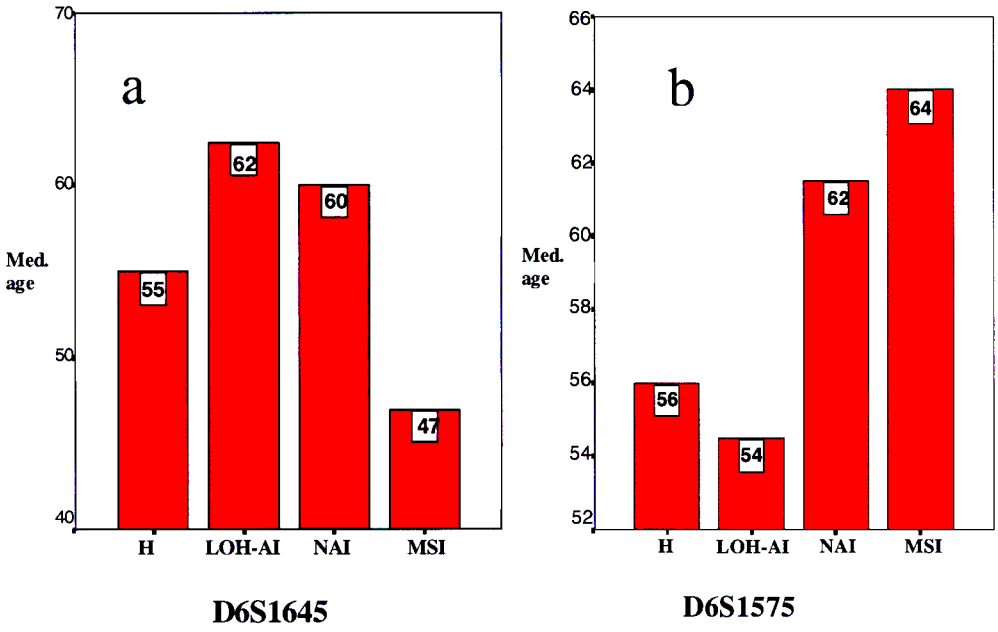

Figure 22: Bar graph plots of median age vs. microsatellite genotype for the *p21*^{CIP1}-linked markers.

3.7.2.2 Chi-squared test and cross tabulation

Chi-squared tests were performed for all microsatellite markers, in relation to patient sex, tumour stage, tumour grade, lymph node metastases, TNM staging and outcome. Cross tabulations for each marker and clinical feature are given in Appendix E1 and E2, alongside the p values of statistical significance. Tumour grade was significantly associated with marker D6S1575 ($p<0.05$). No other significant relationships were observed for the other parameters. The following bar graph plots reflect the trends that were observed:

3.7.2.2.1 Sex

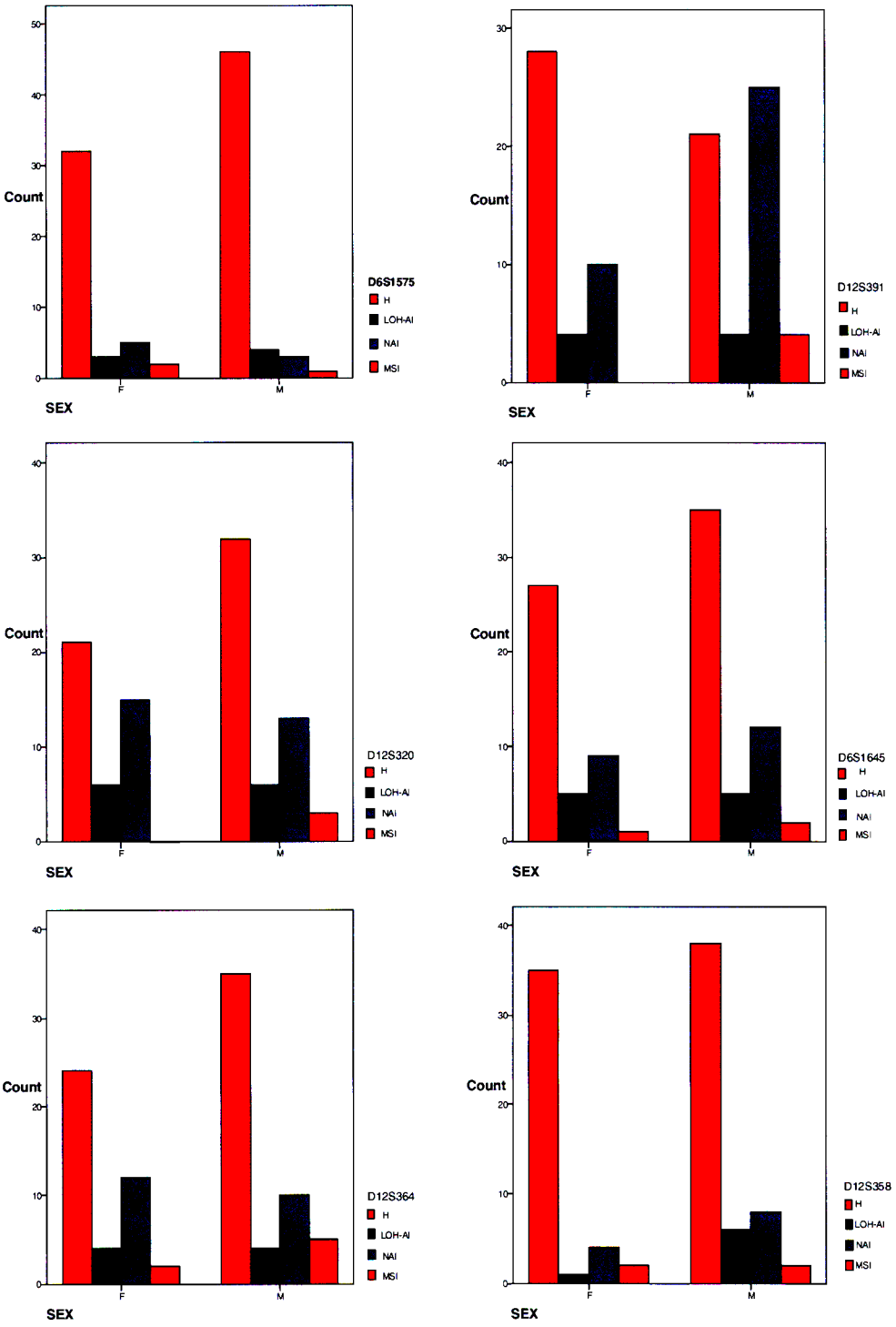

Figure 23: Bar graph plots of sex *vs.* microsatellite genotype frequencies.

3.7.2.2.2 Tumour stage

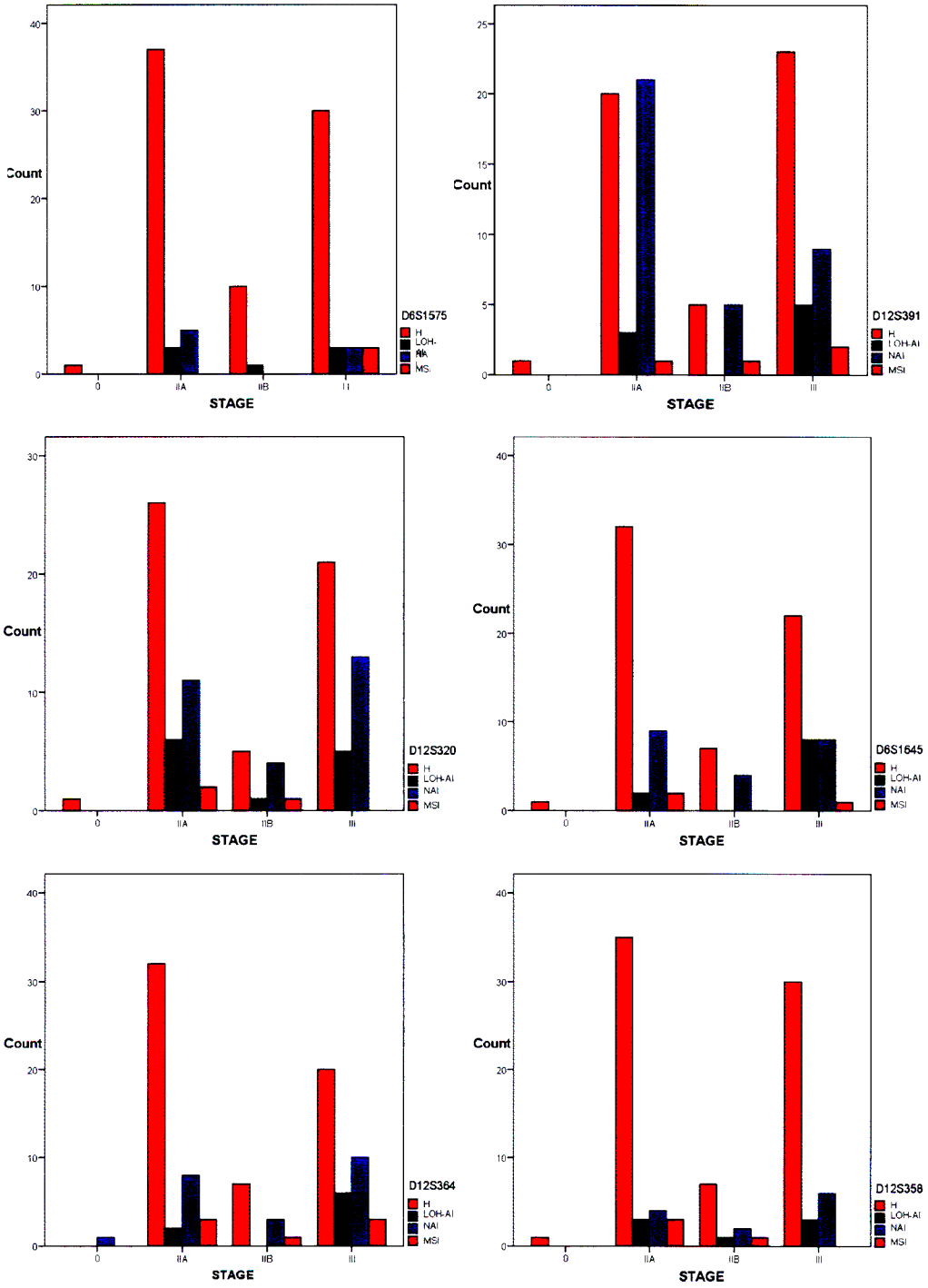

Figure 24: Bar graph plots of tumour stage *vs.* microsatellite genotype frequencies.

3.7.2.2.3 Tumour grade

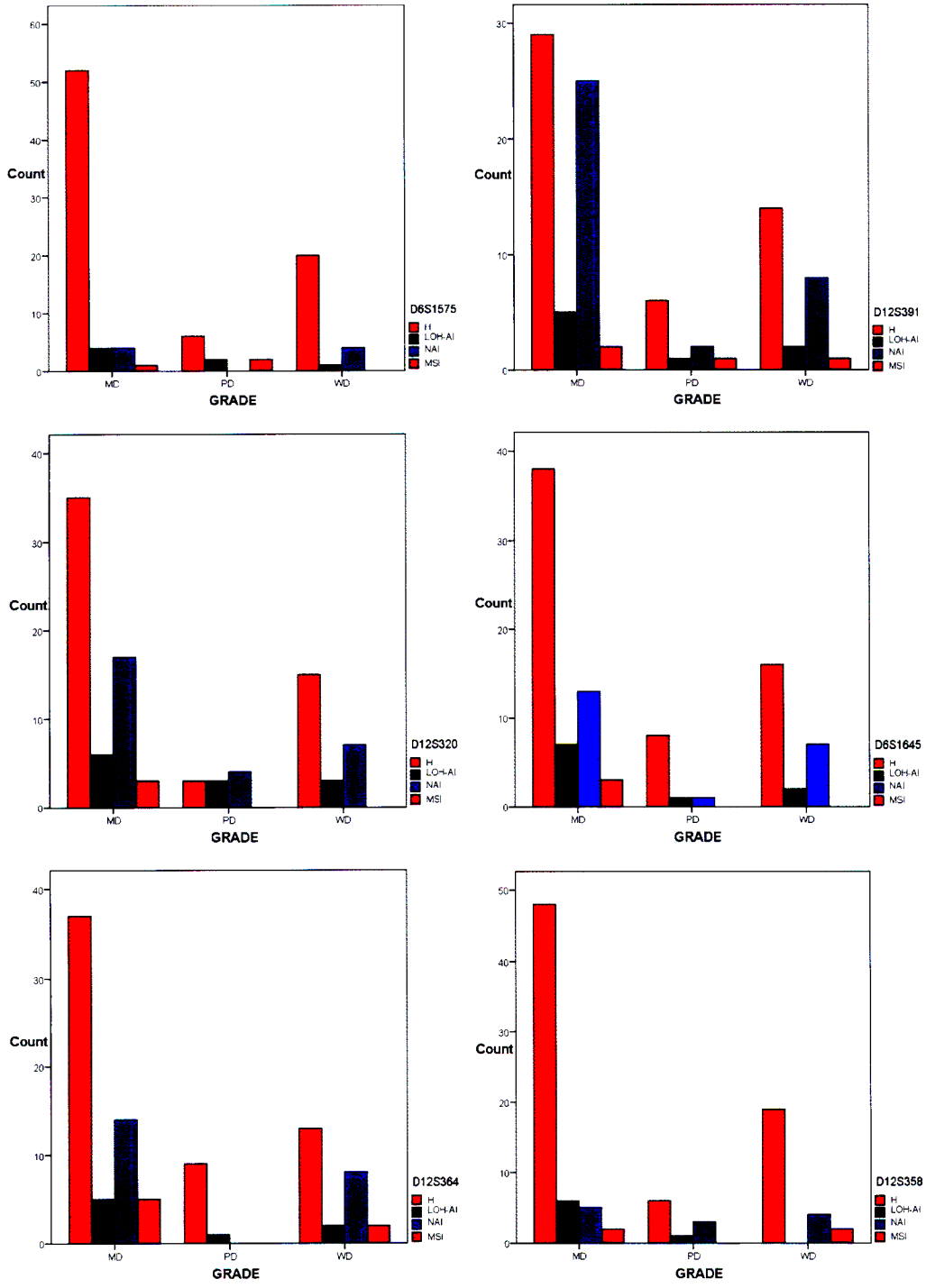

Figure 25: Bar graph plots of tumour grade *vs.* microsatellite genotype frequencies.

3.7.2.2.4 Lymph node metastases

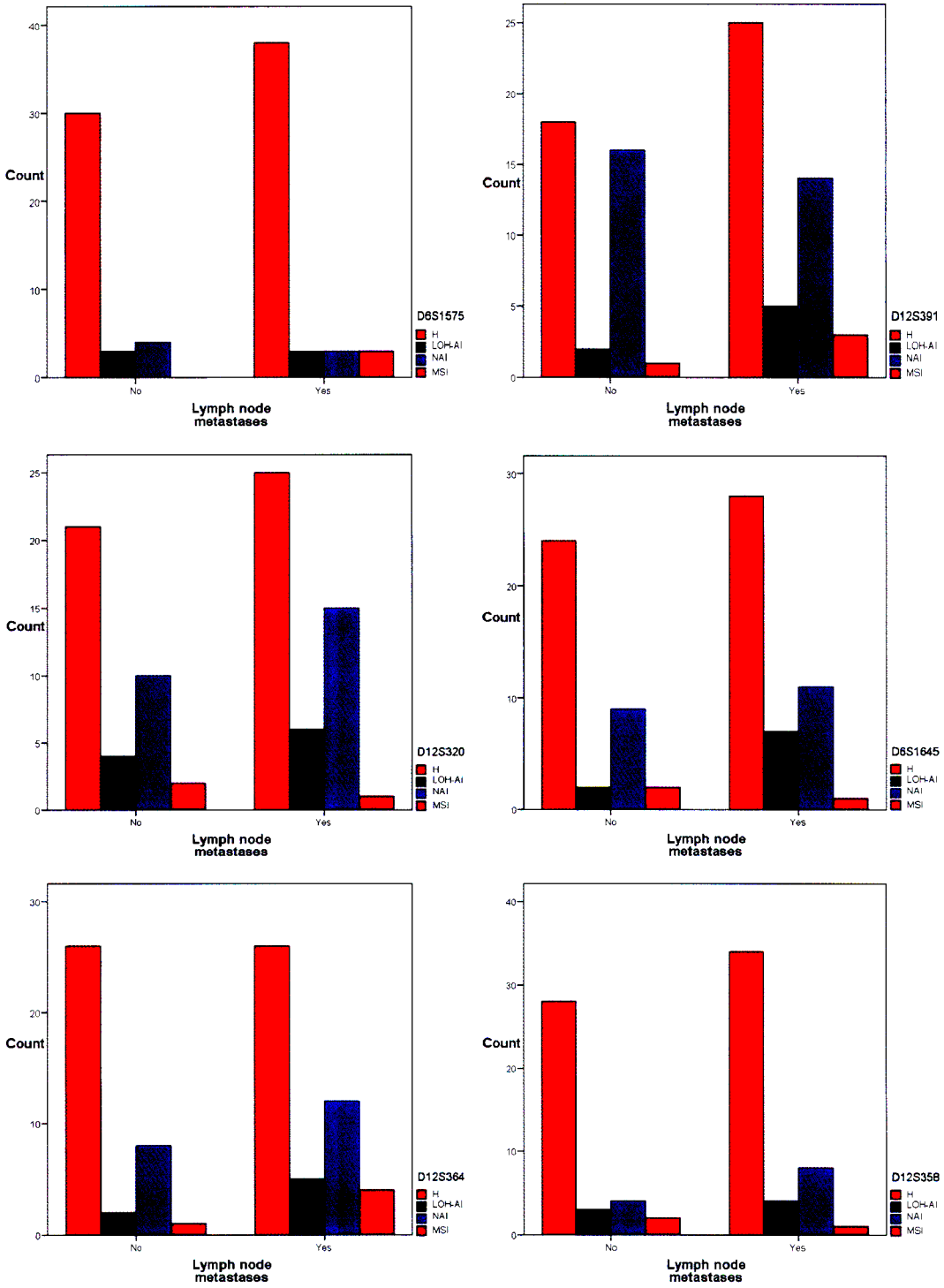

Figure 26: Bar graph plots of lymph node metastases *vs.* microsatellite genotype frequencies.

3.7.2.2.5 TNM staging

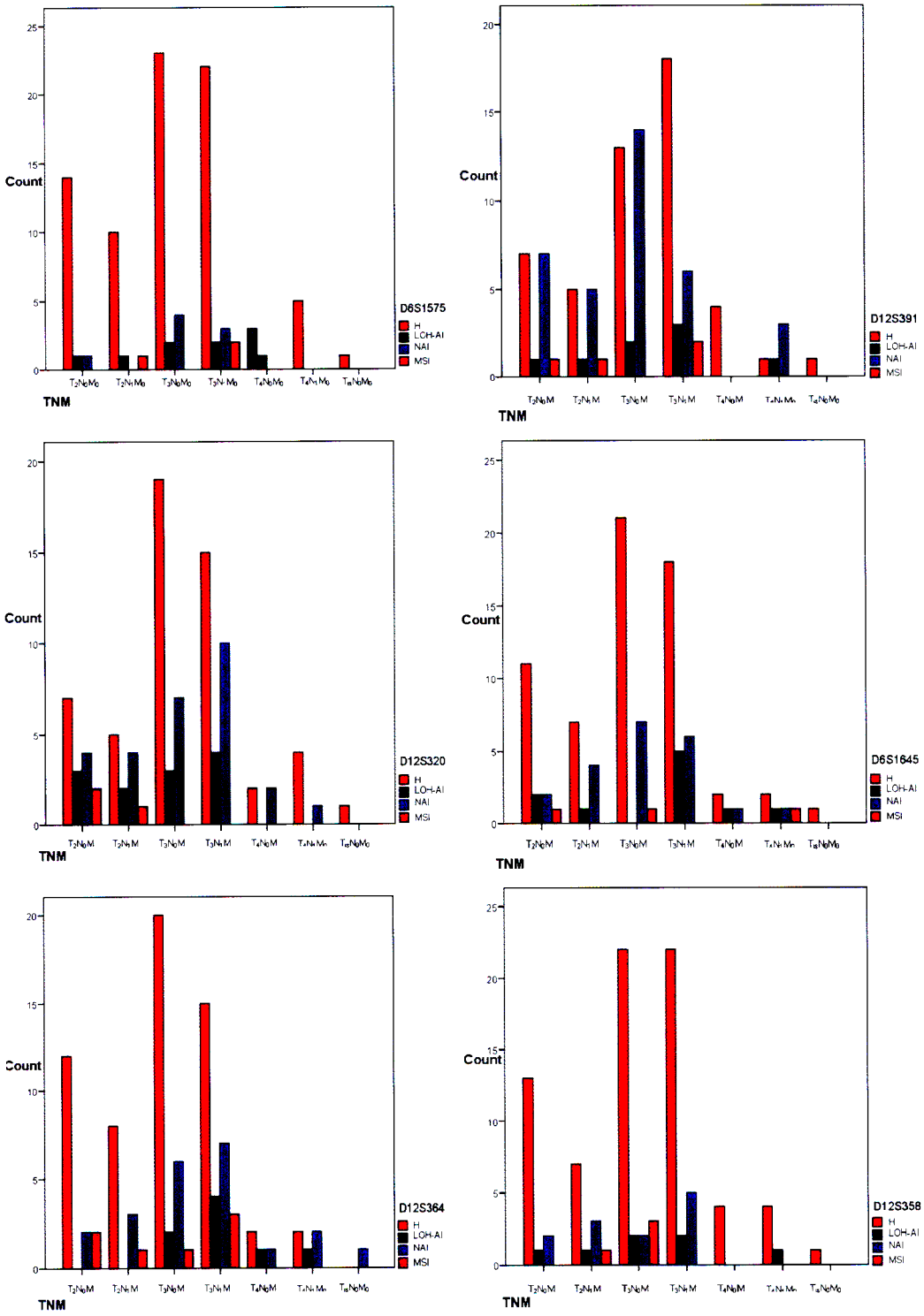

Figure 27: Bar graph plots of TNM stage groups *vs.* microsatellite genotype frequencies.

3.7.2.2.6 Outcome (alive/dead)

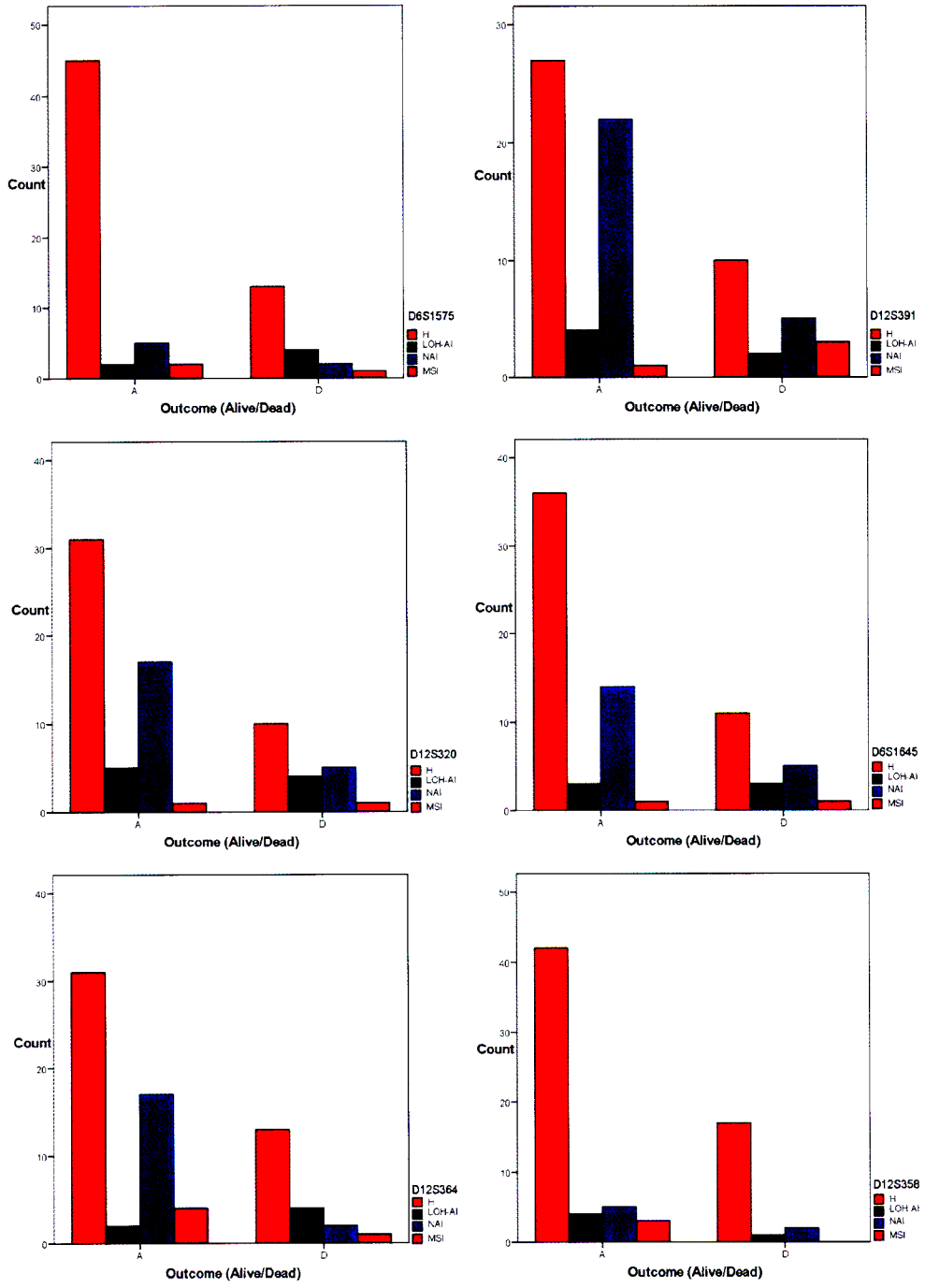

Figure 28: Bar graph plots of outcome vs. microsatellite genotype frequencies.

3.7.2.3 Kaplan-Meier test for survival time

A Kaplan-Meier test for survival time in weeks *vs.* microsatellite genotypes was carried out. The table of statistical significance for all 6 markers is provided below (Table 9). In addition, Figures 29, 30 and 31 that follow illustrates these results. These graphs are plots of survival time *vs.* cumulative survival, for each of the markers. For marker D12S391, MSI is significantly associated with decreased survival time [Figure 29(b)]. Similarly, decreased survival time is significantly associated with marker D12S364 and LOH-AI [Figure 31(a)].

Table 9: Kaplan-Meier test of statistical significance for survival

Microsatellite marker	**P value**	**Significance**
D6S1575	0.11	not significant ($p>0.05$)
D12S391	0.05	significant ($p<0.05$)
D12S320	0.33	not significant ($p>0.05$)
D6S1645	0.16	not significant ($p>0.05$)
D12S364	0.03	significant ($p<0.05$)
D12S358	0.70	not significant ($p>0.05$)

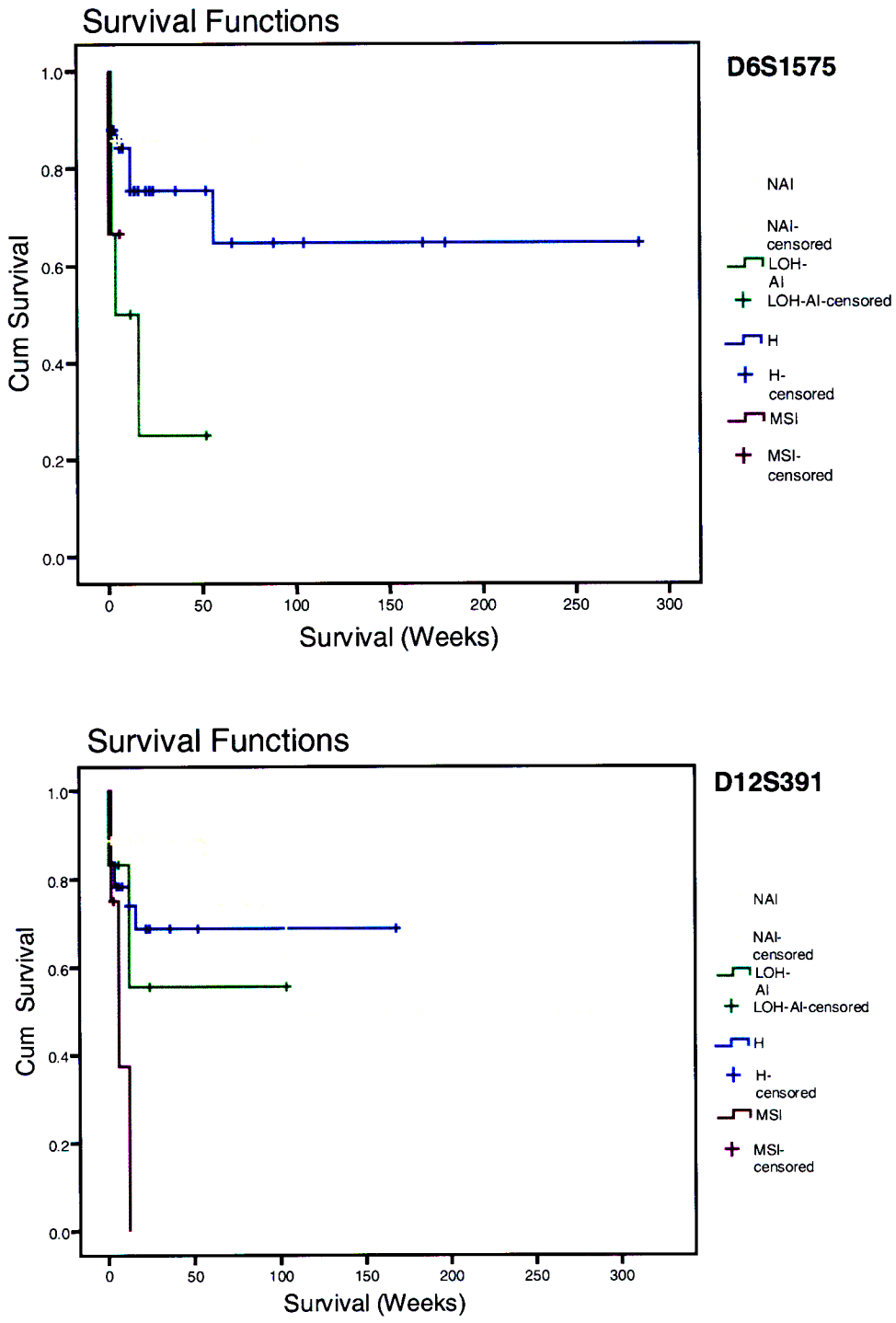

Figure 29: Trends in survival for markers D6S1575 and D12S391.

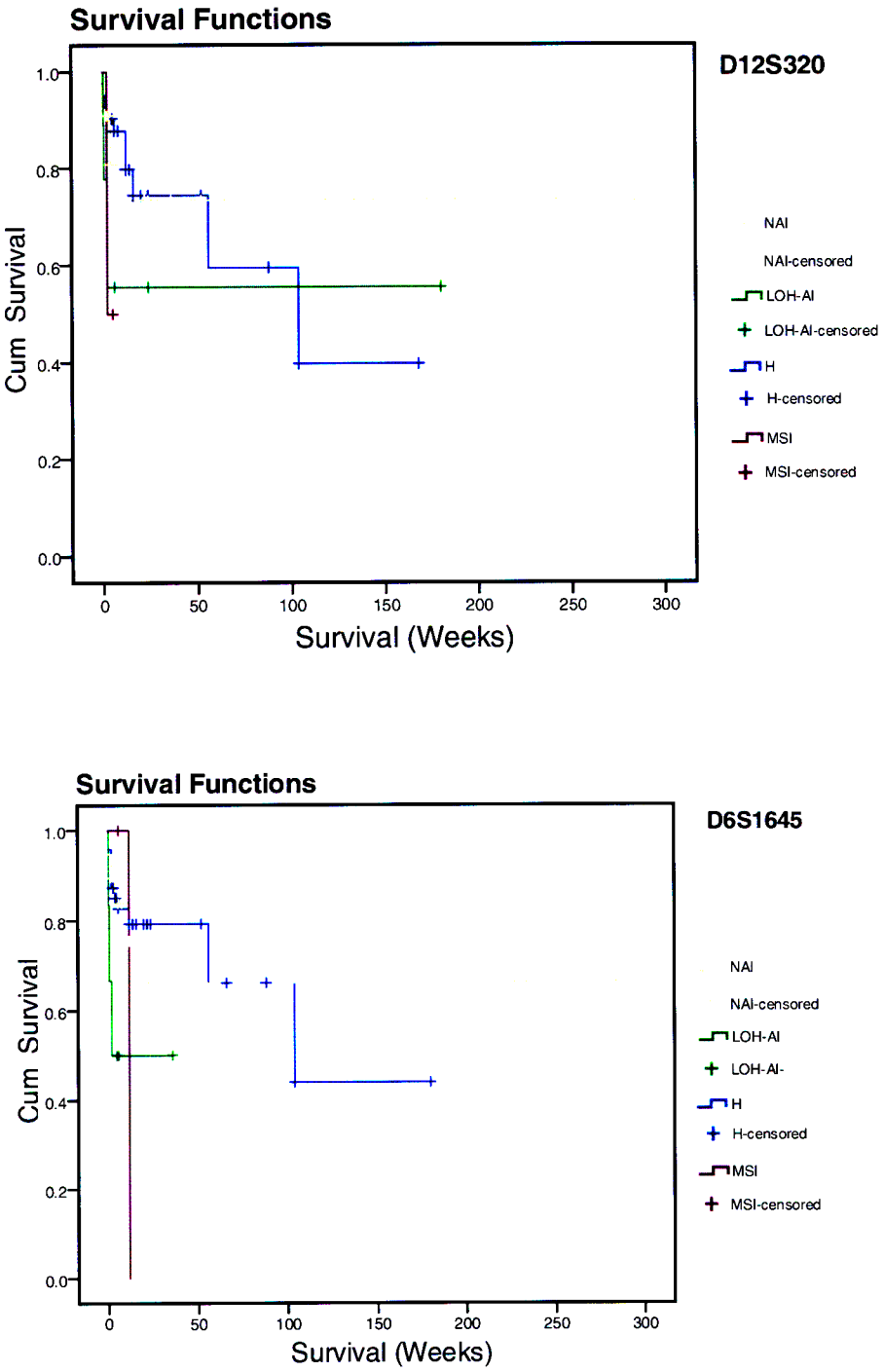

Figure 30: Trends in survival for markers D12S320 and D6S1645

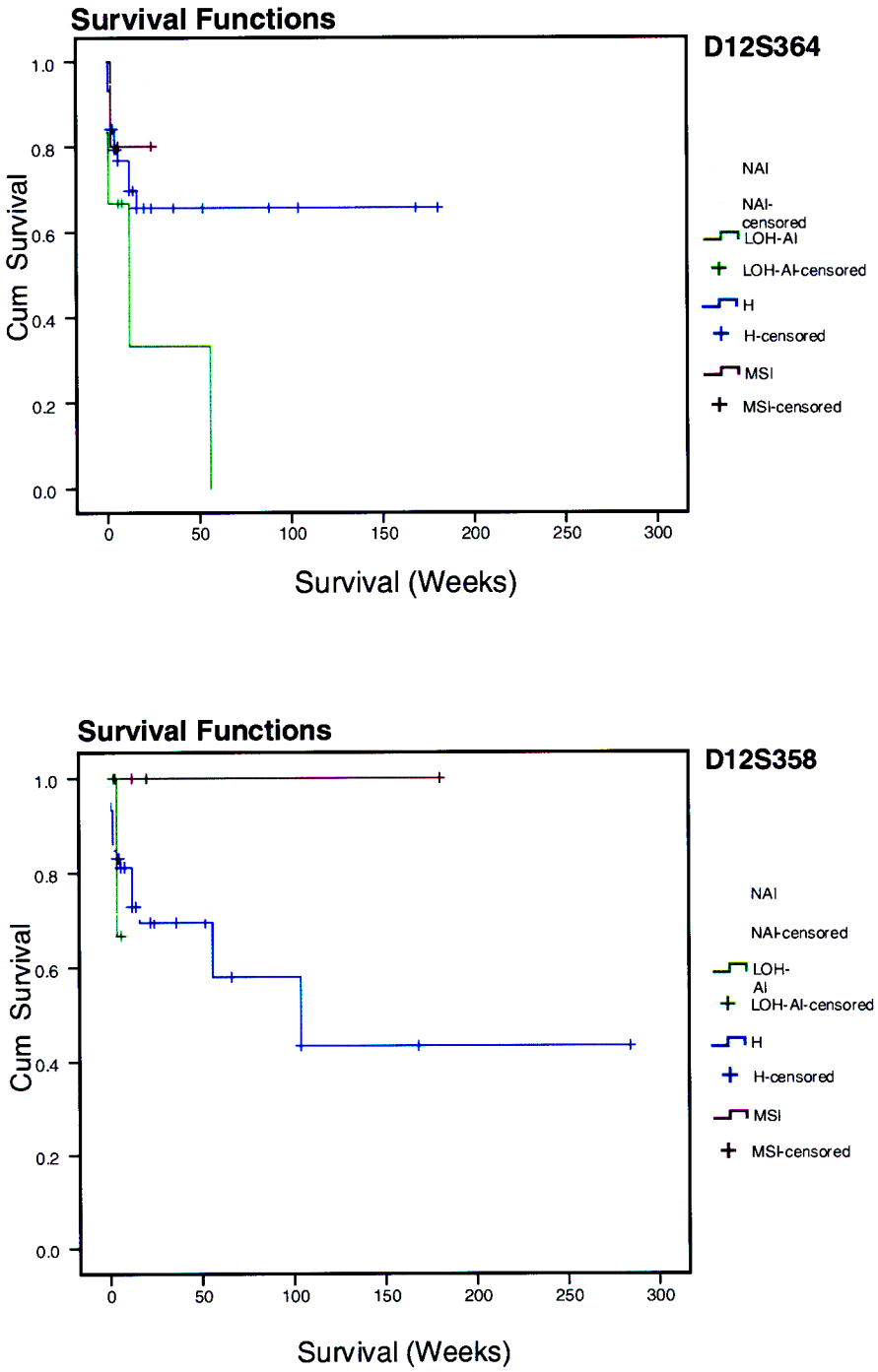

Figure 31: Trends in survival for markers D12S364 and D12S358

CHAPTER FOUR

Discussion

4.1 *p27*-related markers

Several loci in the vicinity of the *p27* gene have been evaluated for their tumour suppressor activity across a wide range of cancers. Hoornaert and colleagues (2003) have summarized and described a commonly deleted region containing tumour suppressor activity between markers D12S77 and D12S358. The 4 markers investigated in this study, as well as the *p27* gene that they surround, are located in this region.

Previous studies have focused on a relatively large region of the 12p locus, which contains *p27* and *ETV6/TEL* (Hetet *et al.*, 2000). LOH-AI was shown to occur frequently in these studies. Such reports on the 12p region uncovered many tumour suppressor genes (TSG's), however the exact role of these genes has not been established (Hetet *et al.*, 2000). In addition, since the deletions occur over a broad area, it is unclear as to which loci within this region are critical to cancer development. Further, no study to date has described in detail the genetic status of this region with regard to OSCC. This is the first study that describes the status of the *p27* gene in a large cohort of OSCC's. Therefore, a comparison of these figures can only be made with other studies involving other cancer types. The frequencies of LOH-AI in the present study range from 19% to 37% (Chapter 3, Table 5, and Appendix E2)

In general, these results are lower than those reported in other cancer types. A study on T-cell leukaemia reported a frequency of 43% (Hetet *et al.*, 2000). Kibel and co-workers (2000) reported LOH frequencies of 23%, 30% and 47% in prostate adenocarcinoma. These increasing percentages were correspondingly associated with increasing disease severity. Takeuchi *et al.* (1996) and Li *et al.* (2003) also found relatively high frequencies of LOH in non-small cell lung carcinoma ranging from 33% to 50%, respectively.

With regard to the relationship between age and microsatellite aberrations, a Kruskal-Wallis test was performed to determine if any association existed. A plot of median age *vs.* microsatellite alteration for each marker (Figures 21 and 22) revealed certain trends. While the results of these tests were not statistically significant ($p>0.05$, Appendix E3), the trends that were indicated are noteworthy. Figures 21 (c) and (d) illustrate markers D12S320 and D12S391, where an increased frequency of LOH-AI is associated with older patients. The median age for the occurrence of LOH-AI in marker D12S391 was found to be 63. Similarly, marker D12S320 showed a median age of 60. These results are in comparison to the other microsatellite alterations that were recorded *viz.*, H, NAI and MSI, where the median age for occurrence ranged from the lower to mid-fifties.

For the other two *p27*-related markers, *viz.* D12S364 and D12S358, a different pattern is configured. Figures 21(a) and (b) indicate that MSI was found to occur most frequently in older patients, when compared to other microsatellite alterations that were recorded. The median age for MSI occurrence in marker D12S364 is 60. Similarly, the median age for marker

D12S358 is 61. H, NAI and LOH-AI occurred most frequently in patients that were younger, with median ages ranging from 53 to 58.

Whilst not statistically significant, the results for age clearly indicate the emergence of a trend for higher frequencies of genetic aberrations among older patients. This would imply that genetic instability is not a significant feature in younger patients with OSCC, in view of the markers selected for this study. A search of the literature available to date shows that patient age has not been significantly associated with microsatellite aberrations in OSCC (Hu *et al.*, 2005; Kubo *et al.*, 2005; Liu *et al.*, 2005). Furthermore, the apparent lack of microsatellite aberrations in younger patients may indicate a greater role for environmental risk factors in the development of OSCC within our geographic setting. Low MSI and LOH frequencies have also been reported in earlier studies conducted within our laboratory. In a study conducted on sporadic gastric cancer, Chetty and co-workers (2002) reported low MSI and LOH frequencies, and no significant correlation with any clinico-pathological parameter. Another study on OSCC and mismatch repair genes, also found similar results (Naidoo *et al.*, 2005).

Microsatellite markers were further analyzed using the chi-squared test for association with sex, tumour type, tumour grade, lymph node metastases, TNM staging and outcome (Appendices E1 & E2). Most of the tests indicated no significant relationship between microsatellite alterations, and the clinico-pathological parameter being investigated.

For the *p27*-related markers, the relationship between sex and marker D12S391 was found to be significant ($p<0.05$, Appendix E1, Table 2). Analysis of the cross tabulation (Appendix E2,

section 2) revealed that the relationship was found to exist between NAI and men. NAI was found to occur in 46.3% of men (Appendix E2, section 2). This result in itself may not be clinically relevant. However, it suggests that marker D12S391 is stable in men, and therefore not significant for OSCC development.

Kibel *et al.* (2000) described increasing LOH frequencies that were associated with increased disease severity in prostate adenocarcinoma. Two of the markers used in the present study, *viz.*, D12S391 and D12S358 were also part of their analyses. These researchers concluded that LOH was strongly associated with primary tumours, as well as metastatic disease. They also found that the pattern of genetic loss was identical in all metastatic sites within an individual. This indicated that LOH occurred before metastases and was clonal in origin. Despite using the same markers, the results obtained in our study were not as significant as Kibel and colleagues, and no similar association was observed in metastatic OSCC. This may be due to the fact that these markers are cancer-specific.

A Kaplan-Meier test for survival showed a significant relationship between survival time after surgery, and markers D12S391 and D12S364 (Chapter 3, Table 9). Marker D12S391, as shown in Figure 29, revealed that MSI is associated with a reduced time for survival following surgery. For marker D12S364, cases that were recorded as LOH-AI were significantly associated with reduced survival time. A study on microsatellite instability in OSCC found similar results using different markers (Eisenberger *et al.*, 2003). Those researchers concluded that whilst clinical follow-up was limited, increased chances of survival were still associated with fewer microsatellite alterations. In our study, follow-up time after surgery was substantial,

and the results obtained are therefore more accurate in describing the relationship between survival and microsatellite alterations.

Despite the fact that there were a limited number of MSI and LOH-AI cases, it does not impact severely on the significance of the result. This is because the number of weeks of survival following surgery in MSI and LOH-AI cases is dramatically lower than that of other microsatellite alterations. Thus, the risk of there being ambiguity in the interpretation of the Kaplan-Meier plots is minimal. These results are significant, as these markers may successfully be applied as independent prognostic tools in predicting the survival probabilities of patients that display an MSI or LOH-AI genotype. For such patients, this finding may afford the clinician the opportunity to decide on management of the disease *via* non-surgical means.

4.2 *p21*-related markers

With regard to the *p21* related markers, D6S1645 shows relatively low LOH-AI at 33% (Table 6). Marker D6S1575 however, displays frequent LOH-AI at 47% (Table 6), and is similar to other reports on the 6p region. Most of those studies used markers that were closely mapped to the human leukocyte antigen (*HLA*) class 1 major histocompatibility complex (*MHC*). Loss of genetic material in the vicinity of the *MHC* genes, which are located at 6p21.3, have been implicated in various malignancies. These include colorectal cancer, head and neck squamous cell carcinoma, cervical cancer, leukaemia and astrocytoma (Honchel *et al.*, 1996); (Saitoh *et al.*, 1998); (Feenstra *et al.*, 1999); (Koopman *et al.*, 2000) and (Bevan *et al.*, 2000).

Very few studies have focused on the 6p21.2 region, which harbours the *p21* gene. A report by (Harima *et al.*, 2000) who investigated this locus for genetic aberrations in cervical cancer found a direct correlation between high LOH frequencies and cancer relapse following chemotherapy. They also found LOH to be significantly associated with a decreased rate of survival. However, no study to date has implicated the 6p21.2 locus in OSCC. The high LOH-AI (47%, Table 6) observed at D6S1575 is noteworthy; in that it may be an important region in OSCC development that warrants further investigation. For the *p21*-related markers in our study, no association could be made between microsatellite alterations and survival.

In a study on OSCC, Nie and co-workers (2001) investigated DNA hypermethylation as a mechanism for loss of expression of the *HLA class I* genes located at 6p21. They found a high frequency of LOH (44%) associated with *p21*, in comparison to that observed among the *HLA-I* genes (8-25%). The LOH frequencies for markers near *p21* are comparable to marker D6S1575 that was used in our study, where LOH-AI occurred at 47%. In addition, those researchers also reported that LOH frequency increased closer to *p21* and beyond downstream of the *HLA-I* genes (Nie *et al.*, 2001). This suggested that either *p21* itself or regions further downstream were targets of inactivation through LOH. These researchers also hypothesized that LOH frequencies were lower because DNA hypermethylation at the *HLA* sites helped to reduce genomic instability at genes located nearby. This may suggest that hypermethylation of genes close to D6S1645 may contribute to the relatively low LOH-AI frequency.

With regard to the Kruskal-Wallis test that was performed for association with age, markers D6S1645 and D6S1575 were not found to be significantly associated. However, as was the

case for the *p27*-related markers, there are clear trends towards an association of LOH-AI and MSI with advanced age. For marker D6S1575, a median age of 64 was found to be associated with MSI cases, in comparison to the other microsatellite alterations, which were associated with younger patients. For D6S1645, LOH-AI cases showed a median age of 62, which was also higher than any other aberration recorded. As was the case with the *p27*-related markers, a pattern of increased genetic instability that is associated with advanced age is observed.

A Chi-squared test for association with the other clinico-pathological parameters was also carried out for the *p21*-related markers. Tumour grade was found to be significantly associated with microsatellite aberrations in marker D6S1575 ($p<0.05$, Appendix E1, Table 1). Analysis of the cross tabulation for this marker shows that the relationship may lie with poorly differentiated (PD) tumours (Appendix E2, section 1). 20% of all PD tumours display LOH-AI and MSI. This is in comparison to the other tumour grades, where LOH-AI ranges from 4% to 6%, and MSI ranges from 0% to 2%. This result must be interpreted with caution, since only 10% of tumours that were analyzed were PD. Future investigations into the relationship between this marker and microsatellite aberrations are required, using a much larger set of PD-graded tumours. This will allow for a more accurate assessment of the exact nature of the relationship between D6S1575 and tumour grade. The relationship between tumour grade and microsatellite aberrations is important, since it would provide invaluable information to the clinician about prognosis.

CHAPTER FIVE

Conclusion

Microsatellite aberrations occur infrequently among the markers that were used in this study, with the exception of marker D6S1575. There was also a significant association between poorly differentiated tumours and this marker. Further investigations into the association between marker D6S1575 and poorly differentiated tumours will provide a more accurate reflection of the nature of the relationship. Amongst the *p27*-related markers, D12S391 and D12S364 aberrations were significantly associated with reduced survival time, indicating that they may be used as predictive markers of survival for patients with OSCC.

The genetic variation due to different geographic locations may be an important feature in OSCC. This would account for the low levels of microsatellite aberrations that were found in this study, in comparison to similar reports elsewhere. Despite the low LOH-AI and MSI levels that are reported, the most significant outcome of this study has been the association between markers D12S391 and D12S364, and reduced survival time. These markers may be used as reliable predictors of survival in OSCC patients, thereby helping clinicians make informed choices about treatment options.

Previously, autoradiography was used in detecting microsatellite PCR products. Most studies now use a fluorescent-based technique, since it has been found to be simpler and more

accurate. The fluorescent-based PCR assay that was used in this study was also found to be accurate and sensitive.

REFERENCES

Ahrendt, S. A., Chow, J. T., Yang, S. C., Wu, L., Zhang, M. J., Jen, J., and Sidransky, D. (2000). Alcohol consumption and cigarette smoking increase the frequency of p53 mutations in non-small cell lung cancer. *Cancer Res* **60**, 3155-3159.

Ajchenbaum, F., Ando, K., DeCaprio, J. A., and Griffin, J. D. (1993). Independent regulation of human D-type cyclin gene expression during G1 phase in primary human T lymphocytes. *J Biol Chem* **268**, 4113-4119.

Allum, W. H., Griffin, S. M., Watson, A., and Colin-Jones, D. (2002). Guidelines for the management of oesophageal and gastric cancer. *Gut* **50 Suppl 5**, v1-23.

Anayama, T., Furihata, M., Ishikawa, T., Ohtsuki, Y., and Ogoshi, S. (1998). Positive correlation between p27Kip1 expression and progression of human esophageal squamous cell carcinoma. *Int J Cancer* **79**, 439-443.

Ashton-Rickardt, P. G., Wyllie, A. H., Bird, C. C., Dunlop, M. G., Steel, C. M., Morris, R. G., Piris, J., Romanowski, P., Wood, R., White, R., and et al. (1991). MCC, a candidate familial polyposis gene in 5q.21, shows frequent allele loss in colorectal and lung cancer. *Oncogene* **6**, 1881-1886.

Baekelandt, M., Holm, R., Trope, C. G., Nesland, J. M., and Kristensen, G. B. (1999). Lack of independent prognostic significance of p21 and p27 expression in advanced ovarian cancer: an immunohistochemical study. *Clin Cancer Res* **5**, 2848-2853.

Bains, M. S. (1995). Ivor Lewis esophagectomy. *Chest Surg Clin N Am* **5**, 515-526.

Balbin, M., Hannon, G. J., Pendas, A. M., Ferrando, A. A., Vizoso, F., Fueyo, A., and Lopez-Otin, C. (1996). Functional analysis of a p21WAF1,CIP1,SDI1 mutant (Arg94 --> Trp) identified in a human breast carcinoma. Evidence that the mutation impairs the ability of p21 to inhibit cyclin-dependent kinases. *J Biol Chem* **271**, 15782-15786.

Barbareschi, M., Doglioni, C., Veronese, S., Bonzanini, M., Dalla Palma, P., Harris, A. L., and Caffo, O. (1996). p21WAF1 and p53 immunohistochemical expression in breast carcinoma may predict therapeutic response to adjuvant treatment. *Eur J Cancer* **32A**, 2182-2183.

Baylin, S. (2001). DNA methylation and epigenetic mechanisms of carcinogenesis. *Dev Biol (Basel)* **106**, 85-87; discussion 143-160.

Bennett, P. (2000). Demystified ... microsatellites. *Mol Pathol* **53**, 177-183.

Bennett, W. P., von Brevern, M. C., Zhu, S. M., Bartsch, H., Muehlbauer, K. R., and Hollstein, M. C. (1997). p53 mutations in esophageal tumors from a high incidence area of China in relation to patient diet and smoking history. *Cancer Epidemiol Biomarkers Prev* **6**, 963-966.

Bevan, S., Catovsky, D., Matutes, E., Antunovic, P., Auger, M. J., Ben-Bassat, I., Bell, A., Berrebi, A., Gaminara, E. J., Junior, M. E., Mauro, F. R., Quabeck, K., Rassam, S. M., Reid, C., Ribeiro, I., Stark, P., van Dongen, J. J., Wimperis, J., Wright, S., Marossy, A., Yuille, M. R., and Houlston, R. S. (2000). Linkage analysis for major histocompatibility complex-related genetic susceptibility in familial chronic lymphocytic leukemia. *Blood* **96**, 3982-3984.

Bhatia, K., Fan, S., Spangler, G., Weintraub, M., O'Connor, P. M., Judde, J. G., and Magrath, I. (1995). A mutant p21 cyclin-dependent kinase inhibitor isolated from a Burkitt's lymphoma. *Cancer Res* **55**, 1431-1435.

Biramijamal, F., Allameh, A., Mirbod, P., Groene, H. J., Koomagi, R., and Hollstein, M. (2001). Unusual profile and high prevalence of p53 mutations in esophageal squamous cell carcinomas from northern Iran. *Cancer Res* **61**, 3119-3123.

Block, M. I., Patterson, G. A., Sundaresan, R. S., Bailey, M. S., Flanagan, F. L., Dehdashti, F., Siegel, B. A., and Cooper, J. D. (1997). Improvement in staging of esophageal cancer with the addition of positron emission tomography. *Ann Thorac Surg* **64**, 770-776; discussion 776-777.

Blot, W. J. (1994). Esophageal cancer trends and risk factors. *Semin Oncol* **21**, 403-410.

Botet, J. F., Lightdale, C. J., Zauber, A. G., Gerdes, H., Urmacher, C., and Brennan, M. F. (1991). Preoperative staging of esophageal cancer: comparison of endoscopic US and dynamic CT. *Radiology* **181**, 419-425.

Boynton, R. F., Blount, P. L., Yin, J., Brown, V. L., Huang, Y., Tong, Y., McDaniel, T., Newkirk, C., Resau, J. H., Raskind, W. H., and et al. (1992). Loss of heterozygosity involving the APC and MCC genetic loci occurs in the majority of human esophageal cancers. *Proc Natl Acad Sci U S A* **89**, 3385-3388.

Brentnall, T. A., Crispin, D. A., Bronner, M. P., Cherian, S. P., Hueffed, M., Rabinovitch, P. S., Rubin, C. E., Haggitt, R. C., and Boland, C. R. (1996). Microsatellite instability in nonneoplastic mucosa from patients with chronic ulcerative colitis. *Cancer Res* **56**, 1237-1240.

Brook, J., McCurrach, M. E., and Harley, H. G. (1992). Molecular basis of myotonic dystrophy: expansion of a trinucleotide (CTG) repeat at the 3' end of a transcript encoding a protein kinase family member. *Cell* **68**, 799-808.

Casson, A. G. (1998). Molecular biology of Barrett's esophagus and esophageal cancer:role of p53. *World J Gastroenterol* **4**, 277-279.

Castelletto, R., Castellsague, X., Munoz, N., Iscovich, J., Chopita, N., and Jmelnitsky, A. (1994). Alcohol, tobacco, diet, mate drinking, and esophageal cancer in Argentina. *Cancer Epidemiol Biomarkers Prev* **3**, 557-564.

Catzavelos, C., Bhattacharya, N., Ung, Y. C., Wilson, J. A., Roncari, L., Sandhu, C., Shaw, P., Yeger, H., Morava-Protzner, I., Kapusta, L., Franssen, E., Pritchard, K. I., and Slingerland, J. M. (1997). Decreased levels of the cell-cycle inhibitor p27Kip1 protein: prognostic implications in primary breast cancer. *Nat Med* **3**, 227-230.

Catzavelos, C., Tsao, M. S., DeBoer, G., Bhattacharya, N., Shepherd, F. A., and Slingerland, J. M. (1999). Reduced expression of the cell cycle inhibitor p27Kip1 in non-small cell lung carcinoma: a prognostic factor independent of Ras. *Cancer Res* **59**, 684-688.

Cawkwell, L., Li, D., Lewis, F. A., Martin, I., Dixon, M. F., and Quirke, P. (1995). Microsatellite instability in colorectal cancer: improved assessment using fluorescent polymerase chain reaction. *Gastroenterology* **109**, 465-471.

Chen, B., Yin, H., and Dhurandhar, N. (1994). Detection of human papillomavirus DNA in esophageal squamous cell carcinomas by the polymerase chain reaction using general consensus primers. *Hum Pathol* **25**, 920-923.

Cheng, J. D., Werness, B. A., Babb, J. S., and Meropol, N. J. (1999). Paradoxical correlations of cyclin-dependent kinase inhibitors p21waf1/cip1 and p27kip1 in metastatic colorectal carcinoma. *Clin Cancer Res* **5**, 1057-1062.

Chetty, R., Naidoo, R., and Schneider, J. (1998). Allelic imbalance and microsatellite instability of the DCC gene in colorectal cancer in patients under the age of 35 using fluorescent DNA technology. *J Clin Pathol:Mol Pathol* **51**, 35-38.

Consigliere, D., Chua, C. L., Hui, F., Yu, C. S., and Low, C. H. (1992). Computed tomography for oesophageal carcinoma: its value to the surgeon. *J R Coll Surg Edinb* **37**, 113-117.

Cordon-Cardo, C., Koff, A., Drobnjak, M., Capodieci, P., Osman, I., Millard, S. S., Gaudin, P. B., Fazzari, M., Zhang, Z. F., Massague, J., and Scher, H. I. (1998). Distinct altered patterns of p27KIP1 gene expression in benign prostatic hyperplasia and prostatic carcinoma. *J Natl Cancer Inst* **90**, 1284-1291.

Cote, R. J., Shi, Y., Groshen, S., Feng, A. C., Cordon-Cardo, C., Skinner, D., and Lieskovosky, G. (1998). Association of p27Kip1 levels with recurrence and survival in patients with stage C prostate carcinoma. *J Natl Cancer Inst* **90**, 916-920.

Crofts, T. J. (2000). Ivor-Lewis oesophagectomy for middle and lower third oesophageal lesions--how we do it. *J R Coll Surg Edinb* **45**, 296-303.

Dahia, P. L., Aguiar, R. C., Honegger, J., Fahlbush, R., Jordan, S., Lowe, D. G., Lu, X., Clayton, R. N., Besser, G. M., and Grossman, A. B. (1998). Mutation and expression analysis of the p27/kip1 gene in corticotrophin-secreting tumours. *Oncogene* **16**, 69-76.

Debrauwere, H., Gendrel, C. G., Lechat, S., and Dutreix, M. (1997). Differences and similarities between various tandem repeat sequences: minisatellites and microsatellites. *Biochimie* **79**, 577-586.

Deng, C., Zhang, P., Harper, J. W., Elledge, S. J., and Leder, P. (1995). Mice lacking p21CIP1/WAF1 undergo normal development, but are defective in G1 checkpoint control. *Cell* **82**, 675-684.

Doki, Y., Imoto, M., Han, E. K., Sgambato, A., and Weinstein, I. B. (1997). Increased expression of the P27KIP1 protein in human esophageal cancer cell lines that over-express cyclin D1. *Carcinogenesis* **18**, 1139-1148.

Eisenberger, C. F., Knoefel, W. T., Peiper, M., Merkert, P., Yekebas, E. F., Scheunemann, P., Steffani, K., Stoecklein, N. H., Hosch, S. B., and Izbicki, J. R. (2003). Squamous cell carcinoma of the esophagus can be detected by microsatellite analysis in tumor and serum. *Clin Cancer Res* **9**, 4178-4183.

el-Deiry, W. S., Harper, J. W., O'Connor, P. M., Velculescu, V. E., Canman, C. E., Jackman, J., Pietenpol, J. A., Burrell, M., Hill, D. E., Wang, Y., and et al. (1994). WAF1/CIP1 is induced in p53-mediated G1 arrest and apoptosis. *Cancer Res* **54**, 1169-1174.

el-Deiry, W. S., Tokino, T., Velculescu, V. E., Levy, D. B., Parsons, R., Trent, J. M., Lin, D., Mercer, W. E., Kinzler, K. W., and Vogelstein, B. (1993). WAF1, a potential mediator of p53 tumor suppression. *Cell* **75**, 817-825.

Enzinger, P. C., and Mayer, R. J. (2003). Esophageal Cancer. *N Engl J Med* **349**, 2241-2252.

Erkal, H. S., Mendenhall, W. M., Amdur, R. J., Villaret, D. B., and Stringer, S. P. (2001). Synchronous and metachronous squamous cell carcinomas of the head and neck mucosal sites. *J Clin Oncol* **19**, 1358-1362.

Erlanson, M., Portin, C., Linderholm, B., Lindh, J., Roos, G., and Landberg, G. (1998). Expression of cyclin E and the cyclin-dependent kinase inhibitor p27 in malignant lymphomas-prognostic implications. *Blood* **92**, 770-777.

Farhadi, M., Tahmasebi, Z., Merat, S., Kamangar, F., Nasrollahzadeh, D., and Malekzadeh, R. (2005). Human papillomavirus in squamous cell carcinoma of esophagus in a high-risk population. *World J Gastroenterol* **11**, 1200-1203.

Feenstra, M., Veltkamp, M., van Kuik, J., Wiertsema, S., Slootweg, P., van den Tweel, J., de Weger, R., and Tilanus, M. (1999). HLA class I expression and chromosomal deletions

at 6p and 15q in head and neck squamous cell carcinomas. *Tissue Antigens* **54**, 235-245.

Fein R, Kelsen D. P., Geller N, Bains M, McCormack P, and Brennan, M. F. (1985). Adenocarcinoma of the esophagus and gastroesophageal junction: prognostic factors and results of therapy. *Cancer* **56**, 2512-2518.

Ferrando, A. A., Balbin, M., Pendas, A. M., Vizoso, F., Velasco, G., and Lopez-Otin, C. (1996). Mutational analysis of the human cyclin-dependent kinase inhibitor p27kip1 in primary breast carcinomas. *Hum Genet* **97**, 91-94.

Fishel, R., Lescoe, M. K., Rao, M. R., Copeland, N. G., Jenkins, N. A., Garber, J., Kane, M., and Kolodner, R. (1993). The human mutator gene homolog MSH2 and its association with hereditary nonpolyposis colon cancer. *Cell* **75**, 1027-1038.

Florenes, V. A., Maelandsmo, G. M., Kerbel, R. S., Slingerland, J. M., Nesland, J. M., and Holm, R. (1998). Protein expression of the cell-cycle inhibitor p27Kip1 in malignant melanoma: inverse correlation with disease-free survival. *Am J Pathol* **153**, 305-312.

Geng, Y., Yu, Q., Sicinska, E., Das, M., Bronson, R. T., and Sicinski, P. (2001). Deletion of the p27Kip1 gene restores normal development in cyclin D1-deficient mice. *Proc Natl Acad Sci U S A* **98**, 194-199.

Gramlich, T. L., Fritsch, C. R., Maurer, D., Eberle, M., and Gansler, T. S. (1994). Differential polymerase chain reaction assay of cyclin D1 gene amplification in esophageal carcinoma. *Diagn Mol Pathol* **3**, 255-259.

Grimm, H., Binmoeller, K. F., Hamper, K., Koch, J., Henne-Bruns, D., and Sochendra, N. (1993). Endosonography for preoperative locoregional staging of esophageal and gastric cancer. *Endoscopy* **25**, 224-230.

Gurski, R., Schirmer, C., Kruel, C., Komlos, F., Kruel, C., and Edelweis, M. (1999). Induction of esophageal carcinogenesis by diethylnitrosamine and assessment of the promoting effect of ethanol and N-nitrosonornicotine: experimental model in mice. *Dis Esophagus* **12**, 99-105.

Gusella, J. F., MacDonald, M. E., Ambrose, C. M., and Duyao, M. P. (1993). Molecular genetics of Huntington's disease. *Arch Neurol* **50**, 1157-1163.

Hamada, M., Naomoto, Y., Fujiwara, T., Kamikawa, Y., and Tanaka, N. (1996). Suppressed apoptotic induction in esophageal squamous cell carcinomas expressing extensive p53 protein. *Jpn J Clin Oncol* **26**, 398-404.

Harada, N., Gansauge, S., Gansauge, F., Gause, H., Shimoyama, S., Imaizumi, T., Mattfeld, T., Schoenberg, M. H., and Beger, H. G. (1997). Nuclear accumulation of p53 correlates significantly with clinical features and inversely with the expression of the cyclin-dependent kinase inhibitor p21(WAF1/CIP1) in pancreatic cancer. *Br J Cancer* **76**, 299-305.

Harima, Y., Harima, K., Sawada, S., Tanaka, Y., Arita, S., and Ohnishi, T. (2000). Loss of heterozygosity on chromosome 6p21.2 as a potential marker for recurrence after radiotherapy of human cervical cancer. *Clin Cancer Res* **6**, 1079-1085.

Harper, J. W., Adami, G. R., Wei, N., Keyomarsi, K., and Elledge, S. J. (1993). The p21 Cdk-interacting protein Cip1 is a potent inhibitor of G1 cyclin-dependent kinases. *Cell* **75**, 805-816.

Hayashi, H., Miyamoto, H., Ito, T., Kameda, Y., Nakamura, N., Kubota, Y., and Kitamura, H. (1997). Analysis of p21Waf1/Cip1 expression in normal, premalignant, and malignant

cells during the development of human lung adenocarcinoma. *Am J Pathol* **151**, 461-470.

Hennings, H., Glick, A. B., Greenhalgh, D. A., Morgan, D. L., Strickland, J. E., Tennenbaum, T., and Yuspa, S. H. (1993). Critical aspects of initiation, promotion, and progression in multistage epidermal carcinogenesis. *Proc Soc Exp Biol Med* **202**, 1-8.

Hetet, G., Dastot, H., Baens, M., Brizard, A., Sigaux, F., Grandchamp, B., and Stern, M. H. (2000). Recurrent molecular deletion of the 12p13 region, centromeric to ETV6/TEL, in T-cell prolymphocytic leukemia. *Hematol J* **1**, 42-47.

Hiltunen, M. O., Alhonen, L., Koistinaho, J., Myohanen, S., Paakkonen, M., Marin, S., Kosma, V. M., and Janne, J. (1997). Hypermethylation of the APC (adenomatous polyposis coli) gene promoter region in human colorectal carcinoma. *Int J Cancer* **70**, 644-648.

Hirai, T., Kuwahara, M., Yoshida, K., Kagawa, Y., Hihara, J., Yamashita, Y., and Toge, T. (1998). Clinical results of transhiatal esophagectomy for carcinoma of the lower thoracic esophagus according to biological markers. *Dis Esophagus* **11**, 221-225.

Holliday, R. (2005). DNA methylation and epigenotypes. *Biochemistry (Mosc)* **70**, 500-504.

Hollywood, D. P and Barton, C. M. (1994). Oncogenes and Tumour Suppressor Genes. In *Cancer: a molecular approach* (N. Lemoine, J. Neoptolemos, and T. Cooke, Eds.), pp. 13-38. Blackwell Scientific Publications, Oxford.

Honchel, R., McDonnell, S., Schaid, D. J., and Thibodeau, S. N. (1996). Tumor necrosis factor-alpha allelic frequency and chromosome 6 allelic imbalance in patients with colorectal cancer. *Cancer Res* **56**, 145-149.

Hoornaert, I., Marynen, P., Goris, J., Sciot, R., and Baens, M. (2003). MAPK phosphatase DUSP16/MKP-7, a candidate tumor suppressor for chromosome region 12p12-13, reduces BCR-ABL-induced transformation. *Oncogene* **22**, 7728-7736.

Hori, H., Kawano, T., Endo, M., and Yuasa, Y. (1997). Genetic polymorphisms of tobacco and alcohol-related metabolizing enzymes and human esophageal squamous cell carcinoma susceptibility. *J Clin Gastroenterol* **25**, 568-575.

Hu, J., Nyren, O., and Wolk, A. (1994). Risk factors for oesophageal cancer in northeast China. *Int J Cancer* **57**, 38-46.

Hu, N., Su, H., Li, W. J., Giffen, C., Goldstein, A. M., Hu, Y., Wang, C., Roth, M. J., Li, G., Dawsey, S. M., Xu, Y., Taylor, P. R., and Emmert-Buck, M. R. (2005). Allelotyping of esophageal squamous-cell carcinoma on chromosome 13 defines deletions related to family history. *Genes Chromosomes Cancer* **44**, 271-278.

Ionov, Y., Peinado, M. A., Malkhosyan, S., Shibata, D., and Perucho, M. (1993). Ubiquitous somatic mutations in simple repeated sequences reveal a new mechanism for colonic carcinogenesis. *Nature* **363**, 558-561.

Isaacson, C. (2005). The change of the staple diet of black South Africans from sorghum to maize (corn) is the cause of the epidemic of squamous carcinoma of the oesophagus. *Med Hypotheses* **64**, 658-660.

Ishikawa, T., Furihata, M., Ohtsuki, Y., Murakami, H., Inoue, A., and Ogoshi, S. (1998). Cyclin D1 overexpression related to retinoblastoma protein expression as a prognostic marker in human oesophageal squamous cell carcinoma. *Br J Cancer* **77**, 92-97.

Iwamoto, M., Ahnen, D. J., Franklin, W. A., and Maltzman, T. H. (2000). Expression of beta-catenin and full-length APC protein in normal and neoplastic colonic tissues. *Carcinogenesis* **21**, 1935-1940.

Jones, G. J., Heiss, N. S., Veale, R. B., and Thornley, A. L. (1993). Amplification and expression of the TGF-alpha, EGF receptor and c-myc genes in four human oesophageal squamous cell carcinoma lines. *Biosci Rep* **13**, 303-312.

Jung, J. M., Bruner, J. M., Ruan, S., Langford, L. A., Kyritsis, A. P., Kobayashi, T., Levin, V. A., and Zhang, W. (1995). Increased levels of p21WAF1/Cip1 in human brain tumors. *Oncogene* **11**, 2021-2028.

Kallioniemi, O. P., Kallioniemi, A., Kurisu, W., Thor, A., Chen, L. C., Smith, H. S., Waldman, F. M., Pinkel, D., and Gray, J. W. (1992). ERBB2 amplification in breast cancer analyzed by fluorescence *in situ* hybridization. *Proc Natl Acad Sci U S A* **89**, 5321-5325.

Kane, M. F., Loda, M., Gaida, G. M., Lipman, J., Mishra, R., Goldman, H., Jessup, J. M., and Kolodner, R. (1997). Methylation of the hMLH1 promoter correlates with lack of expression of hMLH1 in sporadic colon tumors and mismatch repair-defective human tumor cell lines. *Cancer Res* **57**, 808-811.

Kato, H., Kato, S., Kumabe, T., Sonoda, Y., Yoshimoto, T., Han, S. Y., Suzuki, T., Shibata, H., Kanamaru, R., and Ishioka, C. (2000). Functional evaluation of p53 and PTEN gene mutations in gliomas. *Clin Cancer Res* **6**, 3937-3943.

Kawamata, N., Morosetti, R., Miller, C. W., Park, D., Spirin, K. S., Nakamaki, T., Takeuchi, S., Hatta, Y., Simpson, J., Wilcyznski, S., Lee, Y. Y., Bartram, C.and Koeffler, H. P. (1995). Molecular analysis of the cyclin-dependent kinase inhibitor gene p27/Kip1 in human malignancies. *Cancer Res* **55**, 2266-2269.

Kibel, A. S., Suarez, B. K., Belani, J., Oh, J., Webster, R., Brophy-Ebbers, M., Guo, C., Catalona, W. J., Picus, J., and Goodfellow, P. J. (2003). CDKN1A and CDKN1B polymorphisms and risk of advanced prostate carcinoma. *Cancer Res* **63**, 2033-2036.

Knudson, A. G., Jr. (1971). Mutation and cancer: statistical study of retinoblastoma. *Proc Natl Acad Sci U S A* **68**, 820-823.

Koff, A., Giordano, A., Desai, D., Yamashita, K., Harper, J. W., Elledge, S., Nishimoto, T., Morgan, D. O., Franza, B. R., and Roberts, J. M. (1992). Formation and activation of a cyclin E-cdk2 complex during the G1 phase of the human cell cycle. *Science* **257**, 1689-1694.

Koopman, L. A., Corver, W. E., van der Slik, A. R., Giphart, M. J., and Fleuren, G. J. (2000). Multiple genetic alterations cause frequent and heterogeneous human histocompatibility leukocyte antigen class I loss in cervical cancer. *J Exp Med* **191**, 961-976.

Krasna, M. J., Flowers, J. L., Attar, S., and McLaughlin, J. (1996). Combined thoracoscopic/laparoscopic staging of esophageal cancer. *J Thorac Cardiovasc Surg* **111**, 800-806; discussion 806-807.

Kubo, N., Yashiro, M., Ohira, M., Hori, T., Fujiwara, I., and Hirakawa, K. (2005). Frequent microsatellite instability in primary esophageal carcinoma associated with extraesophageal primary carcinoma. *Int J Cancer* **114**, 166-173.

LaBaer, J., Garrett, M. D., Stevenson, L. F., Slingerland, J. M., Sandhu, C., Chou, H. S., Fattaey, A., and Harlow, E. (1997). New functional activities for the p21 family of CDK inhibitors. *Genes Dev* **11**, 847-862.

Lam, A. K. Y. (2000). Molecular Biology of esophageal squamous cell carcinoma. *Crit Rev Onc Hematol* **33**, 71-90.

Lam, K. Y., and Ma, L. (1997). Pathology of esophageal cancers: local experience and current insights. *Chin Med J (Engl)* **110**, 459-464.

Larsson, L. G., Sandstrom, A., and Westling, P. (1975). Relationship of Plummer-Vinson disease to cancer of the upper alimentary tract in Sweden. *Cancer Res* **35**, 3308-3316.

Lehrbach, D. M., Nita, M. E., and Cecconello, I. (2003). Molecular aspects of esophageal squamous cell carcinoma carcinogenesis. *Arq Gastroenterol* **40**, 256-261.

Leone, G., Sears, R., Huang, E., Rempel, R., Nuckolls, F., Park, C. H., Giangrande, P., Wu, L., Saavedra, H. I., Field, S. J., Thompson, M. A., Yang, H., Fujiwara, Y., Greenberg, M. E., Orkin, S., Smith, C., and Nevins, J. R. (2001). Myc requires distinct E2F activities to induce S phase and apoptosis. *Mol Cell* **8**, 105-113.

Liu, F. X., Huang, X. P., Xu, X., Cai, Y., Han, Y. L., Wu, R. L., Wu, M., Zhan, Q. M., and Wang, M. R. (2005). Alterations of MLH1 and microsatellite instability in esophageal squamous cell carcinomas. *Yi Chuan Xue Bao* **32**, 234-242.

Loda, M., Cukor, B., Tam, S. W., Lavin, P., Fiorentino, M., Draetta, G. F., Jessup, J. M., and Pagano, M. (1997). Increased proteasome-dependent degradation of the cyclin-dependent kinase inhibitor p27 in aggressive colorectal carcinomas. *Nat Med* **3**, 231-234.

Loeb, L. A., Loeb, K. R., and Anderson, J. P. (2003). Multiple mutations and cancer. *Proc Natl Acad Sci U S A* **100**, 776-781.

Lu, C. D., Morita, S., Ishibashi, T., Hara, H., Isozaki, H., and Tanigawa, N. (1999). Loss of p27Kip1 expression independently predicts poor prognosis for patients with resectable pancreatic adenocarcinoma. *Cancer* **85**, 1250-1260.

Luketich, J. D., Schauer, P., Landreneau, R., Nguyen, N., Urso, K., Ferson, P., Keenan, R., and Kim, R. (1997). Minimally invasive surgical staging is superior to endoscopic ultrasound in detecting lymph node metastases in esophageal cancer. *J Thorac Cardiovasc Surg* **114**, 817-821; discussion 821-813.

Lundberg, A. S., and Weinberg, R. A. (1998). Functional inactivation of the retinoblastoma protein requires sequential modification by at least two distinct cyclin-cdk complexes. *Mol Cell Biol* **18**, 753-761.

Mandard, A. M., Hainaut, P., and Hollstein, M. (2000). Genetic steps in the development of squamous cell carcinoma of the esophagus. *Mutat Res* **462**, 335-342.

Maniatis, T., Sambrook, J., and Fritsch, E. F. (1989). Chapter 14: *In vitro* amplification of DNA by the polymerase chain reaction. In *Molecular Cloning: A Laboratory Manual* (C. Nolan, Ed.). Cold Spring Harbor Laboratory Press, New York.

Marasas, W. F., van Rensburg, S. J., and Mirocha, C. J. (1979). Incidence of Fusarium species and the mycotoxins, deoxynivalenol and zearalenone, in corn produced in esophageal cancer areas in Transkei. *J Agric Food Chem* **27**, 1108-1112.

Marriette C, Maurel A, Fabre S, Balon J. M., and Triboulet J. P. (2001). Facteurs prognostiques preoperatoires des cancers epidermoides de l'oesophage thoracique. *Gastroenterol Clin Biol* **25**, 468-472.

Martinez, J. D., Parker, M. T., Fultz, K. E., Ignatenko, N. A., and Gerner, E. W. (2003). Molecular Biology of Cancer. In *Burger's Medicinal Chemistry and Drug Discovery* (D. J. Abraham, Ed.), pp. 1-49. John Wiley & Sons, Inc., Tuscon.

Mathew, R., Arora, S., Mathur, M., Chattopadhyay, T. K., and Ralhan, R. (2001). Esophageal squamous cell carcinomas with DNA replication errors (RER+) are associated with p16/pRb loss and wild-type p53. *J Cancer Res Clin Oncol* **127**, 603-612.

Matsushime, H., Roussel, M. F., and Sherr, C. J. (1991). Novel mammalian cyclins (CYL genes) expressed during G1. *Cold Spring Harb Symp Quant Biol* **56**, 69-74.

McCabe, M. L., and Dlamini, Z. (2005). The molecular mechanisms of oesophageal cancer. *Int Immunopharmacology* **5**, 1113-1130.

Minamoto, T., Mai, M., and Ronai, Z. (1999). Environmental factors as regulators and effectors of multistep carcinogenesis. *Carcinogenesis* **20**, 519-527.

Miyake, S., Nagai, K., Yoshino, K., Oto, M., Endo, M., and Yuasa, Y. (1994). Point mutations and allelic deletion of tumor suppressor gene DCC in human esophageal squamous cell carcinomas and their relation to metastasis. *Cancer Res* **54**, 3007-3010.

Moller, M. B. (2000). P27 in cell cycle control and cancer. *Leuk Lymphoma* **39**, 19-27.

Moller, M. B., Skjodt, K., Mortensen, L. S., and Pedersen, N. T. (1999). Clinical significance of cyclin-dependent kinase inhibitor p27Kip1 expression and proliferation in non-Hodgkin's lymphoma: independent prognostic value of p27Kip1. *Br J Haematol* **105**, 730-736.

Montesano, R., Hollstein, M., and Hainaut, P. (1996). Molecular etiopathogenesis of esophageal cancers. *Ann Ist Super Sanita* **32**, 73-84.

Moreira, L. F., Naomoto, Y., Hamada, M., Kamikawa, Y., and Orita, K. (1995). Assessment of apoptosis in oesophageal carcinoma preoperatively treated by chemotherapy and radiotherapy. *Anticancer Res* **15**, 639-644.

Mori, T., Aoki, T., Matsubara, T., Iida, F., Du, X., Nishihira, T., Mori, S., and Nakamura, Y. (1994). Frequent loss of heterozygosity in the region including BRCA1 on chromosome 17q in squamous cell carcinomas of the esophagus. *Cancer Res* **54**, 1638-1640.

Motokura, T., Bloom, T., Kim, H. G., Juppner, H., Ruderman, J. V., Kronenberg, H. M., and Arnold, A. (1991). A novel cyclin encoded by a bcl1-linked candidate oncogene. *Nature* **350**, 512-515.

Mousses, S., Ozcelik, H., Lee, P. D., Malkin, D., Bull, S. B., and Andrulis, I. L. (1995). Two variants of the CIP1/WAF1 gene occur together and are associated with human cancer. *Hum Mol Genet* **4**, 1089-1092.

Muc, R., and Naidoo, R. (2002). Microsatellite instability in diagnostic pathology. *Curr Diagn Pathol*, 1-10.

Munoz, N., Bosch, F. X., de Sanjose, S., Herrero, R., Castellsague, X., Shah, K. V., Snijders, P. J., and Meijer, C. J. (2003). Epidemiologic classification of human papillomavirus types associated with cervical cancer. *N Engl J Med* **348**, 518-527.

Myers, M. H., and Ries, L. A. (1989). Cancer patient survival rates: SEER program results for 10 years of follow-up. *CA Cancer J Clin* **39**, 21-32.

Naidoo, R., Ramburan, A., Reddi, A., and Chetty, R. (2005). Aberrations in the mismatch repair genes and the clinical impact on oesophageal squamous carcinomas from a high incidence area in South Africa. *J Clin Pathol* **58**, 281-284.

Nakagawa, H., Zukerberg, L., Togawa, K., Meltzer, S. J., Nishihara, T., and Rustgi, A. K. (1995). Human cyclin D1 oncogene and esophageal squamous cell carcinoma. *Cancer* **76**, 541-549.

Nass, S. J., Herman, J. G., Gabrielson, E., Iversen, P. W., Parl, F. F., Davidson, N. E., and Graff, J. R. (2000). Aberrant methylation of the estrogen receptor and E-cadherin 5' CpG islands increases with malignant progression in human breast cancer. *Cancer Res* **60**, 4346-4348.

Nelson, M. A., Futscher, B. W., Kinsella, T., Wymer, J., and Bowden, G. T. (1992). Detection of mutant Ha-ras genes in chemically initiated mouse skin epidermis before the development of benign tumors. *Proc Natl Acad Sci U S A* **89**, 6398-6402.

Nevins, J. R. (2001). The Rb/E2F pathway and cancer. *Hum Mol Genet* **10**, 699-703.

Newcomb, E. W., Sosnow, M., Demopoulos, R. I., Zeleniuch-Jacquotte, A., Sorich, J., and Speyer, J. L. (1999). Expression of the cell cycle inhibitor p27KIP1 is a new prognostic marker associated with survival in epithelial ovarian tumors. *Am J Pathol* **154**, 119-125.

Nie, Y., Yang, G., Song, Y., Zhao, X., So, C., Liao, J., Wang, L. D., and Yang, C. S. (2001). DNA hypermethylation is a mechanism for loss of expression of the HLA class I genes in human esophageal squamous cell carcinomas. *Carcinogenesis* **22**, 1615-1623.

Nowell, P. C. (1976). The clonal evolution of tumor cell populations. *Science* **194**, 23-28.

Oda, S., Oki, E., Machara, Y., and Sugimachi, K. (1997). Precise assessment of microsatellite instability using high resolution fluorescent microsatellite analysis. *Nucleic Acids Res* **25**, 3415-3420.

Ogasawara, S., Maesawa, C., Tamura, G., and Satodate, R. (1994). Lack of mutations of the adenomatous polyposis coli gene in oesophageal and gastric carcinomas. *Virchows Arch* **424**, 607-611.

Ohashi, K., Nemoto, T., Eishi, Y., Matsuno, A., Nakamura, K., and Hirokawa, K. (1997). Proliferative activity and p53 protein accumulation correlate with early invasive trend, and apoptosis correlates with differentiation grade in oesophageal squamous cell carcinomas. *Virchows Arch* **430**, 107-115.

Ohbu, M., Saegusa, M., Kobayashi, N., Tsukamoto, H., Mieno, H., Kakita, A., and Okayasu, I. (1997). Expression of bcl-2 protein in esophageal squamous cell carcinomas and its association with lymph node metastasis. *Cancer* **79**, 1287-1293.

Ohbu, M., Saegusa, M., and Okayasu, I. (1995). Apoptosis and cellular proliferation in oesophageal squamous cell carcinomas: differences between keratinizing and nonkeratinizing types. *Virchows Arch* **427**, 271-276.

Ohtsubo, M., Theodoras, A. M., Schumacher, J., Roberts, J. M., and Pagano, M. (1995). Human cyclin E, a nuclear protein essential for the G1-to-S phase transition. *Mol Cell Biol* **15**, 2612-2624.

Orr, H. T., Chung, M. Y., Banfi, S., Kwiatkowski, T. J., Jr., Servadio, A., Beaudet, A. L., McCall, A. E., Duvick, L. A., Ranum, L. P., and Zoghbi, H. Y. (1993). Expansion of an unstable trinucleotide CAG repeat in spinocerebellar ataxia type 1. *Nat Genet* **4**, 221-226.

Ozawa, S., Ueda, M., Ando, N., Shimizu, N., and Abe, O. (1989). Prognostic significance of epidermal growth factor receptor in esophageal squamous cell carcinomas. *Cancer* **63**, 2169-2173.

Pagano, M., Tam, S. W., Theodoras, A. M., Beer-Romero, P., Del Sal, G., Chau, V., Yew, P. R., Draetta, G. F., and Rolfe, M. (1995). Role of the ubiquitin-proteasome pathway in regulating abundance of the cyclin-dependent kinase inhibitor p27. *Science* **269**, 682-685.

Parenti, A. R., Rugge, M., Shiao, Y. H., Ruol, A., Ancona, E., Bozzola, L., and Ninfo, V. (1997). bcl-2 and p53 immunophenotypes in pre-invasive, early and advanced oesophageal squamous cancer. *Histopathology* **31**, 430-435.

Peto, R. (1982). Carcinogenesis as a multistage process--evidence from human studies. *IARC Sci Publ*, 27-28.

Polyak, K., Lee, M. H., Erdjument-Bromage, H., Koff, A., Roberts, J. M., Tempst, P., and Massague, J. (1994). Cloning of p27Kip1, a cyclin-dependent kinase inhibitor and a potential mediator of extracellular antimitogenic signals. *Cell* **78**, 59-66.

Porter, P. L., Malone, K. E., Heagerty, P. J., Alexander, G. M., Gatti, L. A., Firpo, E. J., Daling, J. R., and Roberts, J. M. (1997). Expression of cell-cycle regulators p27Kip1 and cyclin E, alone and in combination, correlate with survival in young breast cancer patients. *Nat Med* **3**, 222-225.

Puglisi, F., Di Loreto, C., Panizzo, R., Avellini, C., Fongione, S., Cacitti, V., and Beltrami, C. A. (1996). Expression of p53 and bcl-2 and response to preoperative chemotherapy and radiotherapy for locally advanced squamous cell carcinoma of the oesophagus. *J Clin Pathol* **49**, 456-459.

Ralhan, R., Agarwal, S., Mathur, M., Wasylyk, B., and Srivastava, A. (2000). Association between polymorphism in p21(Waf1/Cip1) cyclin-dependent kinase inhibitor gene and human oral cancer. *Clin Cancer Res* **6**, 2440-2447.

Ramburan, A., Chetty, R., Hadley, G. P., Naidoo, R., and Govender, D. (2004). Microsatellite analysis of the DCC gene in nephrobalstomas: pathologic correlations and prognostic implications. *Mod Pathol* **17**, 89-95.

Reed, C. E. (1999). Surgical managment of esophageal carcinoma. *The Oncologist* **4**, 95-105.

Ribiero, U., Posner, M. C., Safatle-Ribiero, A. V., and Reynolds, J. C. (1996). Risk factors for squamous cell carcinoma of the esophagus. *Br J Surg* **83**, 1174-1185.

Rolon, P. A., Castellsague, X., Benz, M., and Munoz, N. (1995). Hot and cold mate drinking and esophageal cancer in Paraguay. *Cancer Epidemiol Biomarkers Prev* **4**, 595-605.

Saez, A., Sanchez, E., Sanchez-Beato, M., Cruz, M. A., Chacon, I., Munoz, E., Camacho, F. I., Martinez-Montero, J. C., Mollejo, M., Garcia, J. F., and Piris, M. A. (1999). p27KIP1 is abnormally expressed in Diffuse Large B-cell Lymphomas and is associated with an adverse clinical outcome. *Br J Cancer* **80**, 1427-1434.

Saidi, F., Sepehr, A., Fahimi, S., Farahvash, M. J., Salehian, P., Esmailzadeh, A., Keshoofy, M., Pirmoazen, N., Yazdanbod, M., and Roshan, M. K. (2000). Oesophageal cancer among the Turkomans of northeast Iran. *Br J Cancer* **83**, 1249-1254.

Saitoh, Y., Bruner, J. M., Levin, V. A., and Kyritsis, A. P. (1998). Identification of allelic loss on chromosome arm 6p in human astrocytomas by arbitrarily primed polymerase chain reaction. *Genes Chromosomes Cancer* **22**, 165-170.

Sampliner, R. E. (1998). Practice guidelines on the diagnosis, surveillance, and therapy of Barrett's esophagus. The Practice Parameters Committee of the American College of Gastroenterology. *Am J Gastroenterol* **93**, 1028-1032.

Sandler, R. S., Nyren, O., Ekbom, A., Eisen, G. M., Yuen, J., and Josefsson, S. (1995). The risk of esophageal cancer in patients with achalasia. A population-based study. *Jama* **274**, 1359-1362.

Sarbia, M., Stahl, M., Fink, U., Willers, R., Seeber, S., and Gabbert, H. E. (1998a). Expression of apoptosis-regulating proteins and outcome of esophageal cancer patients treated by combined therapy modalities. *Clin Cancer Res* **4**, 2991-2997.

Sarbia, M., Stahl, M., zur Hausen, A., Zimmermann, K., Wang, L., Fink, U., Heep, H., Dutkowski, P., Willers, R., Muller, W., Seeber, S., and Gabbert, H. E. (1998b). Expression of p21WAF1 predicts outcome of esophageal cancer patients treated by surgery alone or by combined therapy modalities. *Clin Cancer Res* **4**, 2615-2623.

Schoental, R., and Joffe, A. Z. (1974). Lesions induced in rodents by extracts from cultures of Fusarium poae and F. sporotrichioides. *J Pathol* **112**, 37-42.

Schols, L., Vieira-Saecker, A. M., Schols, S., Przuntek, H., Epplen, J. T., and Riess, O. (1995). Trinucleotide expansion within the MJD1 gene presents clinically as spinocerebellar ataxia and occurs most frequently in German SCA patients. *Hum Mol Genet* **4**, 1001-1005.

Sepehr, A., Taniere, P., Martel-Planche, G., Zia'ee, A. A., Rastgar-Jazii, F., Yazdanbod, M., Etemad-Moghadam, G., Kamangar, F., Saidi, F., and Hainaut, P. (2001). Distinct pattern of TP53 mutations in squamous cell carcinoma of the esophagus in Iran. *Oncogene* **20**, 7368-7374.

Shackelford, R. E., Kaufmann, W. K., and Paules, R. S. (1999). Cell cycle control, checkpoint mechanisms, and genotoxic stress. *Environ Health Perspect* **107 Suppl 1**, 5-24.

Shears, L. L., Ribeiro, U., Kane, J., Safatle-Ribeiro, A., Watkins, S., and Posner, M. (1998). Apoptosis in esophageal cancer following induction chemoradiotherapy. *J Surg Res* **79**, 20-24.

Sherr, C. J. (2000). Cell cycle control and cancer. *Harvey Lect* **96**, 73-92.

Sicinski, P., Donaher, J. L., Geng, Y., Parker, S. B., Gardner, H., Park, M. Y., Robker, R. L., Richards, J. S., McGinnis, L. K., Biggers, J. D., Eppig, J. J., Bronson, R. T., Elledge, S. J., and Weinberg, R. A. (1996). Cyclin D2 is an FSH-responsive gene involved in gonadal cell proliferation and oncogenesis. *Nature* **384**, 470-474.

Singh, S. P., Lipman, J., Goldman, H., Ellis, F. H., Jr., Aizenman, L., Cangi, M. G., Signoretti, S., Chiaur, D. S., Pagano, M., and Loda, M. (1998). Loss or altered subcellular localization of p27 in Barrett's associated adenocarcinoma. *Cancer Res* **58**, 1730-1735.

Sondenaa, K., Skaane, P., Nygaard, K., and Skjennald, A. (1992). Value of computed tomography in preoperative evaluation of resectability and staging in oesophageal carcinoma. *Eur J Surg* **158**, 537-540.

Spirin, K. S., Simpson, J. F., Takeuchi, S., Kawamata, N., Miller, C. W., and Koeffler, H. P. (1996). p27/Kip1 mutation found in breast cancer. *Cancer Res* **56**, 2400-2404.

Stein, J. P., Ginsberg, D. A., Grossfeld, G. D., Chatterjee, S. J., Esrig, D., Dickinson, M. G., Groshen, S., Taylor, C. R., Jones, P. A., Skinner, D. G., and Cote, R. J. (1998). Effect of p21WAF1/CIP1 expression on tumor progression in bladder cancer. *J Natl Cancer Inst* **90**, 1072-1079.

Stoner, G. D., and Gupta, A. (2001). Etiology and chemoprevention of esophageal squamous cell carcinoma. *Carcinogenesis* **22**, 1737-1746.

Swanson, S. J., Batirel, H. F., and Bueno, R. (2001). Transthoracic esophagectomy with radical mediastinal and abdominal lymph node dissection and cervical esophagogastrostomy for esophageal carcinoma. *Ann Thorac Surg* **72**, 1918-1925.

Syrjanen, K. J. (2002). HPV infections and oesophageal cancer. *J Clin Pathol* **55**, 721-728.

Thibodeau, S. N., Bren, G., and Schaid, D. (1993). Microsatellite instability in cancer of the proximal colon. *Science* **260**, 816-819.

Tio, T. L., Coene, P. P., Schouwink, M. H., and Tytgat, G. N. (1989). Esophagogastric carcinoma: preoperative TNM classification with endosonography. *Radiology* **173**, 411-417.

Toyoshima, H., and Hunter, T. (1994). p27, a novel inhibitor of G1 cyclin-Cdk protein kinase activity, is related to p21. *Cell* **78**, 67-74.

Tsihlias, J., Kapusta, L. R., DeBoer, G., Morava-Protzner, I., Zbieranowski, I., Bhattacharya, N., Catzavelos, G. C., Klotz, L. H., and Slingerland, J. M. (1998). Loss of cyclin-dependent kinase inhibitor p27Kip1 is a novel prognostic factor in localized human prostate adenocarcinoma. *Cancer Res* **58**, 542-548.

Tuyns, A. J., Castegnaro, M., Toussaint, G., Walker, E. A., Griciute, L. L., Le Talaer, J. Y., Loquet, C., Guerain, J., and Drilleau, J. F. (1980). [Research on the etiological factors of oesophageal cancer in the West of France (author's transl)]. *Bull Cancer* **67**, 15-28.

Urba, S. G., Orringer, M. B., Turrisi, A., Iannettoni, M., Forastiere, A., and Strawderman, M. (2001). Randomized trial of preoperative chemoradiation versus surgery alone in patients with locoregional esophageal carcinoma. *J Clin Oncol* **19**, 305-313.

Vidal, M. J., Loganzo, F., Jr., de Oliveira, A. R., Hayward, N. K., and Albino, A. P. (1995). Mutations and defective expression of the WAF1 p21 tumour-suppressor gene in malignant melanomas. *Melanoma Res* **5**, 243-250.

Vilgrain, V., Mompoint, D., Palazzo, L., Menu, Y., Gayet, B., Ollier, P., Nahum, H., and Fekete, F. (1990). Staging of esophageal carcinoma: comparison of results with endoscopic sonography and CT. *AJR Am J Roentgenol* **155**, 277-281.

Wagata, T., Shibagaki, I., Imamura, M., Shimada, Y., Toguchida, J., Yandell, D. W., Ikenaga, M., Tobe, T., and Ishizaki, K. (1993). Loss of 17p, mutation of the p53 gene, and overexpression of p53 protein in esophageal squamous cell carcinomas. *Cancer Res* **53**, 846-850.

Wang, L. D., Liu, B., and Zheng, S. (2003a). [Analysis of p53 mutational spectra of esophageal squamous cell carcinomas from Linzhou, comparison with esophageal and other cancers from other areas]. *Zhonghua Liu Xing Bing Xue Za Zhi* **24**, 202-205.

Wang, L. D., Zheng, S., Zheng, Z. Y., and Casson, A. G. (2003b). Primary adenocarcinomas of lower esophagus, esophagogastric junction and gastric cardia: in special reference to China. *World J Gastroenterol* **9**, 1156-1164.

Wang, Y. C., Chen, C. Y., Chen, S. K., Cherng, S. H., Ho, W. L., and Lee, H. (1998). High frequency of deletion mutations in p53 gene from squamous cell lung cancer patients in Taiwan. *Cancer Res* **58**, 328-333.

Wong, F. H., Hu, C. P., Chiu, J. H., Huang, B. S., Chang, J. P., Lin, P. J., Chien, K. Y., and Chang, C. (1994). Expression of multiple oncogenes in human esophageal carcinomas. *Cancer Invest* **12**, 121-131.

Wu, C. F., Wu, D. C., Hsu, H. K., Kao, E. L., Lee, J. M., Lin, C. C., and Wu, M. T. (2005). Relationship between genetic polymorphisms of alcohol and aldehyde dehydrogenases and esophageal squamous cell carcinoma in males. *World J Gastroenterol* **11**, 5103-5108.

Wu, J., Shen, Z. Z., Lu, J. S., Jiang, M., Han, Q. X., Fontana, J. A., Barsky, S. H., and Shao, Z. M. (1999). Prognostic role of p27Kip1 and apoptosis in human breast cancer. *Br J Cancer* **79**, 1572-1578.

Wu Y, Chen J, Ohshima H, Pignatelli B, Boreham J, and Li, J. (1993). Geographic association between urinary excretion of *N*-nitroso compounds and oesophageal cancer mortality in China. *Int J Cancer* **54**, 713-719.

Xiong, Y., Hannon, G. J., Zhang, H., Casso, D., Kobayashi, R., and Beach, D. (1993). p21 is a universal inhibitor of cyclin kinases. *Nature* **366**, 701-704.

Yokoyama, A., Kato, H., Yokoyama, T., Tsujinaka, T., Muto, M., Omori, T., Haneda, T., Kumagai, Y., Igaki, H., Yokoyama, M., Watanabe, H., Fukuda, H., and Yoshimizu, H.

(2002). Genetic polymorphisms of alcohol and aldehyde dehydrogenases and glutathione S-transferase M1 and drinking, smoking, and diet in Japanese men with esophageal squamous cell carcinoma. *Carcinogenesis* **23**, 1851-1859.

Yoshida, K., Kyo, E., Tsuda, T., Tsujino, T., Ito, M., Niimoto, M., and Tahara, E. (1990). EGF and TGF-alpha, the ligands of hyperproduced EGFR in human esophageal carcinoma cells, act as autocrine growth factors. *Int J Cancer* **45**, 131-135.

Zhu, D., Wang, L., Zhang, C., Wang, X., Mao, X., Jia, Y., Yan, S., and Wu, M. (1996). No evidence for the amplifications of MDM2 and C-myc genes involved in the genetic susceptibility to esophageal cancer in a high-risk area of north China. *Cancer Genet Cytogenet* **89**, 184-185.

Zhang, J., Chen, X-L., Wang, K-M., Guo, X-D., Zuo, A-L. and Gong, J. (2004). Barrett's esophagus and its correlation with gastrooesophageal reflux in Chinese. *World J Gastroenterol* **10**, 1065-1068.

Ziegler K, Sanft C, M., Z., Friedrich M, Stein H, Haring R, and O, R. E. (1991). Evaluation of endosonography in TN staging of oesophageal cancer. *Gut* **32**, 16-20.

Appendix A1:

DNA Tissue Lysis Buffer

To a 100mL glass beaker, add:

- 1mL of 1M Tris-HCl (pH7.5) [a]
- 1mL of 0.5M EDTA (pH 8.0) [b]
- Heat the solution gently without stirring, and then add 8mL of 5M NaCl.
- Adjust the total volume to 100mL with distilled water and store in an airtight glass bottle at room temperature.

a : For 50mL of 1M Tris-HCl stock solution, dissolve ~7.88g of Tris-HCl in 50mL of distilled water. pH to 7.5

b: For 50mL of 0.5M EDTA, measure ~9.31g of EDTA (MW = 372.24 g/mol) in 50mL of distilled water. pH to 8.0.

Appendix A2:

Phenol-Chloroform-Isoamyl alcohol

- 25mL each of phenol and chloroform is combined into a dark-coloured bottle in the fumehood.
- 330µl of isoamyl alcohol is then added.
- The mixture is then carefully overlaid with 5mL of TE buffer[a].
- Store at 4°C, preferably away from light

a: TE buffer consists of 10mM Tris base (MW = 157.64g/mol) and 1mM EDTA. These solutions are combined in equal parts. pH to 7.4, and store at room temperature.

Appendix A3:

3M Sodium Acetate

- Measure 24.6g of sodium acetate into 15mL of acetic acid.
- Top up the mixture to 100mL with sterile distilled water.
- Autoclave the solution at 121°C for 15 minutes.
- Allow to cool and store at room temperature in an airtight bottle.

Appendix A4:

80% Ethanol

- For a 100mL stock solution, add 20mL of absolute ethanol to 80mL of sterile distilled water.
- Store in an airtight bottle at room temperature.

Appendix A5

TBE Buffer

For a 1L stock solution of 10 X TBE Buffer, measure the following into a 1L conical flask:

- 108 g Tris base (MW=121.1g/mol)
- 55 g boric acid
- 9.3 g of EDTA-disodium salt (MW=372.74g/mol)

Add approximately 800 mL of sterile, distilled dH_2O and dissolve with a magnetic stirrer on medium heat. Filter the solution through a filter paper. Finally, top up the solution to 1L, and store in an airtight bottle at room temperature.

Appendix A6

Bromophenol Blue dye

The dye consisted of the following:

- 0.02% bromophenol blue
- 0.02% xylene cyanol
- 50% glycerol

Appendix A7:

10% Ammonium Persulphate (APS) solution

- Dissolve 1g of APS in 10mL of sterile, distilled water. Make the solution up fresh prior to use.

Appendix B

Table 1: sequence information for the microsatellite markers used in this study

Marker	Linked Gene	Primer Sequence	% Informativity	Size (bp)
D12S391	*p27*^{Kip1}	F: AACAGGATCAATGGATGCAT R: TGGCTTTTAGACCTGGACTG	89	228
D12S320	*p27*^{Kip1}	F: GGCAGCCAAATAACACATCT R: AAAAAGGTGCCTCCCATTTA	82	196-216
D12S364	*p27*^{Kip1}	F: CCAGTCCTGAACAGGC R: CCCTGGAAGTCCCATC	87	277
D12S358	*p27*^{Kip1}	F: GCCTTTGGGAAACTTTGG R: GCACAGATGAGATCCCGT	76	254
D6S1575	*p21*$^{CIP1/WAF1}$	F: GCATCTCCCCAAACACAAAC R: ACTATGCTTCTGGGTCCCTG	82	90
D6S1645	*p21*$^{CIP1/WAF1}$	F: CAGGAGAACCACTTGAACC R: CCCACTTAGCAGACAGAGAG	62	244

APPENDIX C

Electrophoretograms of LOH-AI and MSI

1.1 D6S1575 – LOH/AI

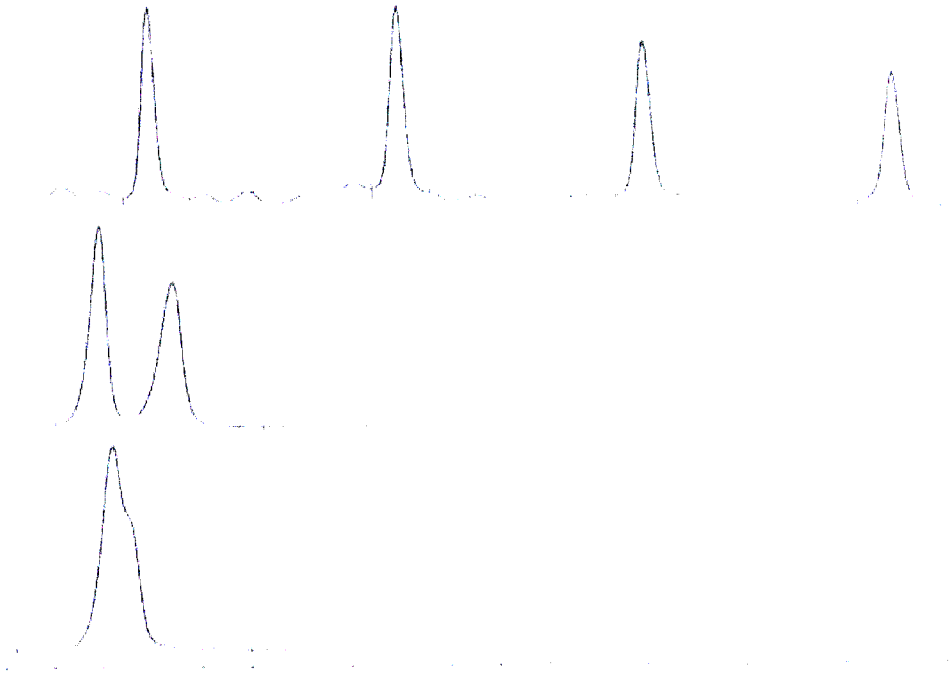

Lane #	Peak #	Run Time	Peak Area	Size (BP)	Quantity
1	1	22:52	169.56	#50.0	1
	2	27:36	134.84	#100.0	0.79522
	3	32:50	145.77	#150.0	0.85971
	4	38:24	131.64	#200.0	0.77635
	5	44:24	133.68	#250.0	0.78836
	6	50:40	109.34	#300.0	0.64482
	7	57:04	98.964	#350.0	0.58365
	8	63:38	86.635	#400.0	0.51094
	9	70:18	66.772	#450.0	0.3938
	10	76:54	41.681	#500.0	0.24582
12	1	26:34	152.64	89.6	1
	2	28:04	149.66	104.6	0.98053
13	1	26:50	130.29	92.3	1

Figure 1.1: electrophoretogram displaying the LOH-AI genotype, as seen in marker D6S1575. Lane 1 contained the 50-500bp CY5-labelled marker. Lane 2 contained normal PCR product (+/- 90bp), with the corresponding tumour sample in lane 3. The table lists the number of peaks that were recorded, as well as their size(s).

1.2 D6S1575 continued – MSI

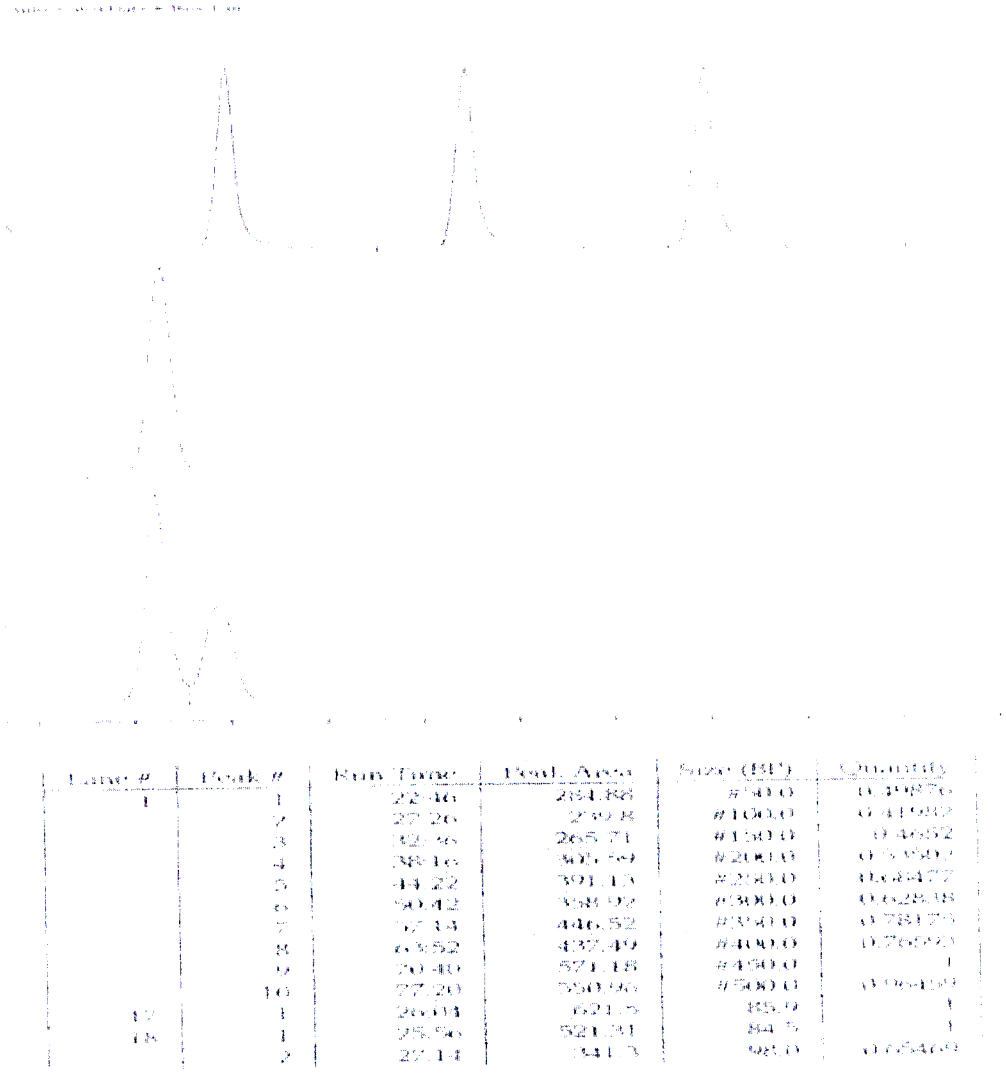

Lane #	Peak #	Run Time	Peak Area	Size (BP)	Quantity
1	1	22.46	284.86	#90.0	0.359876
	2	27.26	2792.8	#100.0	0.411982
	3	32.46	2665.71	#150.0	0.346552
	4	38.16	302.79	#200.0	0.039387
	5	44.22	391.13	#250.0	0.048477
	6	50.42	3586.92	#300.0	0.452838
	7	57.33	446.52	#350.0	0.056376
	8	63.52	4327.49	#400.0	0.546552
	9	70.40	571.18	#450.0	1
	10	77.20	5260.96	#500.0	0.664459
2	1	26.13	821.5	85.9	1
3	1	25.96	821.91	84.5	1
	2	27.14	341.3	98.0	0.415469

Figure 1.2: electrophoretogram displaying the MSI genotype, as seen in marker D6S1575. Lane 1 contained the 50-500bp CY5-labelled marker. Lane 2 contained normal PCR product (+/- 90bp), with the corresponding tumour sample in lane 3. The table lists the number of peaks that were recorded, as well as their size(s).

2.1 D6S1645 – LOH/AI

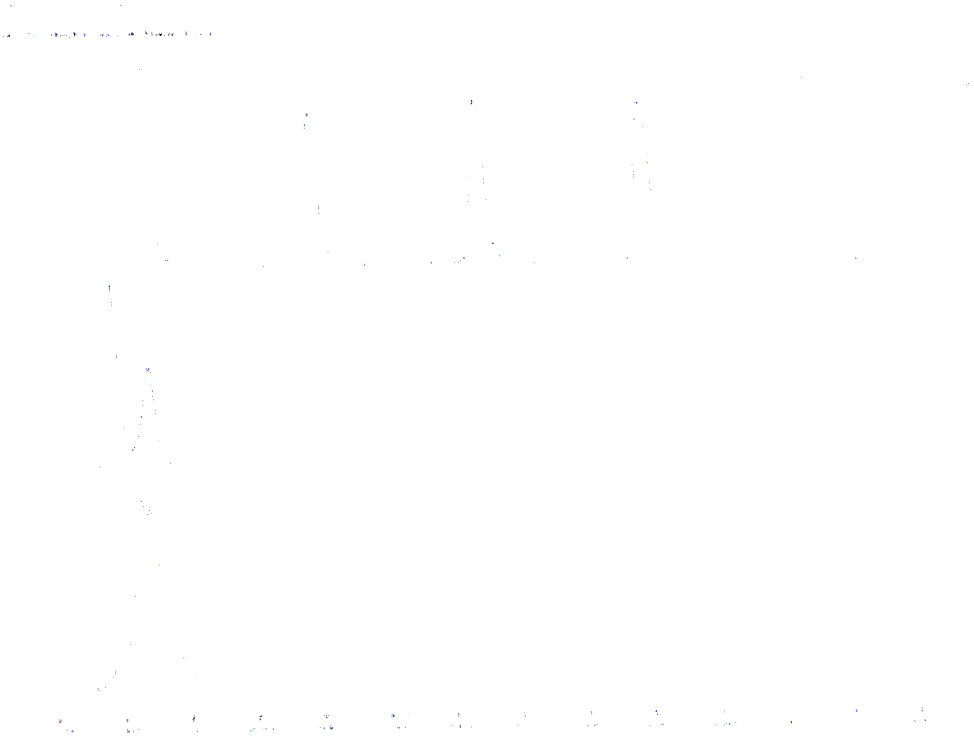

Lane #	Peak #	Run Time	Peak Area	Size (BP)	Quantity
1	1	24.24	131.53	#50.0	0.324.27
	2	29.24	221.5	#100.0	0.54692
	3	35.10	182.9	#150.0	0.45161
	4	41.28	217.44	#200.0	0.53689
	5	48.14	274.06	#250.0	0.6767
	6	55.16	249.88	#300.0	0.61699
	7	62.30	298.84	#350.0	0.73788
	8	69.54	327.03	#400.0	0.80751
	9	77.24	395.08	#450.0	0.97553
	10	84.52	404.99	#500.0	1
28	1	46.42	94.286	238.9	1
	2	48.08	58.754	249.3	0.62343
29	1	47.44	295.52	246.4	1

Figure 2.1: electrophoretogram displaying the LOH-AI genotype, as seen in marker D6S1645. Lane 1 contained the 50-500bp CY5-labelled marker. Lane 2 contained normal PCR product (+/-244bp), with the corresponding tumour sample in lane 3. The table lists the number of peaks that were recorded, as well as their size(s).

2.2 D6S1645 continued – MSI

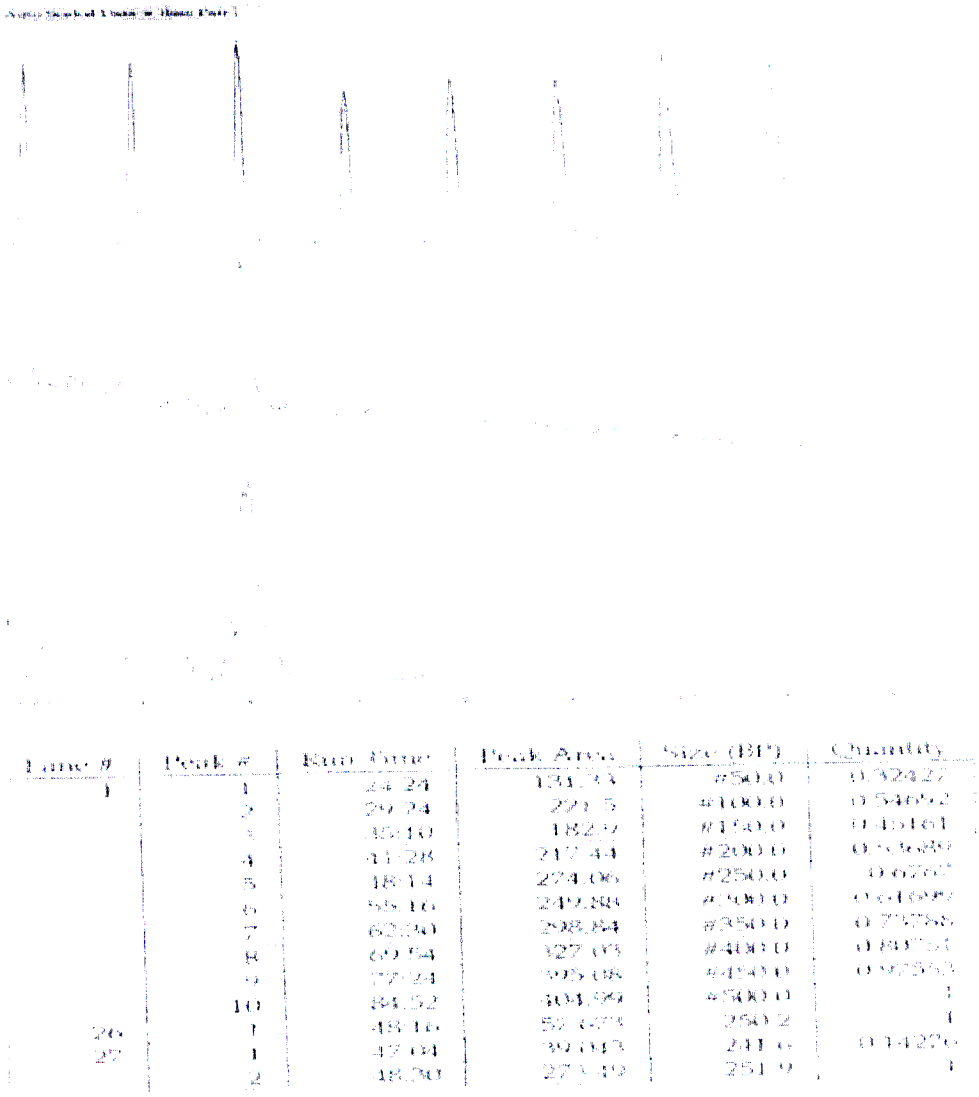

Figure 2.2: electrophoretogram displaying the MSI genotype, as seen in marker D6S1645. Lane 1 contained the 50-500bp CY5-labelled marker. Lane 2 contained normal PCR product (+/- 244bp), with the corresponding tumour sample in lane 3. The table lists the number of peaks that were recorded, as well as their size(s).

3.1 D12S391 – LOH/AI

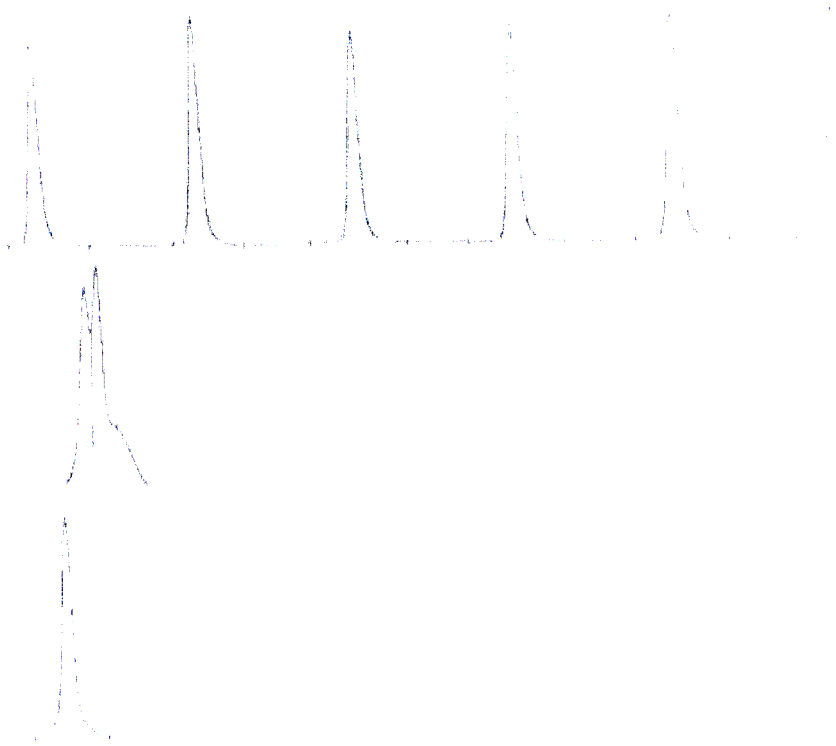

Lane #	Peak #	Size (bp)	Quantity
1	1	50	0.21
	2	100	0.42
	3	150	0.32
	4	200	0.11
	5	250	0.03
	6	300	0.02
	7	350	0.02
	8	400	0.02
	9	450	0.01
	10	500	1
2	1	228	1
	2	230	1
3	1	228	1

Figure 3.1: electrophoretogram displaying the LOH-AI genotype, as seen in marker D12S391. Lane 1 contained the 50-500bp CY5-labelled marker. Lane 2 contained normal PCR product (+/-228bp), with the corresponding tumour sample in lane 3. The table lists the number of peaks that were recorded, as well as their size(s).

3.2 D12S391 continued – MSI

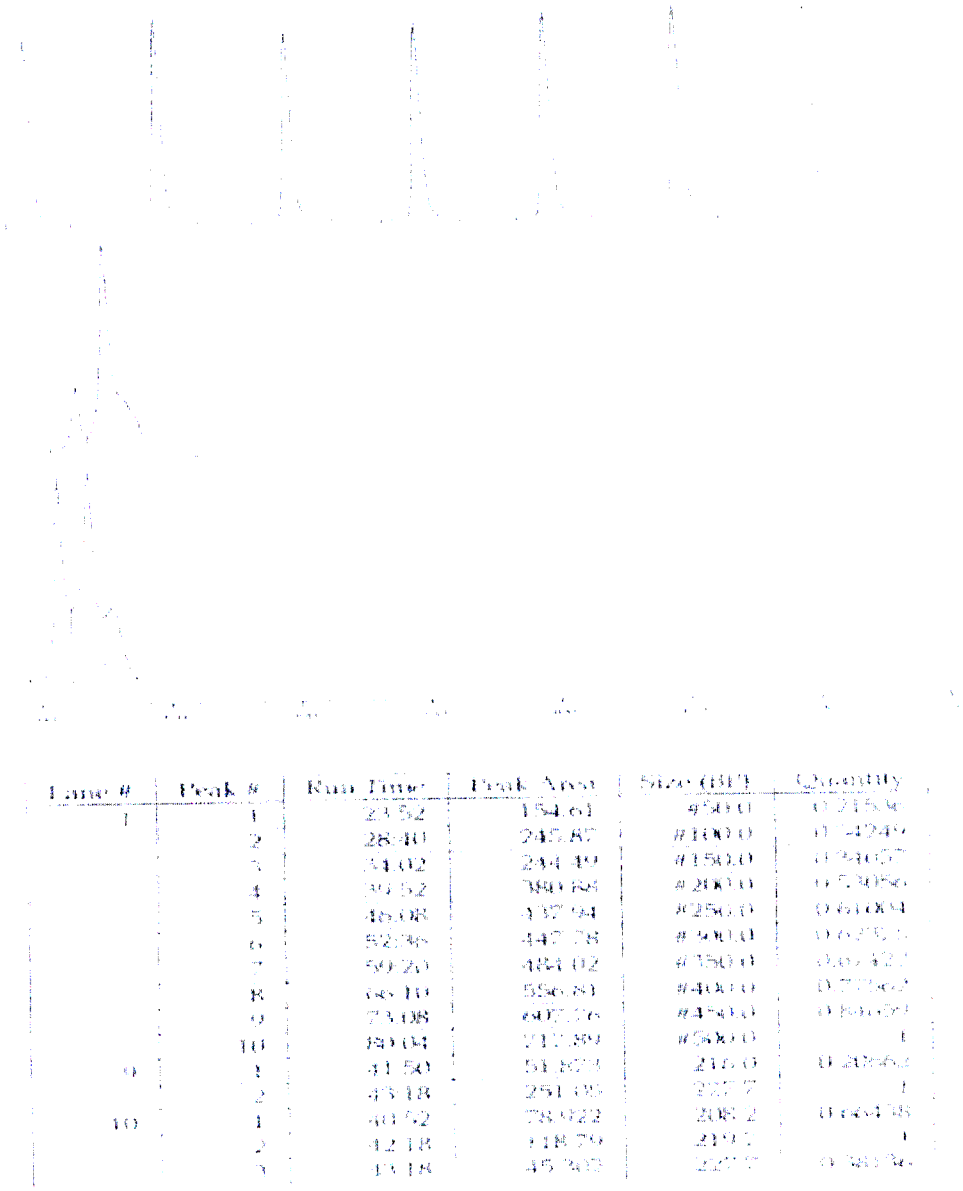

Lane #	Peak #	Run Time	Peak Area	Size (bp)	Quantity
1	1	24.52	154.61	95.01	0.21536
	2	28.40	242.87	118.00	0.42456
	3	34.02	294.49	158.20	0.58057
	4	39.52	388.86	208.00	0.76586
	5	46.08	437.94	258.60	0.86304
	6	52.36	447.78	308.01	0.88245
	7	59.20	484.02	358.01	0.95387
	8	65.10	556.81	408.01	1.09722
	9	73.08	607.26	458.01	1.19677
	10	89.04	512.59	568.01	1
9	1	41.50	51.87	210.6	0.28566
	2	45.18	251.05	227.7	1
10	1	40.52	78.022	208.2	0.44435
	2	42.18	118.79	219.1	1
	3	45.18	45.203	227.7	0.38056

Figure 3.2: electrophoretogram displaying the MSI genotype, as seen in marker D12S391. Lane 1 contained the 50-500bp CY5-labelled marker. Lane 2 contained normal PCR product (+/- 228bp), with the corresponding tumour sample in lane 3. The table lists the number of peaks that were recorded, as well as their size(s).

4.1 D12S320 – LOH/AI

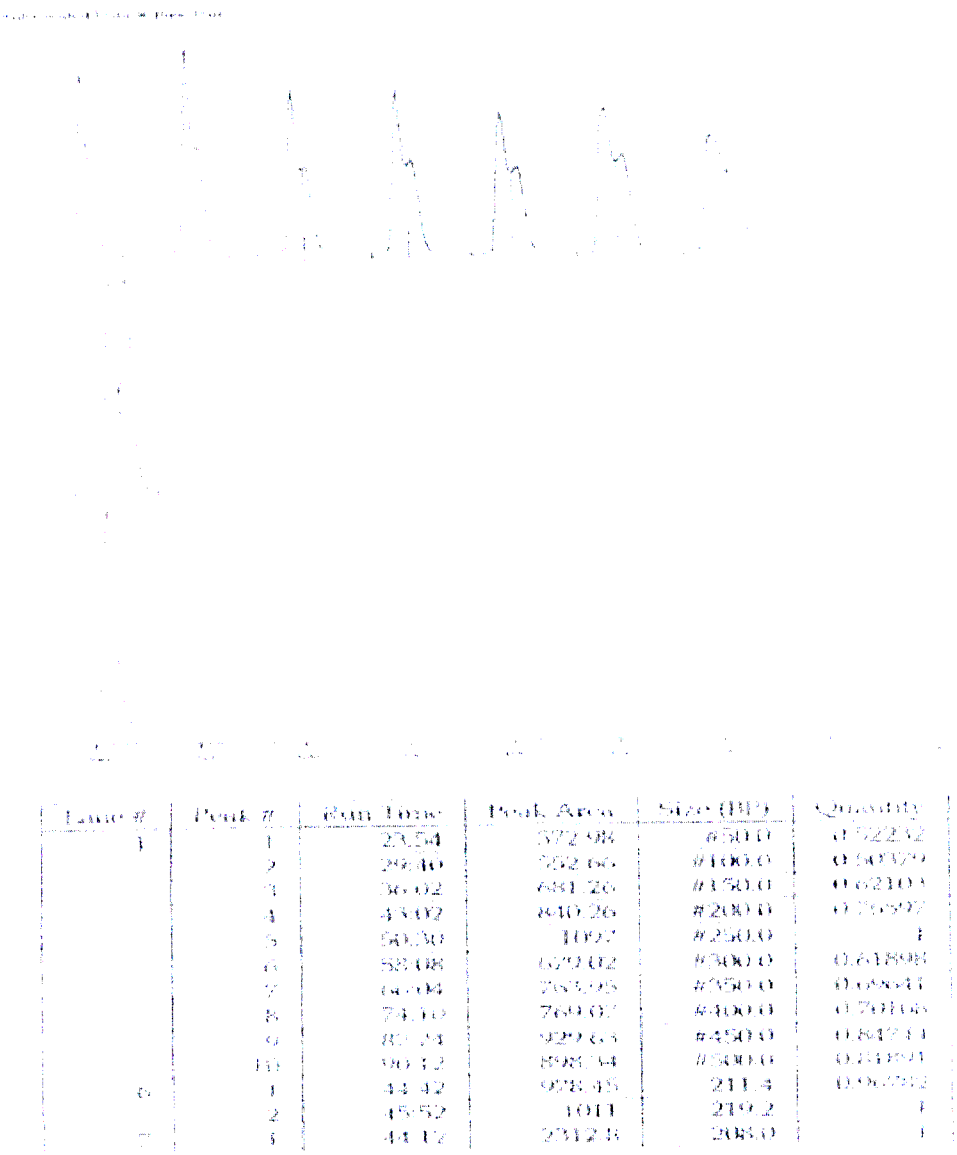

Lane #	Peak #	Dye Type	Peak Area	Size (BP)	Quantity
1	1		23.54		
	2		28.40		
	3		36.02		
	4		43.02		
	5		50.30		
	6		58.08		
	7				
	8				
	9				
	10				
2	1				
	2				
	3				

Figure 4.1: electrophoretogram displaying the LOH-AI genotype, as seen in marker D12S320. Lane 1 contained the 50-500bp CY5-labelled marker. Lane 2 contained normal PCR product (+/- 196-216bp), with the corresponding tumour sample in lane 3. The table lists the number of peaks that were recorded, as well as their size(s).

4.2 D12S320 continued – MSI

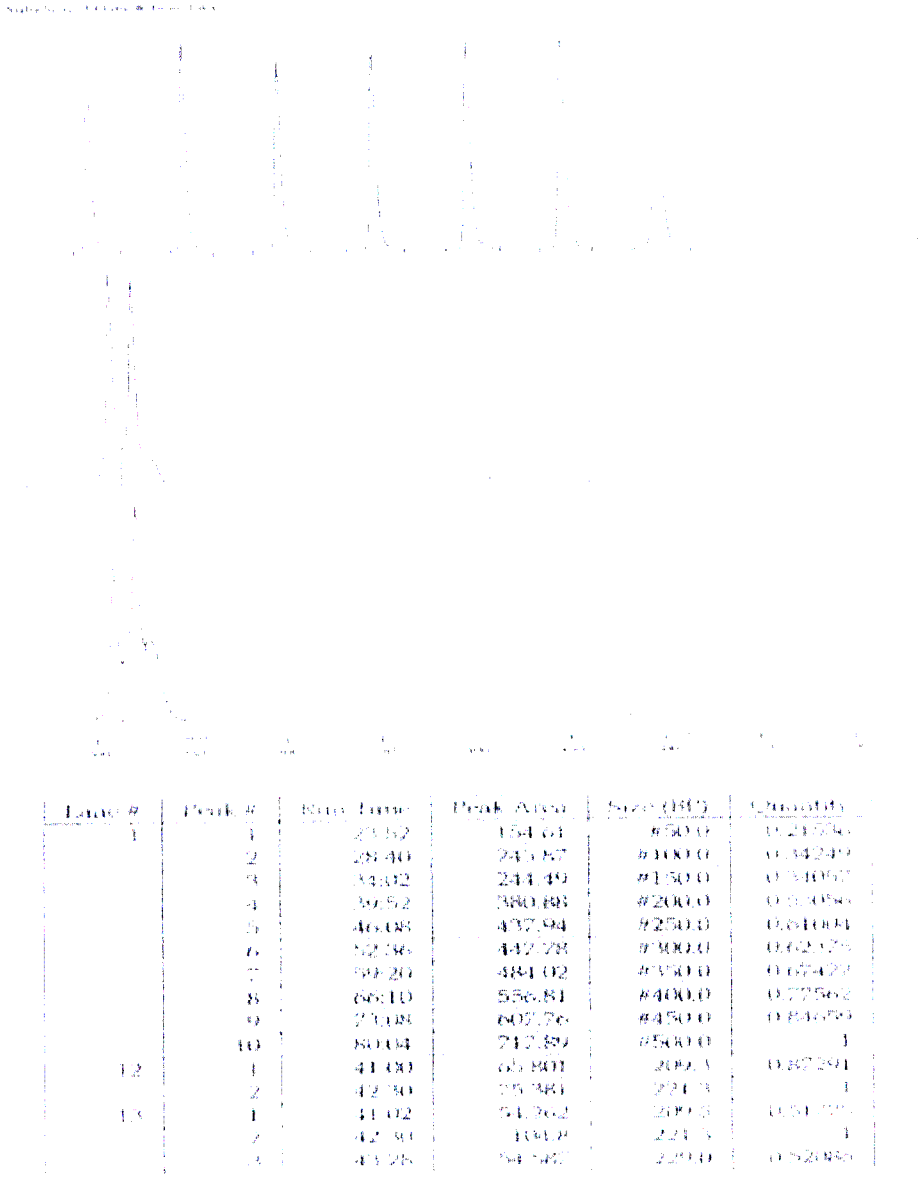

Lane #	Peak #	Size (bp)	Peak Area	Size (bp)	Quantity
1	1	250.52	154.61	#50.0	0.28356
	2	258.40	245.87	#100.0	0.45249
	3	333.02	244.49	#150.0	0.45007
	4	367.52	380.88	#200.0	0.70156
	5	406.08	437.94	#250.0	0.80684
	6	522.86	442.98	#300.0	0.82127
	7	598.20	484.02	#350.0	0.89424
	8	665.10	556.81	#400.0	1.02562
	9	773.08	607.76	#450.0	1.11933
	10	880.04	712.89	#500.0	1
2	1	41.00	65.801	200.1	0.86291
	2	42.30	75.981	224.3	1
3	1	41.02	94.362	200.1	0.91
	2	42.30	103.9	224.3	1
	3	43.26	94.342	250.0	0.9208

Figure 4.2: electrophoretogram displaying the MSI genotype, as seen in marker D12S320. Lane 1 contained the 50-500bp CY5-labelled marker. Lane 2 contained normal PCR product (+/- 196-216bp), with the corresponding tumour sample in lane 3. The table lists the number of peaks that were recorded, as well as their size(s).

5.1 D12S364 – LOH/AI

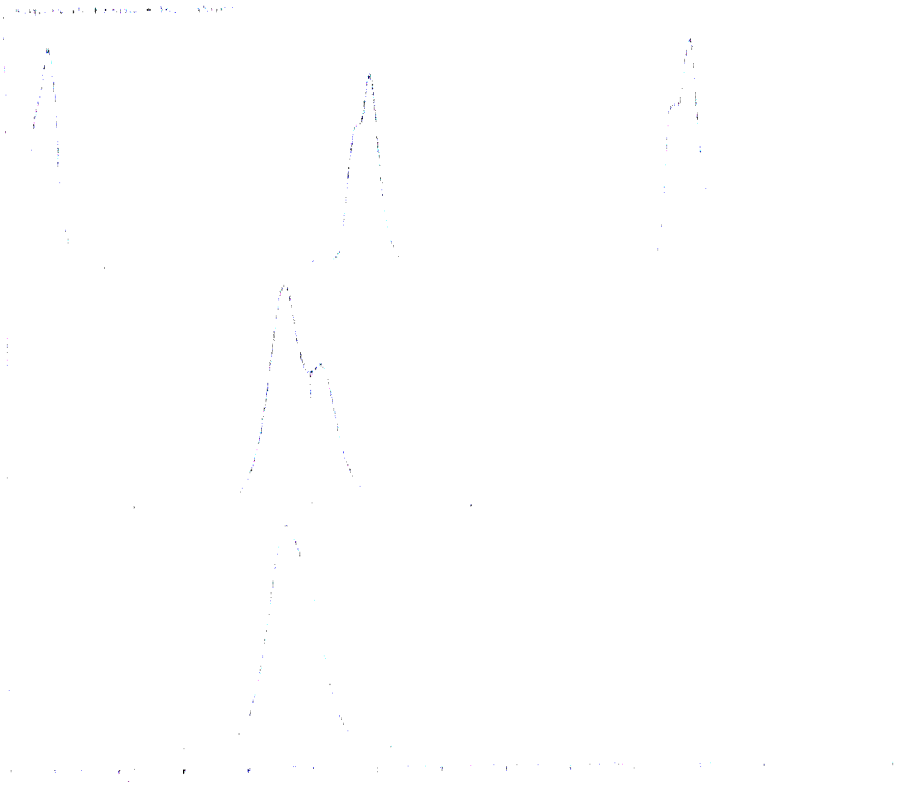

Lane #	Peak #	Run Time	Peak Area	Size (BP)	Quantity
1	1	33.50	163.72	#50.0	0.294464
	2	41.48	293.23	#100.0	0.5277
	3	50.42	263.51	#150.0	0.474121
	4	60.20	339.9	#200.0	0.611669
	5	70.36	446.68	#250.0	0.803985
	6	81.14	421.29	#300.0	0.758819
	7	92.08	555.67	#350.0	1
	8	103.06	378.63	#400.0	0.6814
	9	114.12	511.52	#450.0	0.920954
	10	125.04	383.3	#500.0	0.689079
11	1	78.18	1933.9	286.4	1
	2	79.28	981.44	291.8	0.507749
12	1	78.18	4019.2	286.4	1

Figure 5.1: electrophoretogram displaying the LOH-AI genotype, as seen in marker D12S364. Lane 1 contained the 50-500bp CY5-labelled marker. Lane 2 contained normal PCR product (+/- 277bp), with the corresponding tumour sample in lane 3. The table lists the number of peaks that were recorded, as well as their size(s).

5.2 D12S364 continued – MSI

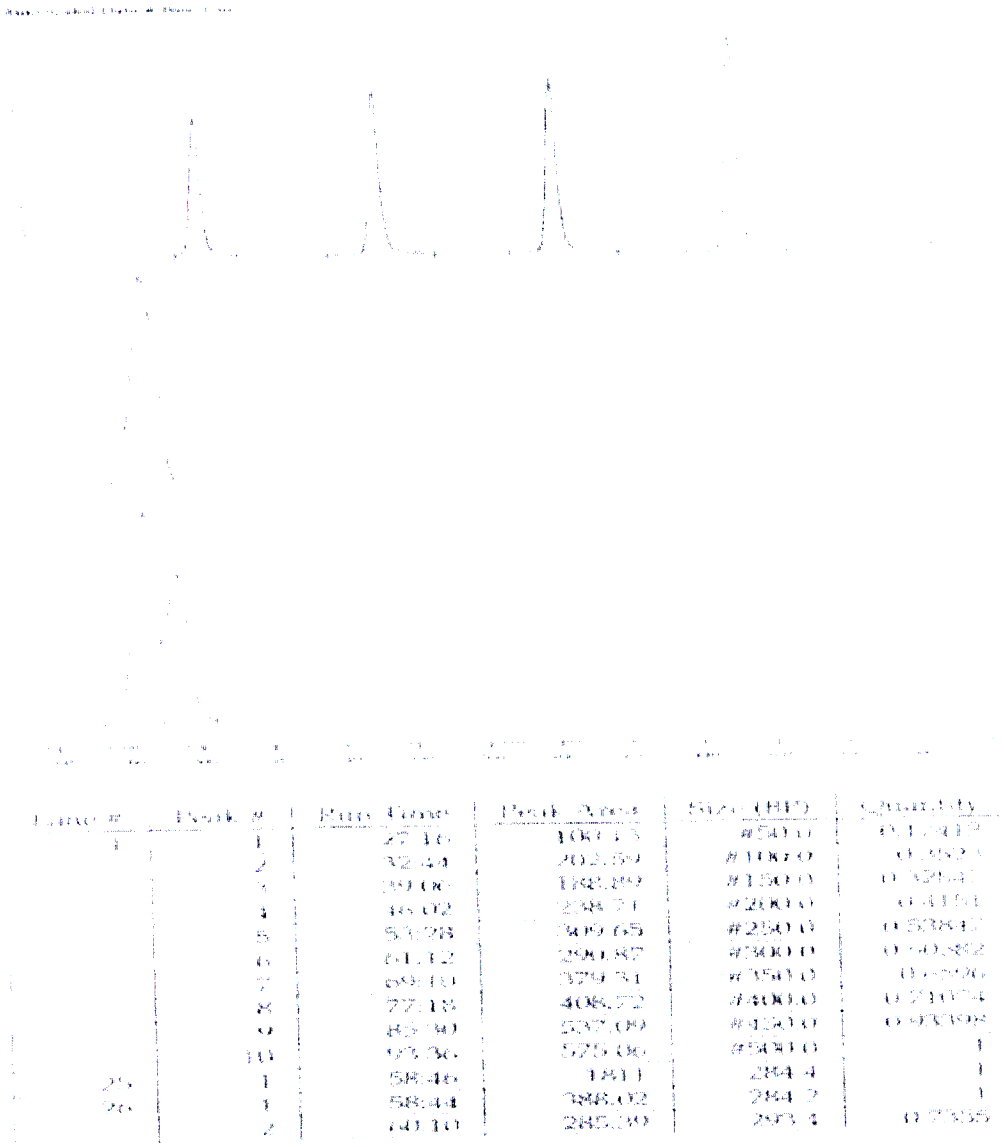

Figure 5.2: electrophoretogram displaying the MSI genotype, as seen in marker D12S364. Lane 1 contained the 50-500bp CY5-labelled marker. Lane 2 contained normal PCR product (+/- 277bp), with the corresponding tumour sample in lane 3. The table lists the number of peaks that were recorded, as well as their size(s).

6.1 D12S358 – LOH/AI

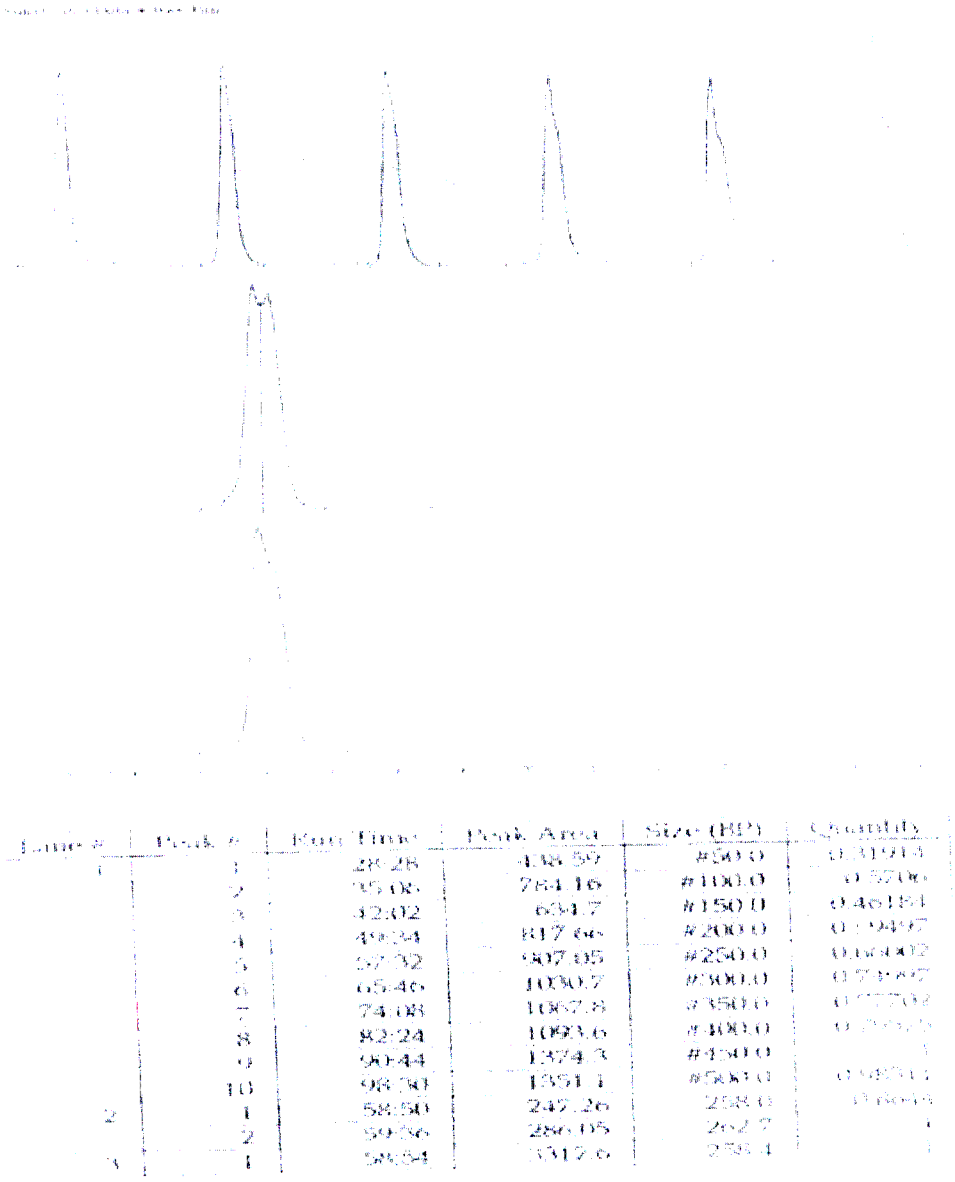

Lane #	Peak #	Run Time	Peak Area	Size (BP)	Quantity
1	1	28:28	438.59	#50.0	0.31914
	2	35:08	764.16	#100.0	0.55586
	3	42:02	654.7	#150.0	0.46184
	4	48:34	817.66	#200.0	0.59467
	5	57:52	807.85	#250.0	0.58752
	6	65:46	1030.7	#300.0	0.74987
	7	74:08	1067.8	#350.0	0.77702
	8	82:24	1093.6	#400.0	0.79579
	9	90:44	1374.3	#450.0	1
	10	98:30	1351.1	#500.0	0.98311
2	1	58:50	242.26	254.0	0.17626
	2	59:36	286.05	262.7	1
3	1	58:54	1312.6	254.4	1

Figure 6.1: electrophoretogram displaying the LOH-AI genotype, as seen in marker D12S358. Lane 1 contained the 50-500bp CY5-labelled marker. Lane 2 contained normal PCR product (+/- 254bp), with the corresponding tumour sample in lane 3. The table lists the number of peaks that were recorded, as well as their size(s).

6.2 D12S358 continued – MSI

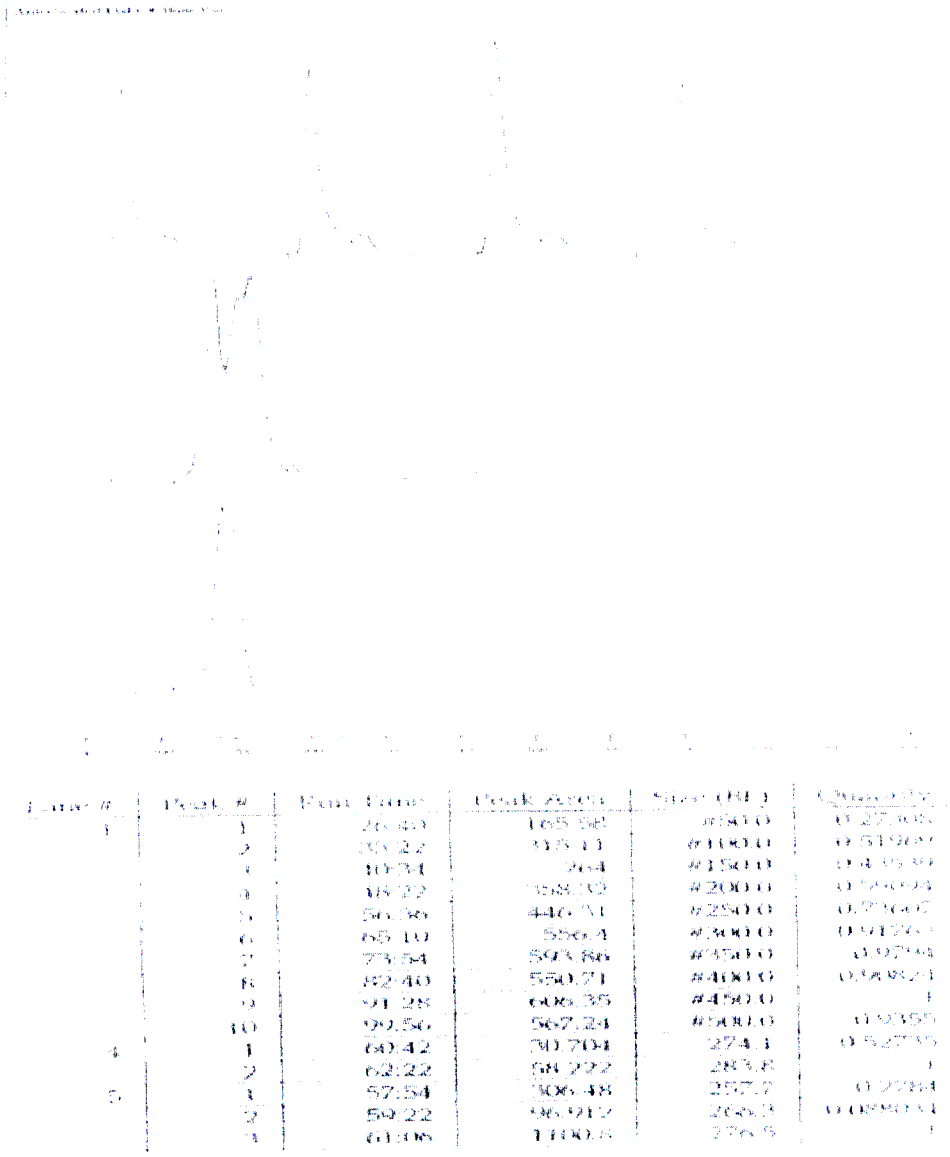

Figure 6.2: electrophoretogram displaying the MSI genotype, as seen in marker D12S358. Lane 1 contained the 50-500bp CY5-labelled marker. Lane 2 contained normal PCR product (+/- 254bp), with the corresponding tumour sample in lane 3. The table lists the number of peaks that were recorded, as well as their size(s).

Appendix D1

Clinico-pathological data

cases	Age	Sex	Stage	Grade	Lymph node metastases	TNM	Outcome (Alive/Dead)	Survival (Weeks)
1	53	F	IIA	MD	No	3, 0, 0	A	2
2	57	F	III	PD	Yes	3, 1, 0	A	88
3	64	F	III	PD	Yes	2, 1, 0	D	0.3
4	68	M	IIA	MD	No	3, 0, 0	A	6
5	50	M	IIA	MD	NR	3, 0, 0	A	8
6	57	M	IIA	WD	No	2, 0, 0	D	6
7	43	M	IIB	MD	Yes	2, 1, 0	A	4
8	50	M	IIB	MD	Yes	2, 1, 0	A	6
9	56	M	IIA	MD	NR	3, 0, 0	A	14
10	50	M	III	MD	Yes	4, 1, 0	A	24
11	61	M	III	MD	Yes	3, 1, 0	D	2
12	53	F	IIA	MD	No	2, 0, 0		
13	62	M	IIB	MD	Yes	2, 1, 0	A	16
14	74	M	IIA	MD	No	2, 0, 0		
15	62	F	IIA	MD	No	2, 0, 0	A	6
16	62	F	III	MD	Yes	3, 1, 0	A	6
17	55	M	IIA	MD	No	2, 0, 0		
18	65	M	IIA	MD	No	2, 0, 0	A	5
19	69	M	III	PD	Yes	3, 1, 0		
20	54	M	IIB	MD	Yes	2, 1, 0	D	2
21	79	F	III	PD	Yes	3, 1, 0	A	6
22	56	F	III	MD	No	4, 0, 0	A	6
23	52	F	IIA	PD	NR	2, 0, 0	D	4
24	28	F	III	WD	NR	4, 0, 0		
25	77	F	III	PD	Yes	3, 1, 0	D	0
26	61	F	III	MD	Yes	3, 1, 0	A	8
27	65	F	III	MD	No	4, 0, 0	A	24
28	42	F	III	MD	Yes	3, 1, 0	A	12
29	35	F	IIA	MD	NR	3, 0, 0	D	2
30	47	F	III	MD	Yes	3, 1, 0	D	0.9
31	35	M	IIB	PD	Yes	2, 1, 0		
32	67	F	IIA	MD	No	3, 0, 0	A	12
33	47	M	IIA	PD	NR	3, 0, 0	D	0.4
34	60	M	III	MD	Yes	3, 1, 0	D	2
35	39	F	III	WD	Yes	3, 1, 0	A	52
36	49	F	IIA	WD	No	3, 0, 0	A	66
37	53	F	III	MD	Yes	3, 1, 0	A	22

cases	Age	Sex	Stage	Grade	Lymph node metastases	TNM	Outcome (Alive/Dead)	Survival (Weeks)
38	61	M	IIA	WD	No	3, 0, 0	A	168
39	51	M	IIA	MD	No	2, 0, 0	A	24
40	58	F	IIA	MD	NR	3, 0, 0		
41	49	F	III	MD	Yes	3, 1, 0	A	36
42	40	M	IIB	MD	Yes	2, 1, 0		
43	49	M	IIA	MD	No	2, 0, 0	A	5
44	55	M	IIA	MD	NR	3, 0, 0		
45	49	M	IIA	MD	NR	3, 0, 0	A	20
46	55	M	III	MD	Yes	3, 1, 0	D	2
47	63	M	IIA	MD	No	3, 0, 0	D	56
48	62	M	III	PD	Yes	3, 1, 0	A	3
49	53	F	IIA	WD	No	3, 0, 0	A	24
50	60	M	IIA	WD	NR	3, 0, 0	D	0.3
51	68	M	IIA	WD	No	3, 0, 0	A	4
52	34	M	IIA	MD	No	3, 0, 0	A	6
53	53	M	IIA	WD	Yes	3, 0, 0	A	52
54	61	M	IIA	WD	NR	2, 0, 0		
55	47	F	IIB	PD	Yes	2, 1, 0		
56	33	M	IIA	WD	No	3, 0, 0	A	104
57	50	F	III	MD	No	4, 0, 0	A	52
58	59	M	IIA	WD	No	2, 0, 0		
59	45	M	IIA	MD	No	3, 0, 0		
60	54	F	IIA	WD	No	3, 0, 0	A	24
61	57	M	IIA	MD	No	3, 0, 0	A	180
62	62	M	III	MD	Yes	3, 1, 0		
63	71	F	III	MD	Yes	3, 1, 0	A	6
64	54	M	III	MD	Yes	3, 1, 0	D	12
65	41	F	IIB	MD	Yes	2, 1, 0		
66	55	M	III	MD	Yes	3, 1, 0	A	6
67	36	M	IIA	WD	No	3, 0, 0	D	16
68	64	F	III	MD	Yes	3, 1, 0		
69	62	M	IIA	WD	No	2, 0, 0		
70	60	M	IIB	MD	Yes	2, 1, 0		
71	65	F	IIA	WD	No	3, 0, 0		
72	48	M	III	MD	Yes	3, 1, 0	A	6
73	65	M	III	WD	Yes	3, 1, 0	A	52
74	60	M	IIA	MD	No	2, 0, 0		
75	71	F	IIB	MD	Yes	2, 1, 0	A	36
76	92	F	IIA	MD	NR	2, 0, 0		
77	54	F	III	MD	Yes	3, 1, 0	D	12
78	44	F	0	WD	No	Tis, 0, 0	A	52
79	49	F	IIA	WD	No	2, 0, 0	A	284
80	71	M	IIA	WD	No	3, 0, 0	A	24
81	68	F	IIB	WD	Yes	2, 1, 0	A	12
82	77	M	IIA	MD	No	3, 0, 0	D	4

cases	Age	Sex	Stage	Grade	Lymph node metastases	TNM	Outcome (Alive/Dead)	Survival (Weeks)
83	57	M	IIA	WD	No	3, 0, 0		
84	63	M	III	MD	Yes	4, 1, 0	A	6
85	65	M	III	WD	Yes	4, 1, 0	A	24
86	48	M	IIA	WD	No	2, 0, 0	A	6
87	52	M	III	MD	Yes	4, 1, 0	A	6
88	47	F	III	MD	Yes	4, 1, 0	D	12
89	54	M	III	MD	Yes	3, 1, 0	A	6
90	44	F	III	MD	Yes	3, 1, 0	A	12
91	60	F	III	MD	Yes	3, 1, 0	A	52
92	61	F	IIA	WD	No	3, 0, 0	D	104
93	68	F	III	MD	Yes	3, 1, 0	A	24
94	38	M	IIA	MD	No	3, 0, 0	A	6
95	62	F	III	MD	Yes	3, 1, 0	A	8
96	68	M	III	MD	Yes	3, 1, 0	D	2

Appendix D2

Microsatellite data

CASES	D6S1575	D12S391	D12S320	D6S1645	D12S364	D12S358
1	H	NAI	NAI	NAI	H	LOH-AI
2	H	NAI	H	H	H	NAI
3	MSI	LOH-AI	LOH-AI	LOH-AI	H	NAI
4	H	LOH-AI	H	H	H	H
5	H	NAI	H	NAI	NAI	H
6	H	MSI	H	H	H	H
7	H	NAI	NAI	H	NAI	H
8	H	H	H	NAI	MSI	H
9	H	NAI	H	H	H	H
10	H	NAI	H	H	H	H
11	H	H	NAI	H	H	H
12	H	NAI	H	H	H	H
13	H	NAI	H	H	H	NAI
14	NAI	H	NAI	H	H	NAI
15	H	H	LOH-AI	H	H	H
16	NAI	LOH-AI	LOH-AI	H	MSI	H
17	H	NAI	H	MSI	H	LOH-AI
18	H	NAI	H	LOH-AI	H	H
19	LOH-AI	H	H	H	H	NAI
20	LOH-AI	MSI	MSI	H	H	H
21	MSI	H	NAI	H	H	H
22	H	H	H	H	NAI	H
23	LOH-AI	H	NAI	H	H	H
24	H	H	NAI	LOH-AI	LOH-AI	H
25	H	H	H	NAI	LOH-AI	H
26	H	H	NAI	NAI	NAI	H
27	H	H	H	NAI	H	H
28	NAI	NAI	H	H	H	H
29	H	NAI	H	H	H	H
30	H	H	H	LOH-AI	LOH-AI	H
31	H	NAI	NAI	H	H	H
32	LOH-AI	H	H	H	NAI	H
33	H	H	LOH-AI	H	H	H
34	H	NAI	LOH-AI	NAI	MSI	H
35	H	NAI	NAI	NAI	H	NAI
36	H	NAI	NAI	H	NAI	H
37	H	H	NAI	H	NAI	H
38	H	H	H	NAI	H	H

CASES	D6S1575	D12S391	D12S320	D6S1645	D12S364	D12S358
39	H	NAI	NAI	H	H	H
40	H	H	NAI	H	H	H
41	H	H	NAI	LOH-AI	H	H
42	H	H	H	NAI	NAI	LOH-AI
43	H	H	MSI	H	H	H
44	H	NAI	H	H	MSI	H
45	H	NAI	H	H	H	MSI
46	LOH-AI	NAI	NAI	H	NAI	NAI
47	H	NAI	H	H	LOH-AI	H
48	H	MSI	NAI	H	H	LOH-AI
49	NAI	H	H	H	H	H
50	NAI	H	H	H	H	H
51	NAI	NAI	NAI	H	H	H
52	H	NAI	NAI	NAI	H	H
53	H	H	H	H	H	H
54	H	H	LOH-AI	H	MSI	H
55	H	H	LOH-AI	H	H	H
56	H	LOH-AI	H	H	H	H
57	LOH-AI	H	NAI	H	H	H
58	H	NAI	LOH-AI	H	H	NAI
59	H	H	H	H	H	H
60	H	H	LOH-AI	H	NAI	H
61	H	NAI	LOH-AI	H	H	MSI
62	H	LOH-AI	NAI	LOH-AI	H	H
63	H	H	H	H	H	H
64	H	MSI	H	NAI	LOH-AI	H
65	H	H	NAI	H	NAI	NAI
66	H	H	H	H	H	NAI
67	LOH-AI	H	H	NAI	H	H
68	H	H	H	LOH-AI	H	H
69	H	NAI	H	LOH-AI	H	H
70	H	NAI	H	H	H	H
71	H	H	H	H	H	MSI
72	MSI	NAI	H	H	NAI	LOH-AI
73	H	H	H	H	NAI	H
74	H	H	MSI	NAI	H	H
75	H	NAI	NAI	NAI	H	H
76	H	LOH-AI	H	H	NAI	H
77	H	LOH-AI	NAI	H	H	H
78	H	H	H	H	NAI	H
79	H	NAI	NAI	NAI	NAI	H
80	H	H	NAI	NAI	NAI	NAI
81	H	H	H	NAI	H	MSI
82	H	H	NAI	NAI	H	LOH-AI
83	H	NAI	H	H	LOH-AI	NAI
84	H	NAI	H	LOH-AI	NAI	H

CASES	D6S1575	D12S391	D12S320	D6S1645	D12S364	D12S358
85	H	LOH-AI	NAI	NAI	NAI	H
86	H	H	H	H	MSI	H
87	H	NAI	H	H	LOH-AI	LOH-AI
88	H	H	H	MSI	H	H
89	H	H	H	H	NAI	H
90	H	H	H	H	NAI	H
91	H	H	H	H	H	H
92	NAI	NAI	H	H	NAI	H
93	NAI	H	LOH-AI	H	MSI	H
94	H	NAI	H	MSI	H	H
95	H	H	H	NAI	LOH-AI	H
96	H	H	LOH-AI	LOH-AI	H	H

Appendix E1: Chi-squared tests

Table 1: Chi-squared test of statistical significance for D6S1575

clinico-pathological feature	chi-squared value	p value	significance
sex	2.021	0.568	not significant ($p>0.05$)
stage	6.240	0.716	not significant ($p>0.05$)
grade	16.464	0.011	significant ($p<0.05$)
lymph node metastases	2.935	0.402	not significant ($p>0.05$)
TNM staging	9.866	0.936	not significant ($p>0.05$)
outcome	5.475	0.140	not significant ($p>0.05$)

Table 2: Chi-squared test of statistical significance for D12S391

clinico-pathological feature	chi-squared value	p value	significance
sex	10.086	0.018	significant ($p<0.05$)
stage	8.481	0.487	not significant ($p>0.05$)
grade	2.618	0.855	not significant ($p>0.05$)
lymph node metastases	2.402	0.493	not significant ($p>0.05$)
TNM staging	14.909	0.668	not significant ($p>0.05$)
outcome	5.780	0.123	not significant ($p>0.05$)

Table 3: Chi-squared test of statistical significance for D12S320

clinico-pathological feature	chi-squared value	p value	significance
sex	3.988	0.263	not significant (p>0.05)
stage	4.692	0.860	not significant (p>0.05)
grade	6.279	0.393	not significant (p>0.05)
lymph node metastases	0.903	0.825	not significant (p>0.05)
TNM staging	13.801	0.742	not significant (p>0.05)
outcome	2.270	0.518	not significant (p>0.05)

Table 4: Chi-squared test of statistical significance for D6S1645

clinico-pathological feature	chi-squared value	p value	significance
sex	0.299	0.960	not significant (p>0.05)
stage	9.548	0.388	not significant (p>0.05)
grade	3.430	0.753	not significant (p>0.05)
lymph node metastases	2.463	0.482	not significant (p>0.05)
TNM staging	15.207	0.648	not significant (p>0.05)
outcome	2.458	0.483	not significant (p>0.05)

Table 5: Chi-squared test of statistical significance for D12S364

clinico-pathological feature	chi-squared value	p value	significance
sex	2.050	0.562	not significant (p>0.05)
stage	9.589	0.385	not significant (p>0.05)
grade	5.740	0.453	not significant (p>0.05)
lymph node metastases	2.734	0.434	not significant (p>0.05)
TNM staging	14.393	0.703	not significant (p>0.05)
outcome	7.670	0.053	not significant (p>0.05)

Table 6: Chi-squared test of statistical significance for D12S358

clinico-pathological feature	chi-squared value	p value	significance
sex	3.584	0.310	not significant (p>0.05)
stage	4.594	0.868	not significant (p>0.05)
grade	7.872	0.248	not significant (p>0.05)
lymph node metastases	1.217	0.749	not significant (p>0.05)
TNM staging	11.914	0.852	not significant (p>0.05)
outcome	1.340	0.720	not significant (p>0.05)

Appendix E2: Cross tabulations

1. Marker D6S1575 genotypes vs. clinico-pathological feature.

Crosstab

			D6S1575				Total
			H	LOH-AI	NAI	MSI	
SEX	F	Count	32	3	5	2	42
		% within sex	76.2%	7.1%	11.9%	4.8%	100.0%
	M	Count	46	4	3	1	54
		% within sex	85.2%	7.4%	5.6%	1.9%	100.0%
Total		Count	78	7	8	3	96
		% within sex	81.3%	7.3%	8.3%	3.1%	100.0%

Crosstab

			D6S1575				Total
			H	LOH-AI	NAI	MSI	
STAGE	0	Count	1	0	0	0	1
		% within stage	100.0%	.0%	.0%	.0%	100.0%
	IIA	Count	37	3	5	0	45
		% within stage	82.2%	6.7%	11.1%	.0%	100.0%
	IIB	Count	10	1	0	0	11
		% within stage	90.9%	9.1%	.0%	.0%	100.0%
	III	Count	30	3	3	3	39
		% within stage	76.9%	7.7%	7.7%	7.7%	100.0%
Total		Count	78	7	8	3	96
		% within stage	81.3%	7.3%	8.3%	3.1%	100.0%

Crosstab

			D6S1575				Total
			H	LOH-AI	NAI	MSI	
GRADE	MD	Count	52	4	4	1	61
		% within grade	85.2%	6.6%	6.6%	1.6%	100.0%
	PD	Count	6	2	0	2	10
		% within grade	60.0%	20.0%	.0%	20.0%	100.0%
	WD	Count	20	1	4	0	25
		% within grade	80.0%	4.0%	16.0%	.0%	100.0%
Total		Count	78	7	8	3	96
		% within grade	81.3%	7.3%	8.3%	3.1%	100.0%

Crosstab

			D6S1575				Total
			H	LOH-AI	NAI	MSI	
Lymph node metastases	No	Count	30	3	4	0	37
		% within Lymph node metastases	81.1%	8.1%	10.8%	.0%	100.0%
	Yes	Count	38	3	3	3	47
		% within Lymph node metastases	80.9%	6.4%	6.4%	6.4%	100.0%
Total		Count	68	6	7	3	84
		% within Lymph node metastases	81.0%	7.1%	8.3%	3.6%	100.0%

Crosstab

			D6S1575				Total
			H	LOH-AI	NAI	MSI	
T, N, M	$T_2N_0M_0$	Count	14	1	1	0	16
		% within TNM	87.5%	6.3%	6.3%	.0%	100.0%
	$T_2N_1M_0$	Count	10	1	0	1	12
		% within TNM	83.3%	8.3%	.0%	8.3%	100.0%
	$T_3N_0M_0$	Count	23	2	4	0	29
		% within TNM	79.3%	6.9%	13.8%	.0%	100.0%
	$T_3N_1M_0$	Count	22	2	3	2	29
		% within TNM	75.9%	6.9%	10.3%	6.9%	100.0%
	$T_4N_0M_0$	Count	3	1	0	0	4
		% within TNM	75.0%	25.0%	.0%	.0%	100.0%
	$T_4N_1M_0$	Count	5	0	0	0	5
		% within TNM	100.0%	.0%	.0%	.0%	100.0%
	$T_{is}N_0M_0$	Count	1	0	0	0	1
		% within TNM	100.0%	.0%	.0%	.0%	100.0%
Total		Count	78	7	8	3	96
		% within TNM	81.3%	7.3%	8.3%	3.1%	100.0%

Crosstab

			D6S1575				Total
			H	LOH-AI	NAI	MSI	
Outcome (Alive/Dead)	A	Count	45	2	5	2	54
		% within Outcome (Alive/Dead)	83.3%	3.7%	9.3%	3.7%	100.0 %
	D	Count	13	4	2	1	20
		% within Outcome (Alive/Dead)	65.0%	20.0%	10.0%	5.0%	100.0 %
Total		Count	58	6	7	3	74
		% within Outcome (Alive/Dead)	78.4%	8.1%	9.5%	4.1%	100.0 %

2. Marker D12S391 genotypes vs. clinico-pathological features.

Crosstab

			D12S391				Total
			H	LOH-AI	NAI	MSI	
SEX	F	Count	28	4	10	0	42
		% within sex	66.7%	9.5%	23.8%	.0%	100.0%
	M	Count	21	4	25	4	54
		% within sex	38.9%	7.4%	46.3%	7.4%	100.0%
Total		Count	49	8	35	4	96
		% within sex	51.0%	8.3%	36.5%	4.2%	100.0%

Crosstab

			D12S391				Total
			H	LOH-AI	NAI	MSI	
STAGE	0	Count	1	0	0	0	1
		% within STAGE	100.0%	.0%	.0%	.0%	100.0%
	IIA	Count	20	3	21	1	45
		% within STAGE	44.4%	6.7%	46.7%	2.2%	100.0%
	IIB	Count	5	0	5	1	11
		% within STAGE	45.5%	.0%	45.5%	9.1%	100.0%
	III	Count	23	5	9	2	39
		% within STAGE	59.0%	12.8%	23.1%	5.1%	100.0%
Total		Count	49	8	35	4	96
		% within STAGE	51.0%	8.3%	36.5%	4.2%	100.0%

Crosstab

			D12S391				Total
			H	LOH-AI	NAI	MSI	
GRADE	MD	Count	29	5	25	2	61
		% within GRADE	47.5%	8.2%	41.0%	3.3%	100.0%
	PD	Count	6	1	2	1	10
		% within GRADE	60.0%	10.0%	20.0%	10.0%	100.0%
	WD	Count	14	2	8	1	25
		% within GRADE	56.0%	8.0%	32.0%	4.0%	100.0%
Total		Count	49	8	35	4	96
		% within GRADE	51.0%	8.3%	36.5%	4.2%	100.0%

Crosstab

			D12S391				Total
			H	LOH-AI	NAI	MSI	
Lymph node metastases	No	Count	18	2	16	1	37
		% within Lymph node metastases	48.6%	5.4%	43.2%	2.7%	100.0%
	Yes	Count	25	5	14	3	47
		% within Lymph node metastases	53.2%	10.6%	29.8%	6.4%	100.0%
Total		Count	43	7	30	4	84
		% within Lymph node metastases	51.2%	8.3%	35.7%	4.8%	100.0%

Crosstab

			D12S391				Total
			H	LOH-AI	NAI	MSI	
TNM	$T_2N_0M_0$	Count	7	1	7	1	16
		% within TNM	43.8%	6.3%	43.8%	6.3%	100.0%
	$T_2N_1M_0$	Count	5	1	5	1	12
		% within TNM	41.7%	8.3%	41.7%	8.3%	100.0%
	$T_3N_0M_0$	Count	13	2	14	0	29
		% within TNM	44.8%	6.9%	48.3%	.0%	100.0%
	$T_3N_1M_0$	Count	18	3	6	2	29
		% within TNM	62.1%	10.3%	20.7%	6.9%	100.0%
	$T_4N_0M_0$	Count	4	0	0	0	4
		% within TNM	100.0%	.0%	.0%	.0%	100.0%
	$T_4N_1M_0$	Count	1	1	3	0	5
		% within TNM	20.0%	20.0%	60.0%	.0%	100.0%
	$T_{IS}N_0M_0$	Count	1	0	0	0	1
		% within TNM	100.0%	.0%	.0%	.0%	100.0%
Total		Count	49	8	35	4	96
		% within TNM	51.0%	8.3%	36.5%	4.2%	100.0%

Crosstab

			D12S391				Total
			H	LOH-AI	NAI	MSI	
Outcome (Alive/Dead)	A	Count	27	4	22	1	54
		% within Outcome (Alive/Dead)	50.0%	7.4%	40.7%	1.9%	100.0%
	D	Count	10	2	5	3	20
		% within Outcome (Alive/Dead)	50.0%	10.0%	25.0%	15.0%	100.0%
Total		Count	37	6	27	4	74
		% within Outcome (Alive/Dead)	50.0%	8.1%	36.5%	5.4%	100.0%

3. Marker D12S320 genotypes vs. clinico-pathological features

Crosstab

			D12S320				Total
			H	LOH-AI	NAI	MSI	
SEX	F	Count	21	6	15	0	42
		% within SEX	50.0%	14.3%	35.7%	.0%	100.0%
	M	Count	32	6	13	3	54
		% within SEX	59.3%	11.1%	24.1%	5.6%	100.0%
Total		Count	53	12	28	3	96
		% within SEX	55.2%	12.5%	29.2%	3.1%	100.0%

Crosstab

			D12S320				Total
			H	LOH-AI	NAI	MSI	
STAGE	0	Count	1	0	0	0	1
		% within STAGE	100.0%	.0%	.0%	.0%	100.0%
	IIA	Count	26	6	11	2	45
		% within STAGE	57.8%	13.3%	24.4%	4.4%	100.0%
	IIB	Count	5	1	4	1	11
		% within STAGE	45.5%	9.1%	36.4%	9.1%	100.0%
	III	Count	21	5	13	0	39
		% within STAGE	53.8%	12.8%	33.3%	.0%	100.0%
Total		Count	53	12	28	3	96
		% within STAGE	55.2%	12.5%	29.2%	3.1%	100.0%

Crosstab

			D12S320				Total
			H	LOH-AI	NAI	MSI	
GRADE	MD	Count	35	6	17	3	61
		% within GRADE	57.4%	9.8%	27.9%	4.9%	100.0%
	PD	Count	3	3	4	0	10
		% within GRADE	30.0%	30.0%	40.0%	.0%	100.0%
	WD	Count	15	3	7	0	25
		% within GRADE	60.0%	12.0%	28.0%	.0%	100.0%
Total		Count	53	12	28	3	96
		% within GRADE	55.2%	12.5%	29.2%	3.1%	100.0%

Crosstab

			D12S320				Total
			H	LOH-AI	NAI	MSI	
Lymph node metastases	No	Count	21	4	10	2	37
		% within Lymph node metastases	56.8%	10.8%	27.0%	5.4%	100.0%
	Yes	Count	25	6	15	1	47
		% within Lymph node metastases	53.2%	12.8%	31.9%	2.1%	100.0%
Total		Count	46	10	25	3	84
		% within Lymph node metastases	54.8%	11.9%	29.8%	3.6%	100.0%

Crosstab

			D12S320				Total
			H	LOH-AI	NAI	MSI	
TNM	$T_2N_0M_0$	Count	7	3	4	2	16
		% within TNM	43.8%	18.8%	25.0%	12.5%	100.0%
	$T_2N_1M_0$	Count	5	2	4	1	12
		% within TNM	41.7%	16.7%	33.3%	8.3%	100.0%
	$T_3N_0M_0$	Count	19	3	7	0	29
		% within TNM	65.5%	10.3%	24.1%	.0%	100.0%
	$T_3N_1M_0$	Count	15	4	10	0	29
		% within TNM	51.7%	13.8%	34.5%	.0%	100.0%
	$T_4N_0M_0$	Count	2	0	2	0	4
		% within TNM	50.0%	.0%	50.0%	.0%	100.0%
	$T_4N_1M_0$	Count	4	0	1	0	5
		% within TNM	80.0%	.0%	20.0%	.0%	100.0%
	$T_{is}N_0M_0$	Count	1	0	0	0	1
		% within TNM	100.0%	.0%	.0%	.0%	100.0%
Total		Count	53	12	28	3	96
		% within TNM	55.2%	12.5%	29.2%	3.1%	100.0%

Crosstab

			D12S320				Total
			H	LOH-AI	NAI	MSI	
Outcome (Alive/Dead)	A	Count	31	5	17	1	54
		% within Outcome (Alive/Dead)	57.4%	9.3%	31.5%	1.9%	100.0%
	D	Count	10	4	5	1	20
		% within Outcome (Alive/Dead)	50.0%	20.0%	25.0%	5.0%	100.0%
Total		Count	41	9	22	2	74
		% within Outcome (Alive/Dead)	55.4%	12.2%	29.7%	2.7%	100.0%

4. Marker D6S1645 genotypes vs. clinico-pathological features.

Crosstab

			D6S1645				Total
			H	LOH-AI	NAI	MSI	
SEX	F	Count	27	5	9	1	42
		% within SEX	64.3%	11.9%	21.4%	2.4%	100.0%
	M	Count	35	5	12	2	54
		% within SEX	64.8%	9.3%	22.2%	3.7%	100.0%
Total		Count	62	10	21	3	96
		% within SEX	64.6%	10.4%	21.9%	3.1%	100.0%

Crosstab

			D6S1645				Total
			H	LOH-AI	NAI	MSI	
STAGE	0	Count	1	0	0	0	1
		% within STAGE	100.0%	.0%	.0%	.0%	100.0%
	IIA	Count	32	2	9	2	45
		% within STAGE	71.1%	4.4%	20.0%	4.4%	100.0%
	IIB	Count	7	0	4	0	11
		% within STAGE	63.6%	.0%	36.4%	.0%	100.0%
	III	Count	22	8	8	1	39
		% within STAGE	56.4%	20.5%	20.5%	2.6%	100.0%
Total		Count	62	10	21	3	96
		% within STAGE	64.6%	10.4%	21.9%	3.1%	100.0%

Crosstab

			D6S1645				Total
			H	LOH-AI	NAI	MSI	
GRADE	MD	Count	38	7	13	3	61
		% within GRADE	62.3%	11.5%	21.3%	4.9%	100.0%
	PD	Count	8	1	1	0	10
		% within GRADE	80.0%	10.0%	10.0%	.0%	100.0%
	WD	Count	16	2	7	0	25
		% within GRADE	64.0%	8.0%	28.0%	.0%	100.0%
Total		Count	62	10	21	3	96
		% within GRADE	64.6%	10.4%	21.9%	3.1%	100.0%

Crosstab

			D6S1645				Total
			H	LOH-AI	NAI	MSI	
Lymph node metastases	No	Count	24	2	9	2	37
		% within Lymph node metastases	64.9%	5.4%	24.3%	5.4%	100.0%
	Yes	Count	28	7	11	1	47
		% within Lymph node metastases	59.6%	14.9%	23.4%	2.1%	100.0%
Total		Count	52	9	20	3	84
		% within Lymph node metastases	61.9%	10.7%	23.8%	3.6%	100.0%

Crosstab

			D6S1645				Total
			H	LOH-AI	NAI	MSI	
TNM	$T_2N_0M_0$	Count	11	2	2	1	16
		% within TNM	68.8%	12.5%	12.5%	6.3%	100.0%
	$T_2N_1M_0$	Count	7	1	4	0	12
		% within TNM	58.3%	8.3%	33.3%	.0%	100.0%
	$T_3N_0M_0$	Count	21	0	7	1	29
		% within TNM	72.4%	.0%	24.1%	3.4%	100.0%
	$T_3N_1M_0$	Count	18	5	6	0	29
		% within TNM	62.1%	17.2%	20.7%	.0%	100.0%
	$T_4N_0M_0$	Count	2	1	1	0	4
		% within TNM	50.0%	25.0%	25.0%	.0%	100.0%
	$T_4N_1M_0$	Count	2	1	1	1	5
		% within TNM	40.0%	20.0%	20.0%	20.0%	100.0%
	$T_{is0}M_0$	Count	1	0	0	0	1
		% within TNM	100.0%	.0%	.0%	.0%	100.0%
Total		Count	62	10	21	3	96
		% within TNM	64.6%	10.4%	21.9%	3.1%	100.0%

Crosstab

			D6S1645				Total
			H	LOH-AI	NAI	MSI	
Outcome (Alive/Dead)	A	Count	36	3	14	1	54
		% within Outcome (Alive/Dead)	66.7%	5.6%	25.9%	1.9%	100.0 %
	D	Count	11	3	5	1	20
		% within Outcome (Alive/Dead)	55.0%	15.0%	25.0%	5.0%	100.0 %
Total		Count	47	6	19	2	74
		% within Outcome (Alive/Dead)	63.5%	8.1%	25.7%	2.7%	100.0 %

5. Marker D12S364 genotypes vs. clinico-pathological features

Crosstab

			D12S364				Total
			H	LOH-AI	NAI	MSI	
SEX	F	Count	24	4	12	2	42
		% within SEX	57.1%	9.5%	28.6%	4.8%	100.0%
	M	Count	35	4	10	5	54
		% within SEX	64.8%	7.4%	18.5%	9.3%	100.0%
Total		Count	59	8	22	7	96
		% within SEX	61.5%	8.3%	22.9%	7.3%	100.0%

Crosstab

			D12S364				Total
			H	LOH-AI	NAI	MSI	
STAGE	0	Count	0	0	1	0	1
		% within STAGE	.0%	.0%	100.0%	.0%	100.0%
	IIA	Count	32	2	8	3	45
		% within STAGE	71.1%	4.4%	17.8%	6.7%	100.0%
	IIB	Count	7	0	3	1	11
		% within STAGE	63.6%	.0%	27.3%	9.1%	100.0%
	III	Count	20	6	10	3	39
		% within STAGE	51.3%	15.4%	25.6%	7.7%	100.0%
Total		Count	59	8	22	7	96
		% within STAGE	61.5%	8.3%	22.9%	7.3%	100.0%

Crosstab

			D12S364				Total
			H	LOH-AI	NAI	MSI	
GRADE	MD	Count	37	5	14	5	61
		% within GRADE	60.7%	8.2%	23.0%	8.2%	100.0%
	PD	Count	9	1	0	0	10
		% within GRADE	90.0%	10.0%	.0%	.0%	100.0%
	WD	Count	13	2	8	2	25
		% within GRADE	52.0%	8.0%	32.0%	8.0%	100.0%
Total		Count	59	8	22	7	96
		% within GRADE	61.5%	8.3%	22.9%	7.3%	100.0%

Crosstab

			D12S364				Total
			H	LOH-AI	NAI	MSI	
Lymph node metastases	No	Count	26	2	8	1	37
		% within Lymph node metastases	70.3%	5.4%	21.6%	2.7%	100.0%
	Yes	Count	26	5	12	4	47
		% within Lymph node metastases	55.3%	10.6%	25.5%	8.5%	100.0%
Total		Count	52	7	20	5	84
		% within Lymph node metastases	61.9%	8.3%	23.8%	6.0%	100.0%

Crosstab

			D12S364				Total
			H	LOH-AI	NAI	MSI	H
TNM	$T_2N_0M_0$	Count	12	0	2	2	16
		% within TNM	75.0%	.0%	12.5%	12.5%	100.0%
	$T_2N_1M_0$	Count	8	0	3	1	12
		% within TNM	66.7%	.0%	25.0%	8.3%	100.0%
	$T_3N_0M_0$	Count	20	2	6	1	29
		% within TNM	69.0%	6.9%	20.7%	3.4%	100.0%
	$T_3N_1M_0$	Count	15	4	7	3	29
		% within TNM	51.7%	13.8%	24.1%	10.3%	100.0%
	$T_4N_0M_0$	Count	2	1	1	0	4
		% within TNM	50.0%	25.0%	25.0%	.0%	100.0%
	$T_4N_1M_0$	Count	2	1	2	0	5
		% within TNM	40.0%	20.0%	40.0%	.0%	100.0%
	$T_{IS}N_0M_0$	Count	0	0	1	0	1
		% within TNM	.0%	.0%	100.0%	.0%	100.0%
Total		Count	59	8	22	7	96
		% within TNM	61.5%	8.3%	22.9%	7.3%	100.0%

Crosstab

			D12S364				Total
			H	LOH-AI	NAI	MSI	
Outcome (Alive/Dead)	A	Count	31	2	17	4	54
		% within Outcome (Alive/Dead)	57.4%	3.7%	31.5%	7.4%	100.0%
	D	Count	13	4	2	1	20
		% within Outcome (Alive/Dead)	65.0%	20.0%	10.0%	5.0%	100.0%
Total		Count	44	6	19	5	74
		% within Outcome (Alive/Dead)	59.5%	8.1%	25.7%	6.8%	100.0%

6. Marker D12S358 genotypes vs. clinic-pathological features.

Crosstab

			D12S358				Total
			H	LOH-AI	NAI	MSI	
SEX	F	Count	35	1	4	2	42
		% within SEX	83.3%	2.4%	9.5%	4.8%	100.0%
	M	Count	38	6	8	2	54
		% within SEX	70.4%	11.1%	14.8%	3.7%	100.0%
Total		Count	73	7	12	4	96
		% within SEX	76.0%	7.3%	12.5%	4.2%	100.0%

Crosstab

			D12S358				Total
			H	LOH-AI	NAI	MSI	
STAGE	0	Count	1	0	0	0	1
		% within STAGE	100.0%	.0%	.0%	.0%	100.0%
	IIA	Count	35	3	4	3	45
		% within STAGE	77.8%	6.7%	8.9%	6.7%	100.0%
	IIB	Count	7	1	2	1	11
		% within STAGE	63.6%	9.1%	18.2%	9.1%	100.0%
	III	Count	30	3	6	0	39
		% within STAGE	76.9%	7.7%	15.4%	.0%	100.0%
Total		Count	73	7	12	4	96
		% within STAGE	76.0%	7.3%	12.5%	4.2%	100.0%

Crosstab

			D12S358				Total
			H	LOH-AI	NAI	MSI	
GRADE	MD	Count	48	6	5	2	61
		% within GRADE	78.7%	9.8%	8.2%	3.3%	100.0%
	PD	Count	6	1	3	0	10
		% within GRADE	60.0%	10.0%	30.0%	.0%	100.0%
	WD	Count	19	0	4	2	25
		% within GRADE	76.0%	.0%	16.0%	8.0%	100.0%
Total		Count	73	7	12	4	96
		% within GRADE	76.0%	7.3%	12.5%	4.2%	100.0%

Crosstab

			D12S358				Total
			H	LOH-AI	NAI	MSI	
Lymph node metastases	No	Count	28	3	4	2	37
		% within Lymph node metastases	75.7%	8.1%	10.8%	5.4%	100.0%
	Yes	Count	34	4	8	1	47
		% within Lymph node metastases	72.3%	8.5%	17.0%	2.1%	100.0%
Total		Count	62	7	12	3	84
		% within Lymph node metastases	73.8%	8.3%	14.3%	3.6%	100.0%

Crosstab

			D12S358				Total
			H	LOH-AI	NAI	MSI	
TNM	$T_2N_0M_0$	Count	13	1	2	0	16
		% within TNM	81.3%	6.3%	12.5%	.0%	100.0%
	$T_2N_1M_0$	Count	7	1	3	1	12
		% within TNM	58.3%	8.3%	25.0%	8.3%	100.0%
	$T_3N_0M_0$	Count	22	2	2	3	29
		% within TNM	75.9%	6.9%	6.9%	10.3%	100.0%
	$T_3N_1M_0$	Count	22	2	5	0	29
		% within TNM	75.9%	6.9%	17.2%	.0%	100.0%
	$T_4N_0M_0$	Count	4	0	0	0	4
		% within TNM	100.0%	.0%	.0%	.0%	100.0%
	$T_4N_1M_0$	Count	4	1	0	0	5
		% within TNM	80.0%	20.0%	.0%	.0%	100.0%
	$T_{IS}N_0M_0$	Count	1	0	0	0	1
		% within TNM	100.0%	.0%	.0%	.0%	100.0%
Total		Count	73	7	12	4	96
		% within TNM	76.0%	7.3%	12.5%	4.2%	100.0%

Crosstab

			D12S358				Total
			H	LOH-AI	NAI	MSI	
Outcome (Alive/Dead)	A	Count	42	4	5	3	54
		% within Outcome (Alive/Dead)	77.8%	7.4%	9.3%	5.6%	100.0%
	D	Count	17	1	2	0	20
		% within Outcome (Alive/Dead)	85.0%	5.0%	10.0%	.0%	100.0%
Total		Count	59	5	7	3	74
		% within Outcome (Alive/Dead)	79.7%	6.8%	9.5%	4.1%	100.0%

Appendix E3:

Kruskal-Wallis test for age *vs.* microsatellite genotypes

Table 1: Kruskal-Wallis test of statistical significance for age

microsatellite marker	**p value**	**significance**
D6S1575	0.300	not significant (p>0.05)
D12S391	0.077	not significant (p>0.05)
D12S320	0.527	not significant (p>0.05)
D6S1645	0.461	not significant (p>0.05)
D12S364	0.834	not significant (p>0.05)
D12S358	0.485	not significant (p>0.05)

Appendix F: PCR optimization

1. $MgCl_2$ optimization

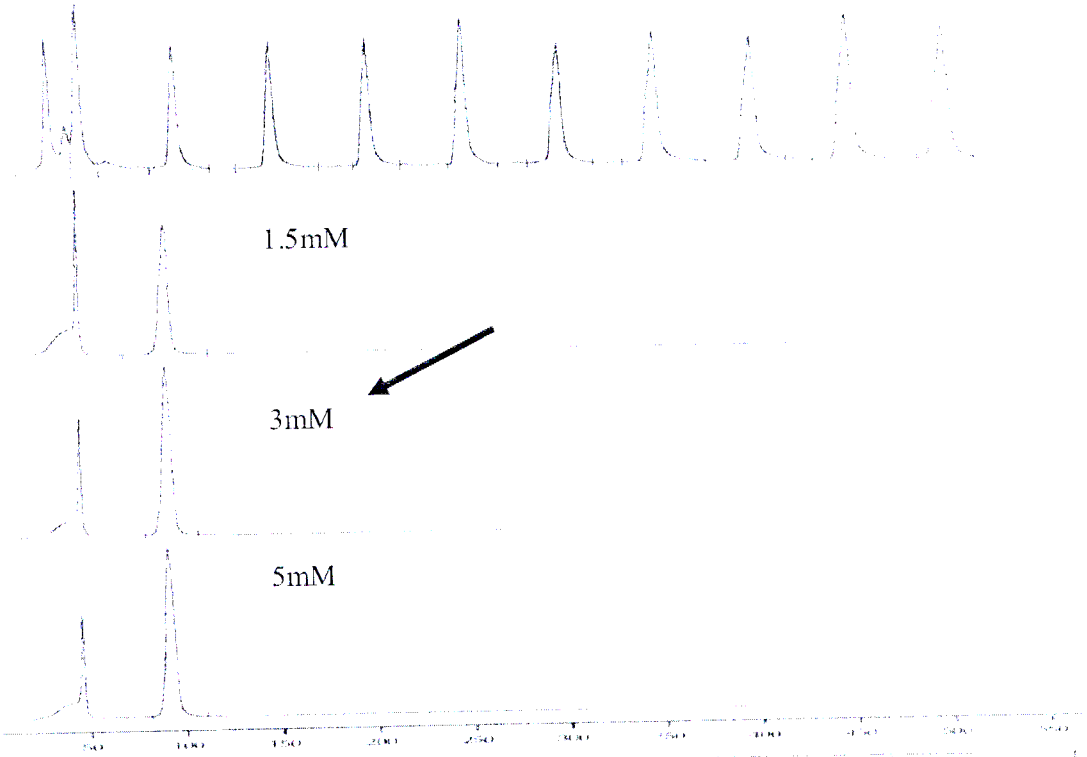

Lane #	Peak #	Run Time	Peak Area	Size (BP)	Quantity
1	1	22:46	284.88	#50.0	0.49876
	2	27:26	239.8	#100.0	0.41982
	3	32:36	265.71	#150.0	0.4652
	4	38:16	305.59	#200.0	0.535502
	5	44:22	391.13	#250.0	0.68477
	6	50:42	358.92	#300.0	0.628488
	7	57:14	446.52	#350.0	0.78175
	8	63:52	437.49	#400.0	0.76593
	9	70:40	571.18	#450.0	1
	10	77:20	550.96	#500.0	0.96459
12	1	26:44	637.41	92.8	1
13	1	26:40	730.64	92.1	1
14	1	26:40	667.27	92.1	1

Figure 1: A representative electrophoretogram of a $MgCl_2$ titration for marker D6S1575. Lane 1 contained the 50-500 CY5-labelled marker. Lanes 2, 3 and 4 contained $MgCl_2$ concentrations of 1.5, 3 and 5mM as indicated. The arrow indicates the chosen approximate concentration used in all subsequent PCR reactions.

Appendix F continued…

2. Template concentration optimization

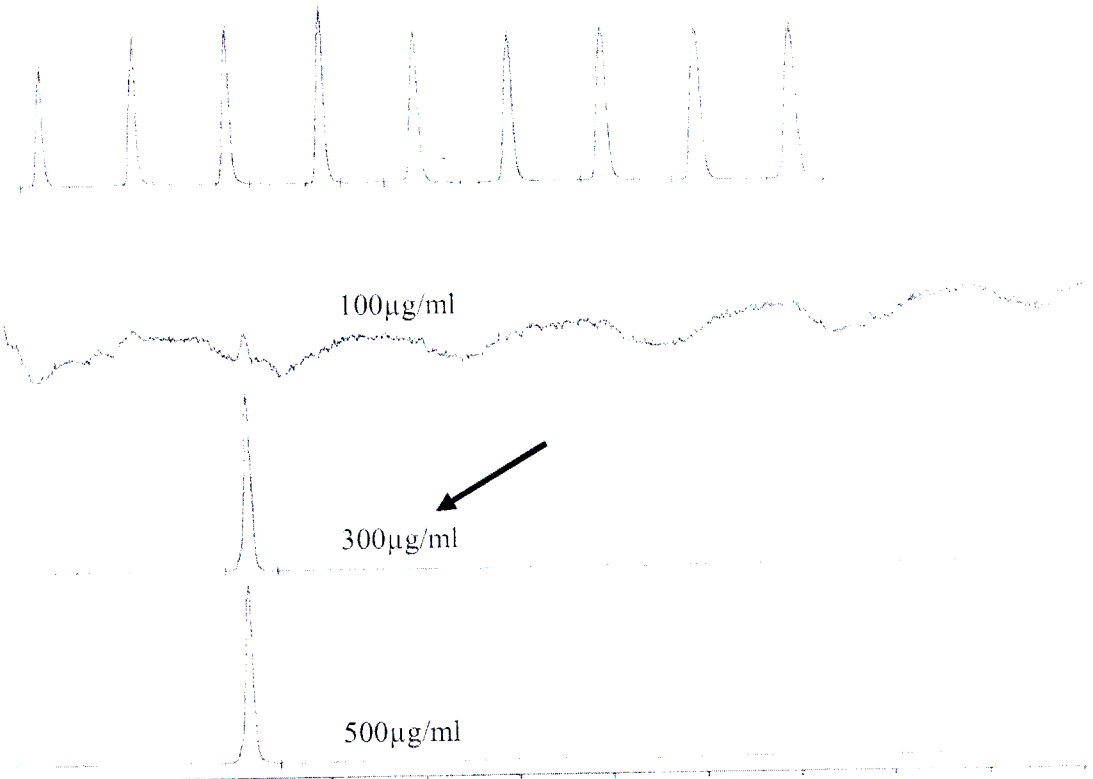

Lane #	Peak #	Run Time	Peak Area	Size (BP)	Quantity
1	1	24:48	263.1	#50.0	0.39519
	2	29:54	210.08	#100.0	0.31556
	3	35:38	293.12	#150.0	0.44029
	4	42:00	348.12	#200.0	0.5229
	5	48:40	440.27	#250.0	0.66132
	6	55:48	458.14	#300.0	0.68816
	7	62:58	473.79	#350.0	0.71167
	8	70:30	551.58	#400.0	0.82853
	9	78:00	594.27	#450.0	0.89264
	10	85:38	665.74	#500.0	1
4	1	43:00	161.31	207.6	1
5	1	42:56	145.53	207.1	1

Figure 2: A representative electrophoretogram of a template titration for marker D12S391. Lane 1 contained the 50-500 CY5-labelled marker. Lanes 2, 3 and 4 contained template concentrations of 100, 300 and 500µg/ml as indicated. The arrow indicates the chosen concentration used in all subsequent PCR reactions.

Appendix F continued…

3. Annealing temperature optimization

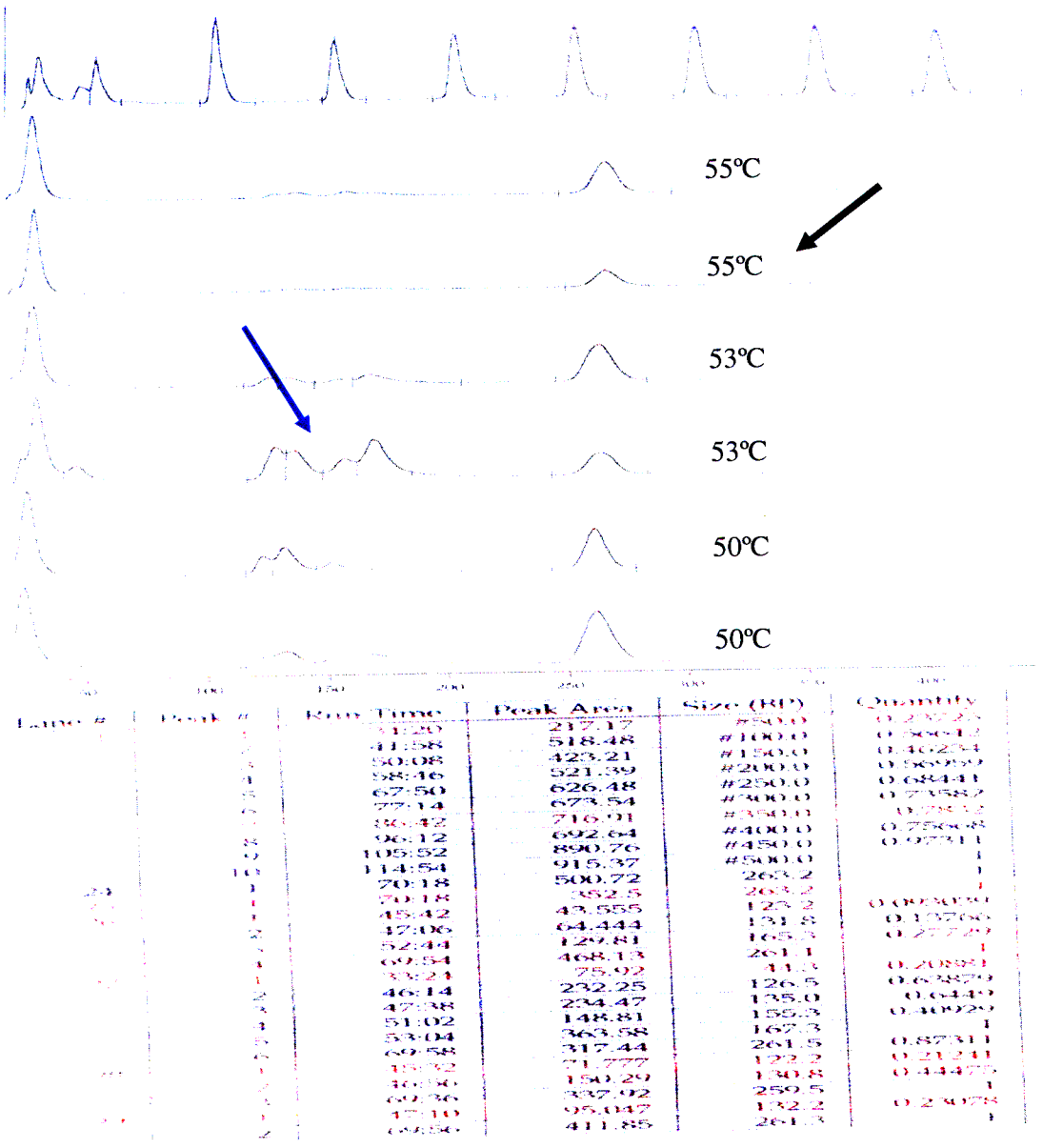

Figure 3: A representative electrophoretogram of an annealing temperature titration for marker D12S358. Lane 1 contained the 50-500 CY5-labelled marker. Lanes 2, 3 ,4, 5, 6 and 7 represent annealing temperatures of 55, 53 and 50 °C as indicated. Additional peaks (indicated by blue arrow) show non-specific amplification, indicative of less stringent primer annealing conditions. The black arrow indicated the chosen annealing temperature that was used in all subsequent PCR reactions.

Appendix F continued…

2. Template concentration optimization

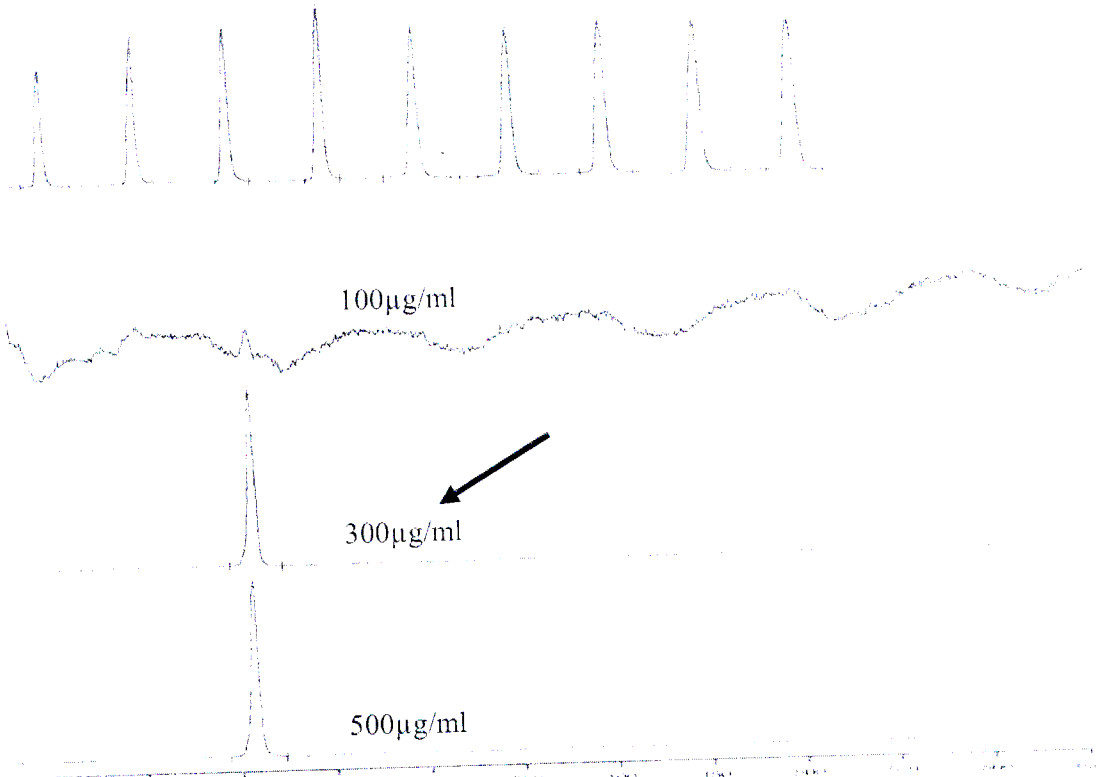

Lane #	Peak #	Run Time	Peak Area	Size (BP)	Quantity
1	1	24:48	263.1	#50.0	0.39519
	2	29:54	210.08	#100.0	0.31556
	3	35:38	293.12	#150.0	0.44029
	4	42:00	348.12	#200.0	0.5229
	5	48:40	440.27	#250.0	0.66132
	6	55:48	458.14	#300.0	0.68816
	7	62:58	473.79	#350.0	0.71167
	8	70:30	551.58	#400.0	0.82853
	9	78:00	594.27	#450.0	0.89264
	10	85:38	665.74	#500.0	1
4	1	43:00	161.31	207.6	1
5	1	42:56	145.53	207.1	1

Figure 2: A representative electrophoretogram of a template titration for marker D12S391. Lane 1 contained the 50-500 CY5-labelled marker. Lanes 2, 3 and 4 contained template concentrations of 100, 300 and 500µg/ml as indicated. The arrow indicates the chosen concentration used in all subsequent PCR reactions.

Appendix F continued…

3. Annealing temperature optimization

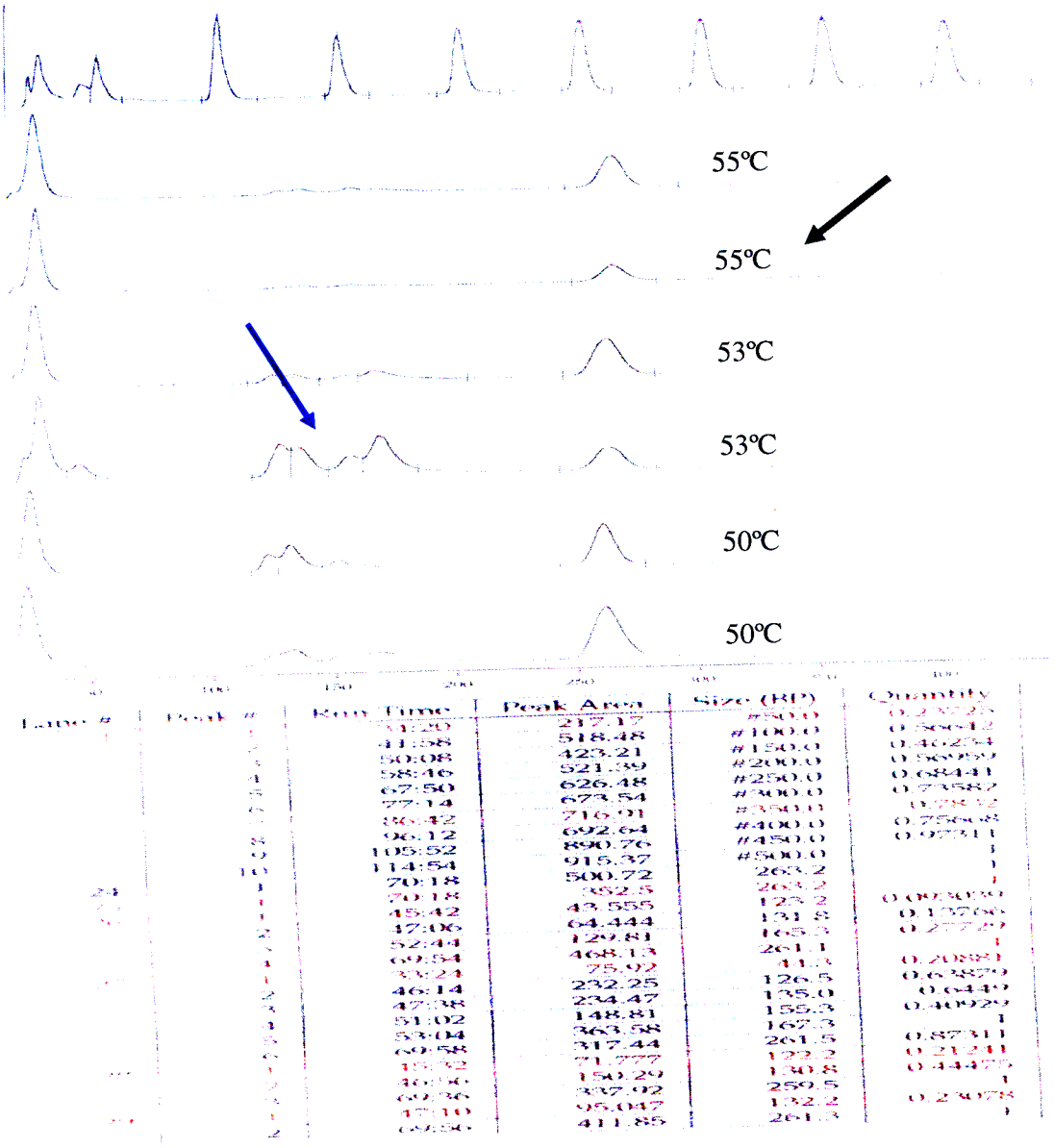

Figure 3: A representative electrophoretogram of an annealing temperature titration for marker D12S358. Lane 1 contained the 50-500 CY5-labelled marker. Lanes 2, 3 ,4, 5, 6 and 7 represent annealing temperatures of 55, 53 and 50 °C as indicated. Additional peaks (indicated by blue arrow) show non-specific amplification, indicative of less stringent primer annealing conditions. The black arrow indicated the chosen annealing temperature that was used in all subsequent PCR reactions.